PREPRINT: This manuscript is a preprint submitted to EarthArXiv. This version 3 reflects the revisions made in response to a second round of peer-review by the GSA Books volume “Jurassic–Paleogene tectonic evolution of the North American Cordillera” of the Geological Society of America (resubmitted to the editors on 2025/02/22).

Tomotectonics of Cordilleran North America since Jurassic times: double-sided subduction, archipelago collisions, and Baja-BC translation

Karin Sigloch[1] & Mitchell G. Mihalynuk[2]

1) Université Côte d’Azur, Observatoire Côte d’Azur, CNRS, IRD. Géoazur, Sophia Antipolis, France. sigloch@geoazur.unice.fr
2) British Columbia Geological Survey. Ministry of Energy, Mines and Low Carbon Innovation British Columbia. Victoria, Canada. Mitch.Mihalynuk@gov.bc.ca

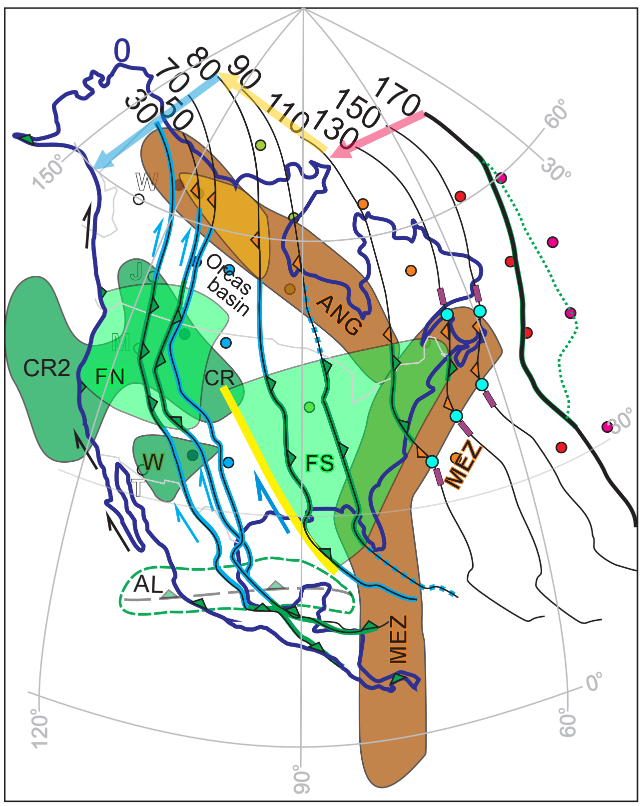

0
30
70
50
80
90
110
130
150
170
150°
60°
30°
W
J
M
Orcas basin
ANG
CR2
FN
CR
FS
W
T
MEZ
AL
MEZ
30°
0°
120°
90°
60°

Figure 1. Roadmap figure for this study: the superposition of subducted lithosphere (slabs) in the mantle with continental drift, reconstructed with respect to the mantle. Coloured polygons show outlines of major slabs under North America from teleseismic P-wave tomography (Sigloch 2011). Slabs inferred to have been deposited by westward subduction are coloured in orange, those generated by eastward (Farallon) subduction in green. Darker colour shades are applied to lower-mantle slabs (MEZ, ANG and CR/CR2/W; light shades to shallower slabs: FS (400-1000 km deep), FN (0-700 km), and to the shallow western end of ANG. Superimposed are time snapshots tracking the westward migrating margin of North America, reconstructed in a mantle reference frame, which is constrained between 0-120 Ma by moving hotspots (Dubrovine et al., 2012) and 120-170 Ma by true polar wander-corrected paleomagnetic data (Torsvik et al., 2019). Colored arrows connecting the northern end points of the paleo-coastlines highlight three distinct episodes of absolute plate motion.

If the slabs sank vertically in place then a continental margin overlying a slab indicates a continent-arc interaction – because a slab constrains a paleo-subduction zone, which must have hosted a paleo-arc. Symbols on the paleo-margins indicate the nature of the tectonic regime along the margin, as inferable from the tomotectonic principles developed in the text. Orange barbs: NAM-beneath-arc collision (westward subducting slab located underneath). Green barbs: subduction beneath NAM (eastward subduction), with arc built on NAM. Light blue lines and arrows: transform boundary along the margin (no slab underneath). Black line: (quasi-)passive continental margin (no slab underneath, and no pre-existing plate boundary along the margin). Yellow line traces the sharp western edge of FS slab, associated with a sudden transition from eastward subduction to transform margin ~80 Ma. The starting point of our inference is ~170 Ma, the time when North America separated from Pangaea, and when absolute paleo-positioning in plate reconstructions becomes reasonably reliable.

Slab abbreviations: MEZ – Mezcalera, ANG – Angayucham, CR & CR2 – Cascadia Root, FN – Farallon North, FS – Farallon South, AL – Alisitos. W is a non-interpretive name.

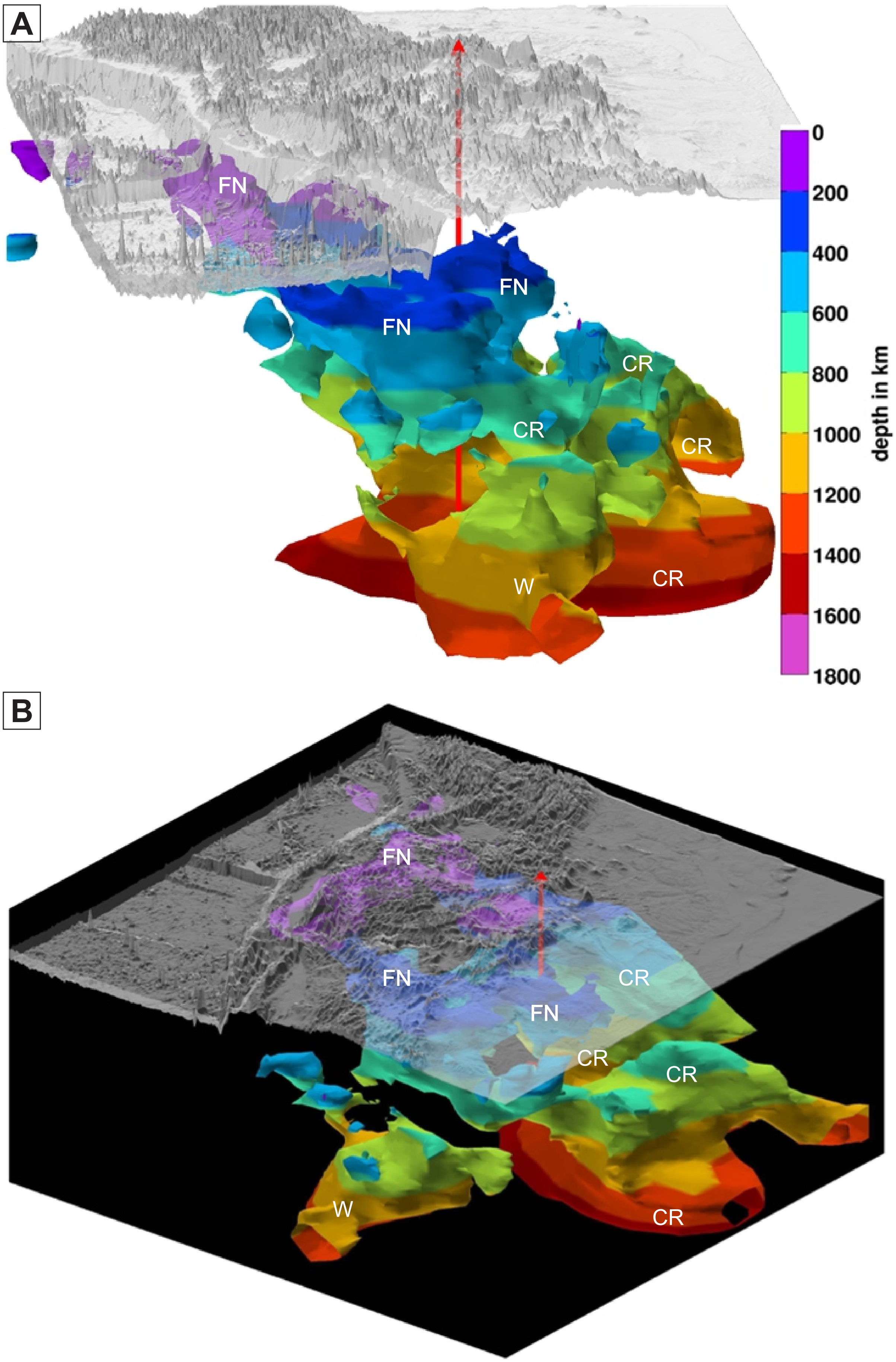
A
FN
FN
FN
CR
CR
CR
W
CR
0
200
400
600
800
1000
1200
1400
1600
1800
depth in km
B
FN
FN
FN
CR
CR
CR
W
CR

Figure 2. Mantle tomography: 3-D isosurface rendering of seismically fast anomalies imaged under the western U.S.A., from the surface to ~1800 km depth, in the teleseismic P-wave tomography model of Sigloch (2011). The isosurface rendering threshold is $dVp/Vp>0.25\%$. Color signals depth and changes in increments of 200 km. This structure represents subducted oceanic lithosphere (slab) of the former Farallon plate, dipping eastward down from beneath the Cascades (Juan de Fuca) trench. Surface topography of the North American Cordillera and the Pacific basin are overlain in translucent gray, with strong vertical exaggeration. Yellowstone (red triangle) and its vertical downward continuation are shown for visual reference. Seismically slow anomalies are not rendered (e.g., Yellowstone plume). Shallow fast anomalies representing the thick continental lithosphere of NAM are masked out as they would block the 3-D view on the slabscape. Panels A and B present alternative view angles on the same scene, comprising the FN and CR slabs of Figure 1 (subdivided at ~600 km depth, where structural breaks are visible especially in panel B). Slab W is also visible in the foreground. Deep CR2 slab under the Pacific is not rendered.

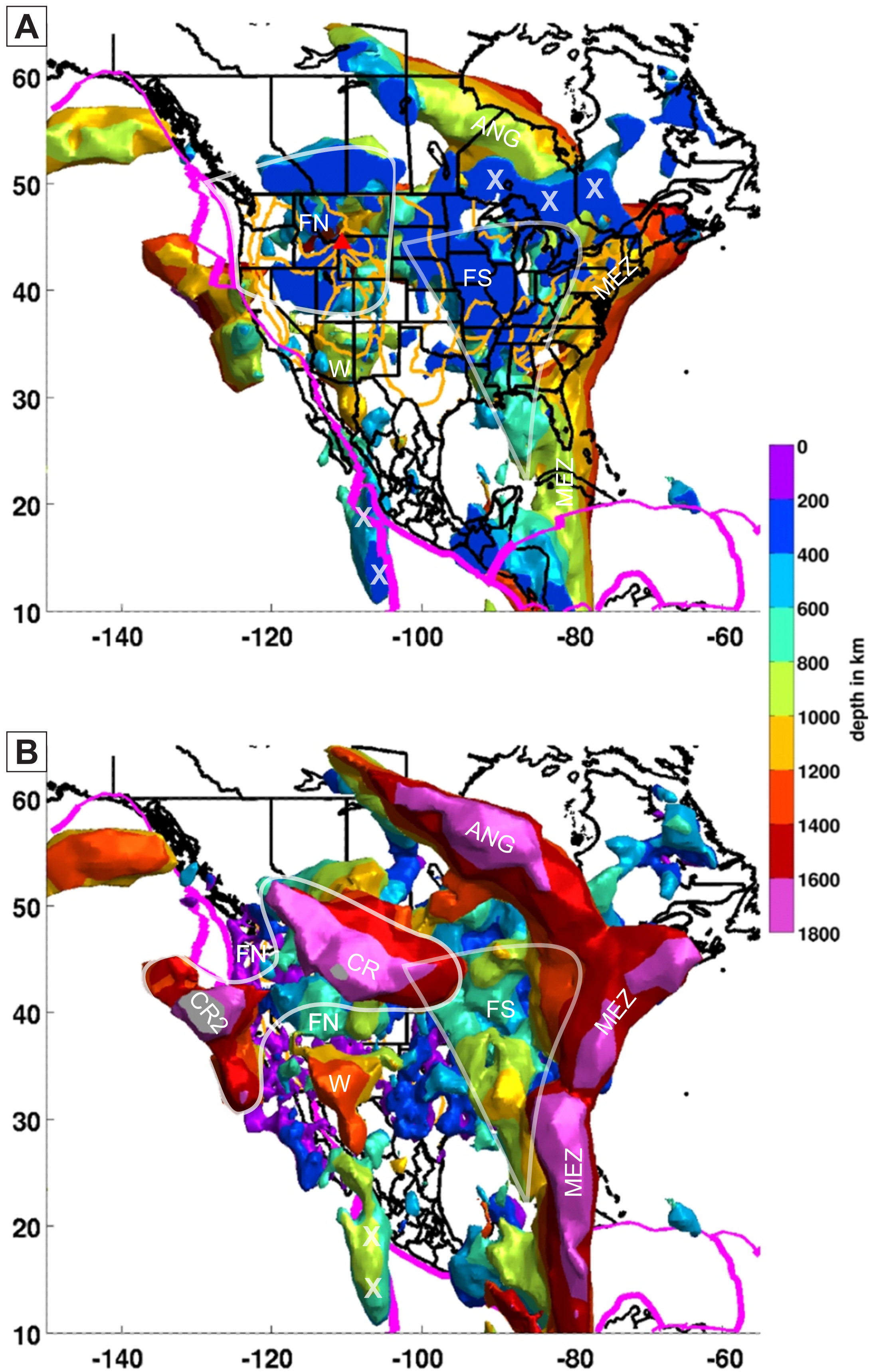

A
ANG
X
X
X
FN
FS
MEZ
W
MEZ
X
X
60
50
40
30
20
10
-140
-120
-100
-80
-60
B
ANG
FN
CR
CR2
FN
FS
MEZ
W
MEZ
X
X
0
200
400
600
800
1000
1200
1400
1600
1800
depth in km

Figure 3. Three-dimensional isosurface rendering of all seismically fast P-wave anomalies (subducted slabs) in the upper and lower mantle beneath North America. Tomography model, rendering threshold and color scheme as in Figure 2. (A) Top-down view of fast structure below 400 km (in order to exclude the overlying lithosphere, which is fast but does not represent slab). Strictly speaking, the view is from ~390 km down due to slight interpolation smoothing of the contouring algorithm, explaining why the shallowest anomalies appear in dark blue, as part of the 200-400 km layer. (B) Inside-out view of all fast structure from the surface down, with the deepest structure (slab walls MEZ, ANG, CR/CR2) emerging to the foreground. Imaging limitations include artifacts, especially near the margins of the regional dataset: resolution lost into the ocean basins and north of 55°. Two downward smearing artifacts are labeled with white x's and are not interpreted.

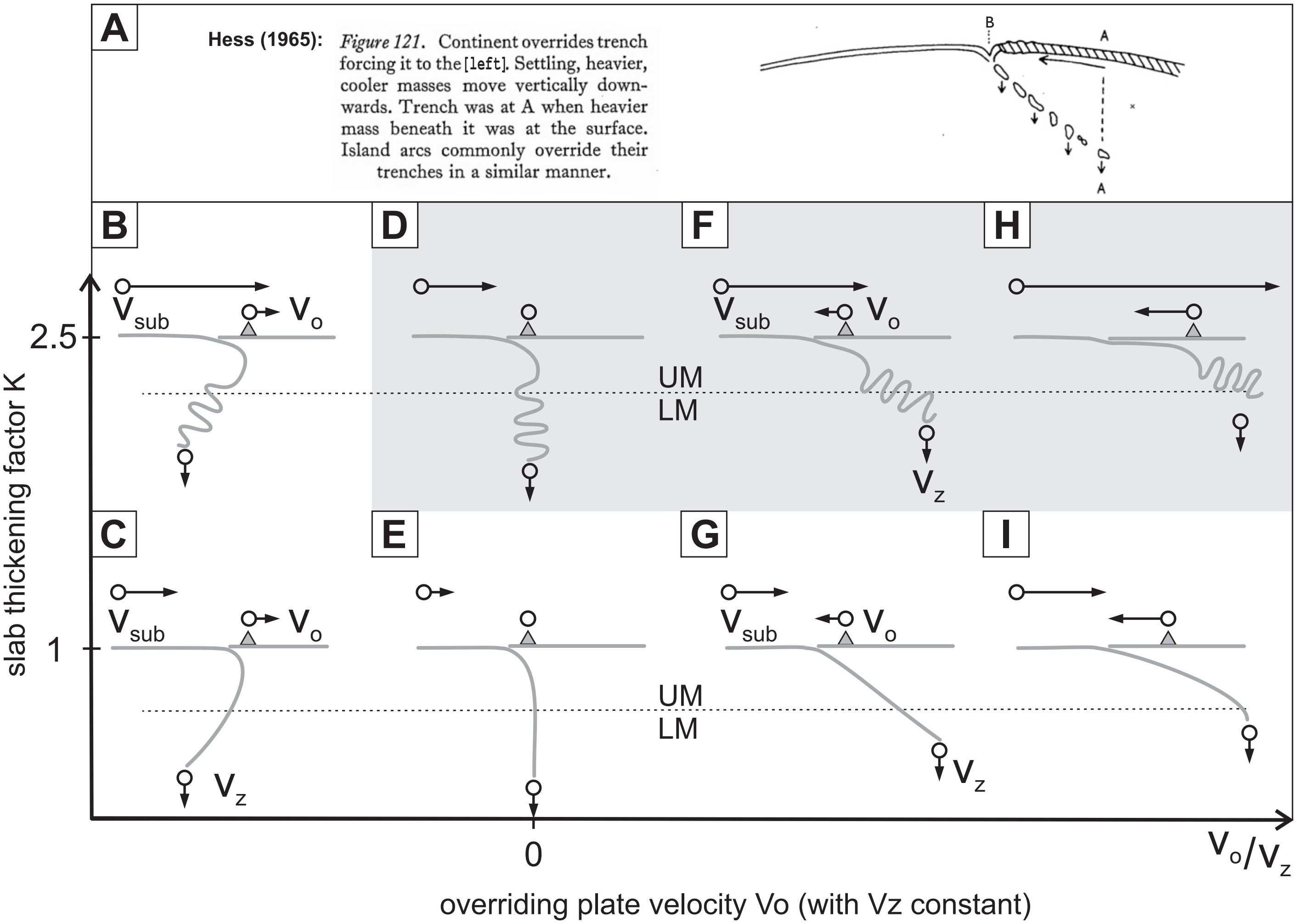
A
Hess (1965):
Figure 121. Continent overrides trench forcing it to the [left]. Settling, heavier, cooler masses move vertically downwards. Trench was at A when heavier mass beneath it was at the surface. Island arcs commonly override their trenches in a similar manner.
B
A
A
B
D
F
H
C
E
G
I
Vsub
Vo
Vz
UM
LM
2.5
1
slab thickening factor K
0
Vo/Vz
overriding plate velocity Vo (with Vz constant)

Figure 4. (A) The tomotectonic null hypothesis of vertical slab sinking, as envisioned by the very first cartoon of subduction to be published, by Harry Hess in 1965. Motions are drawn in a mantle reference frame, with the overriding plate moving laterally but not the subducting plate. (B)-(I) Range of possible slab geometries predicted for when oceanic lithosphere sinks vertically after entering the trench, as a function of the parameters v_o, the velocity of the overriding plate (or arc) on the x-axis, and of K, a measure for the vigor of subduction, on the y-axis. Dashed lines represent the viscosity discontinuity between upper mantle (UM) and lower mantle (LM), where the mantle becomes 1-2 orders of magnitude more viscous, resisting further slab sinking. Motions are drawn relative to the mantle, and velocity arrows are drawn to scale relative to each other. v_z, the slab sinking velocity in the lower mantle, is kept fixed in all panels (a typical value being 10 mm/year). Kinematic ratio $K = v_{sub}/v_{acc}$ is the ratio of slab length subducted per unit time versus the length of accommodation space created for it, by means of the vertical sinking away of older slab and the migration v_o of the trench away from the site of older subduction (see Cerpa et al. 2022, eq. 1, for exact definition). K>1 indicates "traffic jam conditions", where plate convergence is too rapid to be accommodated undeformed, so that slab is forced to thicken (probably by folding). The average value observed for present-day trenches is K~2.5 (Cerpa et al. 2022), with the associated slab types highlighted by grey shaded panels D, F, H. $v_o < 0$ (trench advance, panels B & C) is practically not observed.

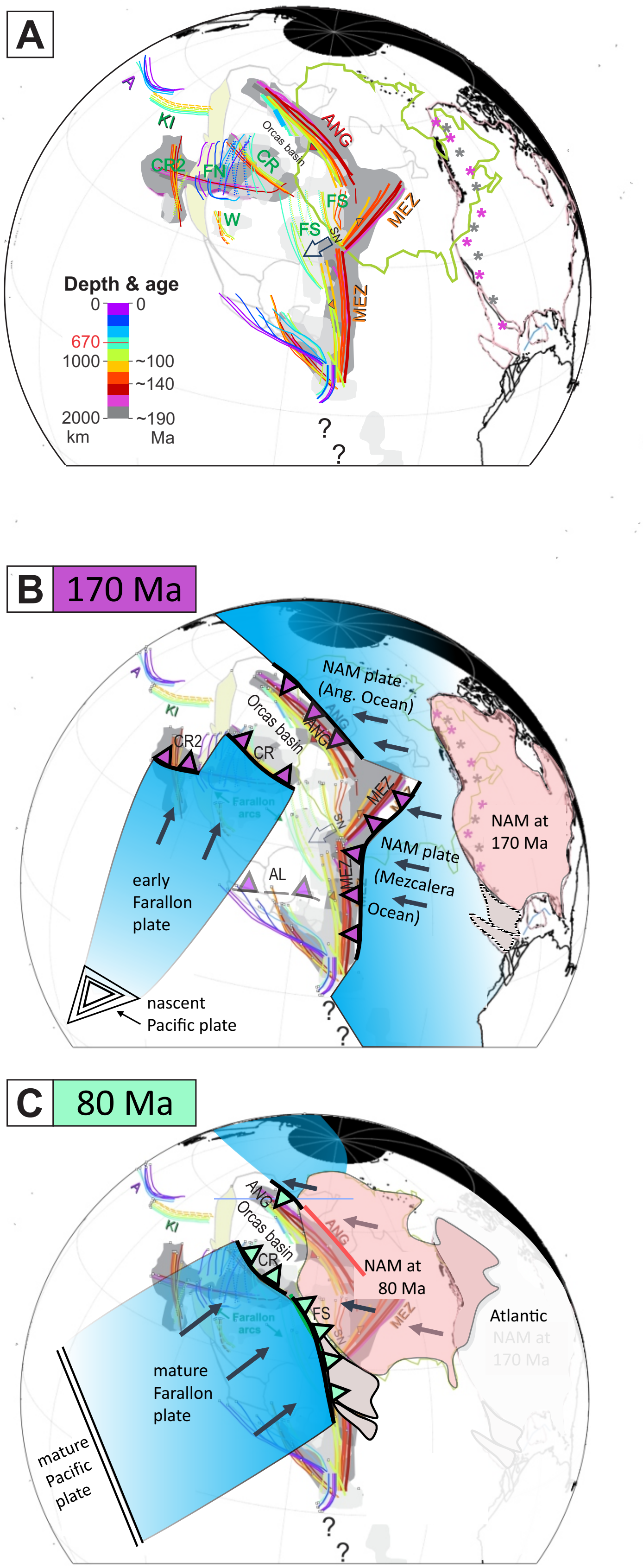
A
A
KI
CR2
FN
CR
Orcas basin
ANG
FS
W
FS
SN
MEZ
MEZ
Depth & age
0
0
670
1000
~100
~140
2000
km
~190
Ma
?
?
B
170 Ma
NAM plate
(Ang. Ocean)
Orcas basin
CR2
CR
ANG
MEZ
Farallon arcs
NAM at
170 Ma
NAM plate
(Mezcalera
Ocean)
AL
early
Farallon
plate
nascent
Pacific plate
C
80 Ma
ANG
Orcas basin
CR
NAM at
80 Ma
FS
MEZ
Atlantic
NAM at
170 Ma
mature
Farallon
plate
mature
Pacific
plate

Figure 5. Paleo-trenches in absolute (mantle) coordinates, as predicted by the observed slab geometries of Figure 3 if the slabs sank vertically. **(A)** Slab-to-trench transcriptions are drawn in depth increments of 100 km, using the same depth-to-colour mapping as Figure 3. Tracks of paleo-trench (or arc) locations are shown as thick lines if inferred to be produced by westward subduction, and thin lines if produced by eastward subduction or subduction of ambiguous polarity (mostly Farallon). For laterally extended slabs (FS, FN, CR, presumably produced as in figs 4F/H), the arc lines are shown as dashed when a locus of slab deposition is poorly constrained laterally, for a given depth. The colour bar also shows an indicative mapping of slab depth to time of subduction, using 10 mm/year as a typical, heuristic value for slab sinking rate. The coastlines of NAM reconstructed at times 170 Ma (black), ~80 Ma (green), and present day (grey). Grey polygons indicate slab footprints at 800 km depth (in light grey) and at 1400 km (dark grey). Label SN marks the approximate position of the Sierra Nevada batholith; the arrow denotes possible extents of the Hess-Shatsky Rise conjugate plateau. Arc abbreviations: A = Aleutian, KI = Kula-Izanagi. Purple-grey stars on western NAM mark the previous generation of arcs IMS & NJ, extinct and accreted by 170 Ma.

(B) Tomotectonically inferred trenches and plates at 170 Ma, before NAM started its westward drift. All arcs are intra-oceanic at this time. AL trench will start up ~130 Ma, when the Farallon plate has grown southeastward. Trenches/arcs active at the respective reconstruction times are highlighted with barbs and the colors corresponding to their depths, and are plotted on the basemap of panel A.

(C) Trenches and plates at 80 Ma when override is far advanced, with the westward subduction system almost overridden. Farallon plate subducts into a margin-hugging trench in the south (FS) but remains offshore farther north (CR).

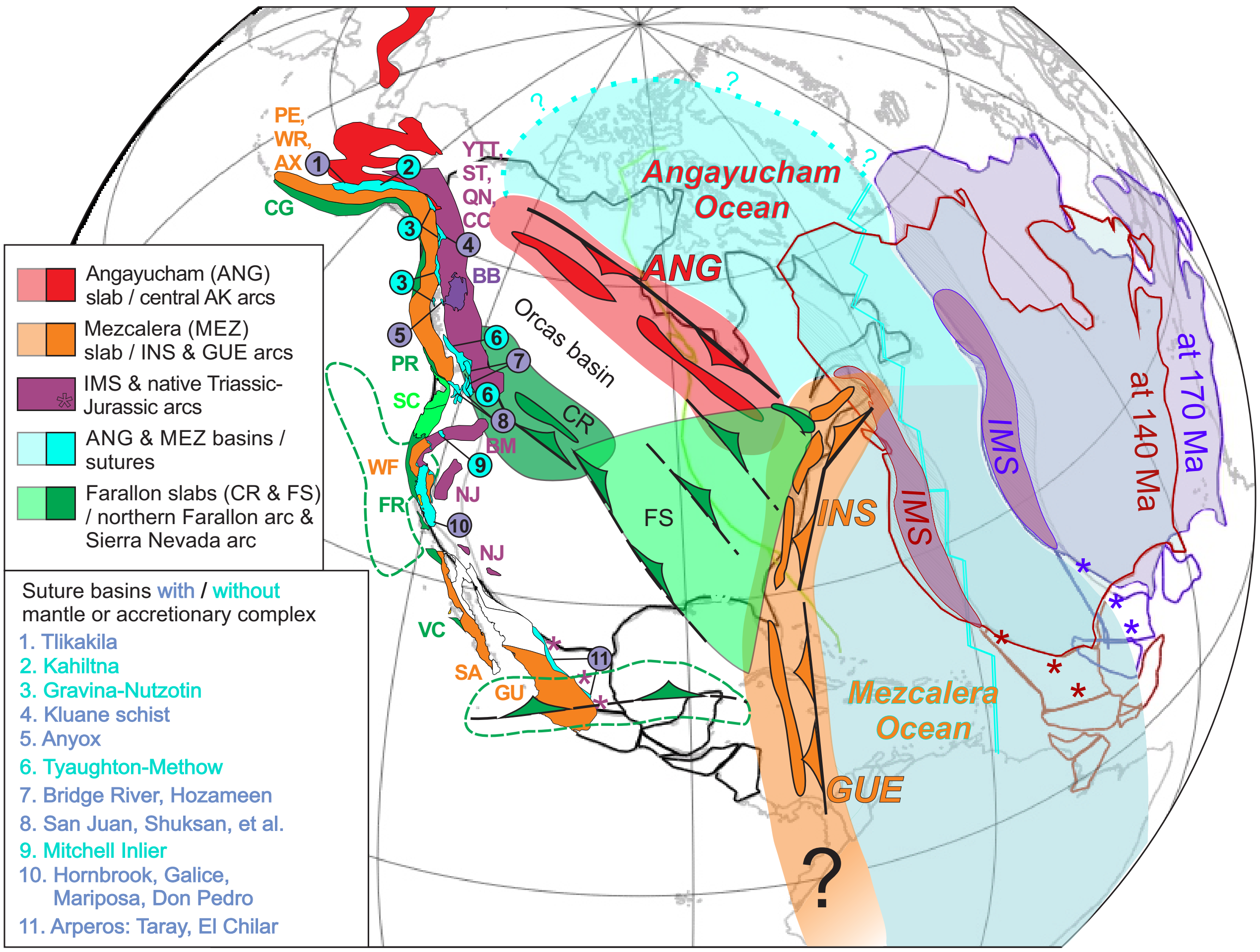

Angayucham (ANG) slab / central AK arcs
Mezcalera (MEZ) slab / INS & GUE arcs
IMS & native Triassic-Jurassic arcs
ANG & MEZ basins / sutures
Farallon slabs (CR & FS) / northern Farallon arc & Sierra Nevada arc
Suture basins with / without mantle or accretionary complex
1. Tlikakila
2. Kahiltna
3. Gravina-Nutzotin
4. Kluane schist
5. Anyox
6. Tyaughton-Methow
7. Bridge River, Hozameen
8. San Juan, Shuksan, et al.
9. Mitchell Inlier
10. Hornbrook, Galice, Mariposa, Don Pedro
11. Arperos: Taray, El Chilar
Angayucham Ocean
ANG
Orcas basin
CR
FS
INS
IMS
GUE
Mezcalera Ocean
at 170 Ma
at 140 Ma
PE, WR, AX
CG
YTT, ST, QN, CC
BB
PR
SC
WF
FR
BM
NJ
VC
SA
GU
?

Figure 6. Arc terranes matched to slabs. Every substantive slab should be associated with a geologically known arc, and every known arc should be associated with a slab. Arc (super-)terranes are shown in their present positions in the Cordillera on the left part of the map. The same arc terranes are schematically reconstructed above their matched slabs and paleo-trenches, in absolute positions relative to the lower mantle. Colour legend gives the interpreted matches of slabs to geologically known arcs. Superterranes, slabs, arcs and trenches are coloured green if associated with Farallon Ocean subduction; orange if associated with Mezcalera Ocean subduction, and red if associated with Angayucham Ocean subduction. The reconstruction time for the arcs and slab walls corresponds to ~170 Ma (before Archipelago override began), except in the case of the SW-ward migrating southern Farallon (Sierra Nevada Batholith) arc, which is shown in several time snapshots migrating across the area occupied by its associated FS slab. North America is reconstructed at 170 Ma, 140 Ma and 0 Ma. Intermontane Superterrane (IMS) and its continental prolongation, the Native Jurassic arc (NJ) are coloured purple; by 170 Ma, their arc activity had ceased and IMS is shown docked against NAM. The interpreted suture of MEZ arcs (Insular & Guerrero Superterranes INS, orange) against IMS/NJ terranes, is represented by a dozen of collapsed oceanic basins colored cyan and numbered/labeled in the legend.
Abbreviations: Guerrero-Insular arc terranes include WR (Wrangellia), AX (Alexander), PE (Peninsular), GU (Guerrero), WF (Western Jurassic, Western Hayfork, Foothills, and related terranes), SA (Santa Ana). Terranes are associated with Farallon subduction include CG—Chugach; FR—Franciscan; PR—Pacific Rim; SC—Siletz-Crescent; VC—Vizcaino.
IMS Superterrane (purple) includes terranes BM (Blue Mountains, CC (Cache Creek), QN (Quesnel), ST (Stikine) and YTT (Yukon Tanana). NJ (Native Jurassic arc) is the onshore continuation of IMS arcs, as is presumably its along-strike continuation of extensional magmatism in Mexico ("Nazas arc", cf. Busby and Centeno-García, 2022), shown by purple asterisks.

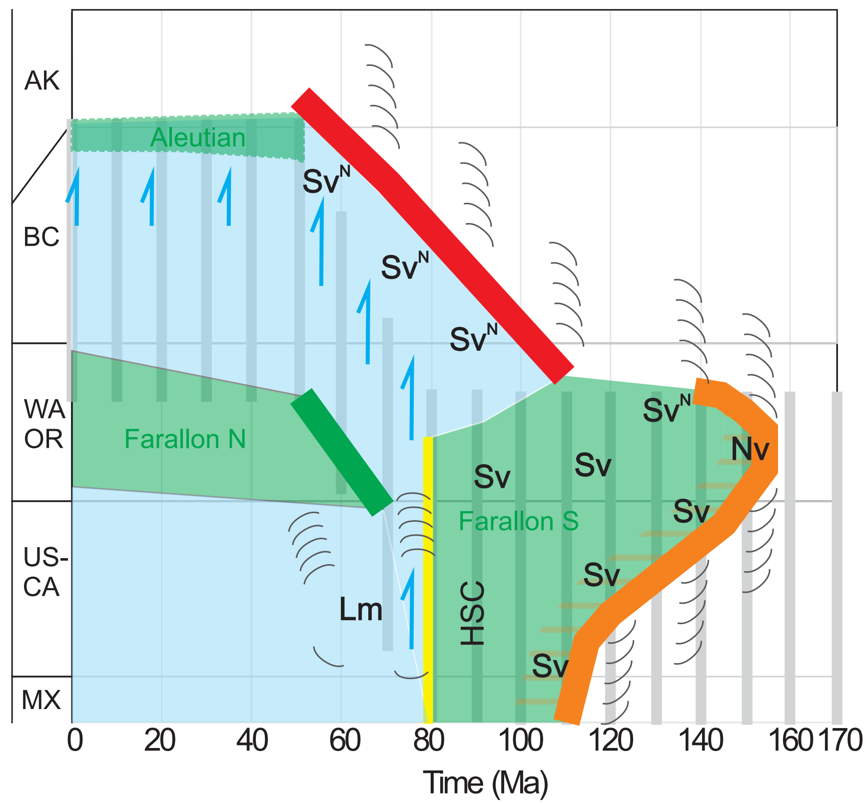

AK
BC
WA
OR
US-
CA
MX
Aleutian
Sv^N
Sv^N
Sv^N
Sv^N
Farallon N
Nv
Sv
Sv
Farallon S
Sv
Sv
Sv
Lm
HSC
0
20
40
60
80
100
120
140
160
170
Time (Ma)

Figure 7. Predicted and observed tectonic events along the NAM continental margin over geological time. The x-axis represents past time (in Ma), the y-coordinate is a distance measure roughly proportional to latitude, which runs the length of the western NAM margin, from northern MX to AK. The reference frame is stable NAM: a point in (x,y)-space represents, at time x, a coast-perpendicular swath at length y, from the immediate offshore to several hundred kilometers into the interior. A coast-proximal point on stable NAM over time runs on a horizontal trajectory (although outboard, translating elements in its swath may change); a vertical line represents synchronous events on and near the margin at fixed time x. Three separate layers of information are distinguished by the use of color. Layer 1 (margin): Colored areas represent the tectonic regime of the marginal plate boundary, as inferred by tomotectonics: white — quasi-passive margin, blue — transform boundary, green — Farallon or Pacific subduction zone, bold green, orange or red: override of an active arc on the CR, MEZ or ANG slab, respectively. Blue arrows are proportional margin-parallel motion during BajaBC times (fast) and its aftermath (moderate). Yellow line: Big Break.
Layer 2 (interior): Black elements denote geologically observed deformation in the hinterland of swath y at time x. Orogeny abbreviations: Nv – Nevadan, Sv— Sevier, SvN — Sevier North (Columbian), Lm — Laramide orogeny. HSC: Hess Shatsky Conjugate plateau. Scalloped symbols show extents of observed continental deformation (orogeny, DeCelles, 2004; Yonkee and Weil, 2015; Pană, 2021), which is interpreted to radiate to the hinterland and margin-parallel from the (colored) locations of arc- or plateau collision (Humphreys et al., 2025, this volume). Layer 3 (Insular microntinent): grey vertical bars represent the latitudinal extent of INS every 10 m.y. INS is located offshore while in the white (x,y) space and accreted while in a colored (x,y) space.

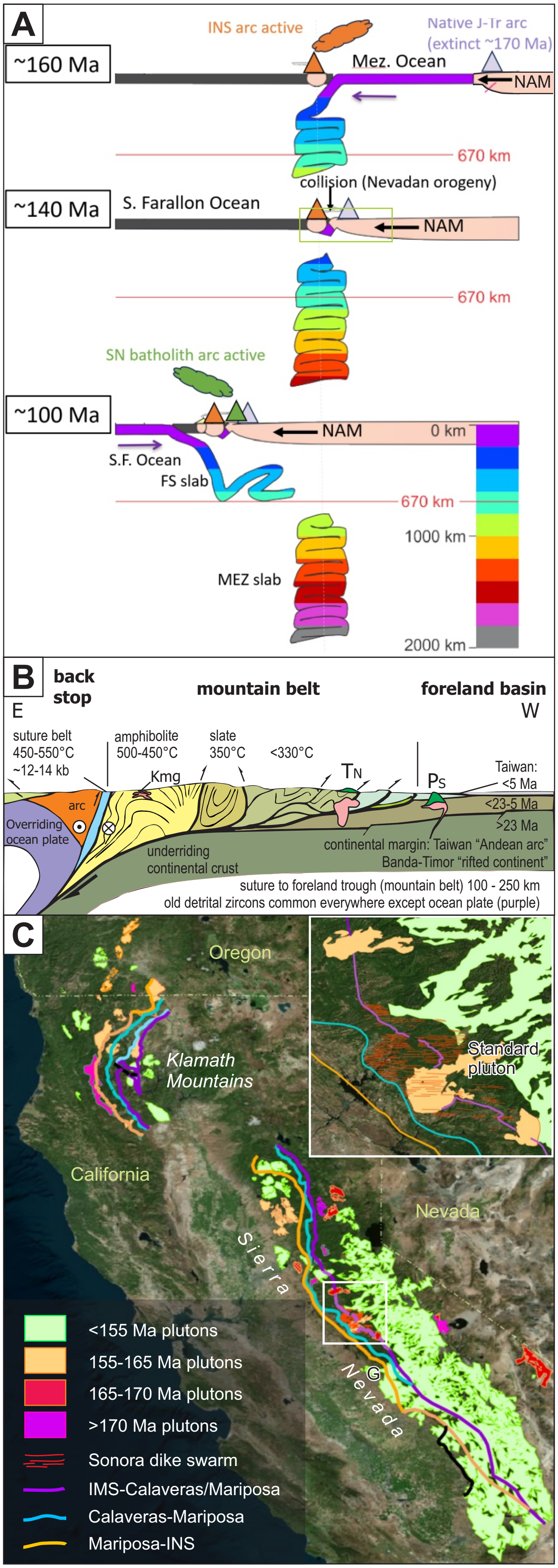
A
~160 Ma
INS arc active
Native J-Tr arc
(extinct ~170 Ma)
Mez. Ocean
NAM
670 km
collision (Nevadan orogeny)
~140 Ma
S. Farallon Ocean
NAM
670 km
SN batholith arc active
~100 Ma
NAM
0 km
S.F. Ocean
FS slab
670 km
1000 km
MEZ slab
2000 km
B
back stop
mountain belt
foreland basin
E
W
suture belt
450-550°C
~12-14 kb
amphibolite
500-450°C
slate
350°C
<330°C
Kmg
TN
PS
Taiwan:
<5 Ma
<23-5 Ma
>23 Ma
arc
Overriding ocean plate
underriding continental crust
continental margin: Taiwan "Andean arc"
Banda-Timor "rifted continent"
suture to foreland trough (mountain belt) 100 - 250 km
old detrital zircons common everywhere except ocean plate (purple)
C
Oregon
Klamath Mountains
California
Nevada
Sierra
Nevada
G
Standard pluton
<155 Ma plutons
155-165 Ma plutons
165-170 Ma plutons
>170 Ma plutons
Sonora dike swarm
IMS-Calaveras/Mariposa
Calaveras-Mariposa
Mariposa-INS

Figure 8. Collisional deformation since ~155 Ma, when NAM first rode into the intra-oceanic MEZ arc and welded it onto the continent's westward-subducting margin. **(A)** Progression of deformation in three time slices before, during and after suturing. **At 160 Ma**, arc magmatism above the westward-subducting Mezcalera Ocean, at the leading edge of North America (NAM), adds crust to the Insular Superterrane (INS) arc and lithosphere to the MEZ slab wall. Circa 155 Ma, the last of Mezcalera lithosphere is consumed between NAM and easternmost INS: NAM collides with INS microcontinent, resulting in the Nevadan orogeny **At 140 Ma,** deformation at the California margin and upward truncation of the slab wall. As NAM is still being pulled westward (by intact trench segments in and out of the figure plane), subduction polarity at the collided segment is forced to flip. **At 100 Ma,** subduction has flipped to eastward beneath the margin. Its slab, deposited by subduction of the Southern Farallon plate), creates an east-dipping blanket (100 Ma panel) as the trench is forced westward in front of advancing NAM. This subduction is building new, margin-hugging arcs that overprint the NAM-INS suture (including the Sierra Nevada batholith). Both north and south of the initial collision site, NAM continues to collide with microcontinental INS, resulting in widening Sevier deformation (Columbian orogeny in Canada).
(B) Generalized cross-section through a modern continent-beneath-arc suture, such as between Australia and Asia, Asia beneath the Philippine arc, or NAM beneath INS or ANG. This spatial zoom into the green box in the 140-Ma panel of A is based on a stylized cross section through central Taiwan (after Angelier et al., 1990; Beyssac et al., 2007; section oriented normal to the suture). All of these sutures show widespread distribution of units containing old detrital zircons, tectonically exhumed forearc (tectonically removed), and high grade, rapidly exhumed metamorphic rocks immediately inboard of the suture. Kmg is Cretaceous orthogneiss (Chipan gneiss) that has cooled through 240 °C in the past million years (Beyssac et al., 2007). P_S and T_N are volcanic (green) and plutonic (pink) representations of magmatic rocks of the Penghu Island group and of Tatun volcano (magma chamber imaged by Huang et al., 2021 has no perceivable connection to the mantle wedge), projected from south and north into the line of the section.
(C) Map of accretionary mélanges and plutons pertaining to the inferred Mezcalera Ocean suture between INS and cratonic NAM in California. Colored lines delineate two accretionary mélanges in the Sierra Nevada against their surrounding basement: Calaveras, associated with NJT/IMS arc on NAM; and Mariposa, associated with MEZ arc on INS. Cyan line traces the interpreted boundary between the two complexes. Schweickert (2015) maps the Calaveras complex in Sierra Nevada foothills as bordered by Mariposa Formation or similar strata of the Don Pedro terrane. An equivalent contact has not been identified in the Klamath Mountains, but possible traces are shown, based on the compilation of Dickinson (2008). Plutons are colored by age, see legend. The choice of age bins is hypothesis driven around events at 170 Ma (end of NJT arc) and 155 Ma (closure of the mélange basins), see text. Inset: zoom into the area of the ?extension-related, east-west-elongated Standard pluton (166 Ma) and Calaveras Complex, which are cut by the Sonora dike swarm (159-157 Ma) (after Schweickert, 2015). Pluton distribution and ages after (Ludington et al. 2007), except where superseded in California by Cecil et al. (2012) and Schweickert (2015). Pluton ages in Nevada are from John et al. (1994), Castellanos-Melendez et al. (2024). Paleozoic plutons are omitted.

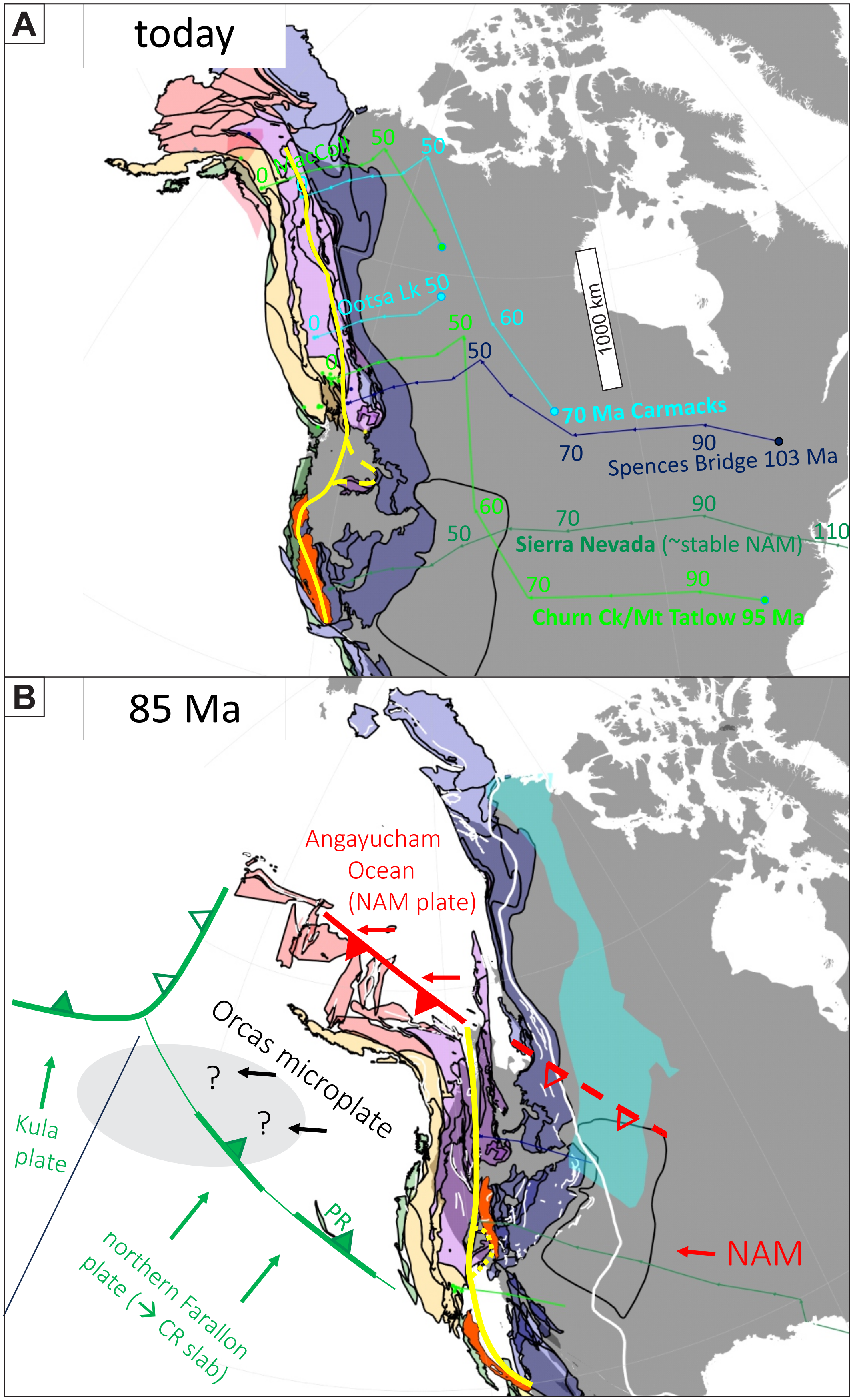
A
today
0 MacColl 50
50
Ootsa Lk 50
0
50
60
0
50
1000 km
70 Ma Carmacks
70
90
Spences Bridge 103 Ma
60
70
90
50
Sierra Nevada (~stable NAM)
110
70
90
Churn Ck/Mt Tatlow 95 Ma
B
85 Ma
Angayucham
Ocean
(NAM plate)
Orcas microplate
?
?
Kula
plate
PR
northern Farallon
plate (→ CR slab)
NAM

Figure 9. Margin-parallel terrane translations based principally on paleomagnetic data from Late Cretaceous and Eocene strata. These data constrain the tomotectonic terrane reconstruction model of Clennett et al. (2020), which is modified in the figures. (A) Present-day terrane map shows the current locations of a half-dozen units that are very robustly constrained. The green/blue lines, with nodes every 10 Ma and date labels (in Ma) at key times, represent the spatio-temporal trajectories into the past of these units, back to when they were deposited. A 1000-km scale bar is shown for reference. Trajectories are in absolute coordinates relative to the lower mantle, according to our Clennett et al. 2020 reconstruction. This reconstruction honors the displacement constraints of the most solid paleomag sites, Carmacks & Mount Tatlow/Churn Creek, but Spences Bridge is not honored since it does not fully pass the fold test. The model is based on globally derived apparent polar wander paths (APWP), which reach the same conclusion as for APWP derived solely from North American rock units (Housen, 2021; Tikoff et al., 2022). The *main* BajaBC translations are implemented 70-50 Ma along the yellow line, which runs mainly through Intermontane terranes (and their left-behind correlatives in the Blue Mountains/U.S.). This Baja-BC fault line is necessarily speculative, but it must run inboard of all paleomag sites that show significant offsets (details in section 6.2). The trajectory of the Sierra Nevada, illustrative of a non-translated site on stable NAM, is shown in dark green. Accreted superterrane packages follow the colour scheme of Figure 7; additional pericratonic blocks are colored dark and light purple.

(B) Tomotectonic reconstruction of the assembly of Alaska from Baja-BC and Angayucham terrane translations. This 85-Ma snapshot f the Clennett et al. 2020 model reconstructs the configuration of Baja-BC (comprising at a minimum the terranes west of the yellow line) at the onset of its northward sprint. The locations of the Angayucham (red barbs) and northern Farallon trenches (green solid barbs) are constrained by the ANG and CR slabs, respectively. The terranes of the then-active ANG arc (Koyukuk, future Central Alaska, in red) were welded into the Orcas microplate, but gradually being dislodged and rotated by the obliquely colliding NAM – the "Great Alaskan Terrane Wreck" of Johnston (2001). The northern Farallon arc terranes (Pacific Rim, PR, and others now underplating INS) were also intruded into the Orcas plate and slowly accreted against INS. During its northward sprint, Baja-BC effectively became part of the Orcas plate, separated from NAM by the "Baja-BC fault" (yellow line) or collection of faults.

Baja-BC passes *inboard* of, and unimpeded by, the CR Farallon trench, which still sits offshore. As NAM advances westward, Orcas is squeezed out toward the west or north. It may have subducted into one of two small slabs observed under the grey areas (see text). Due to the small size and mobility of the plate, its disappearance can be rapid, and the Baja-BC and Central Alaskan terranes on it are transported along (the "sprint" phase). As the Orcas seafloor subducts, the northern Farallon trench persists and makes landfall on NAM, becoming the continental Cascades arc by ~50 Ma, which shut off this northwestern passage for shuffling terranes. Baja-BC and Central Alaska collapse against each other and against NAM, completing the assembly of Alaska. The angle between the yellow line (paralleling the NAM margin) and the ANG slab (red line) sets the angle of the Alaskan orocline.

Tomotectonics of Cordilleran North America since Jurassic times: double-sided subduction, archipelago collisions, and Baja-BC translation

Karin Sigloch[1] and Mitchell G. Mihalynuk[2]
[1] Université Côte d'Azur, Observatoire de la Côte d'Azur, CNRS, IRD, Géoazur, 250 rue Albert Einstein, Sophia Antipolis 06560 Valbonne, France
[2] British Columbia Geological Survey, PO Box Stn Prov Govt, Victoria, BC, V8W 9N3, Canada

Abstract

Tomotectonics hindcasts paleo-trenches, through the spatiotemporal superposition of subducted lithosphere (slabs imaged in the earth's mantle) with plate reconstructions (constrained by seafloor isochrons). The two geophysical datasets are linked through the tomotectonic null hypothesis, that oceanic lithosphere sinks vertically down after entering in the mantle. This linkage permits simple and testable predictions about the location and lifespan of volcanic arcs, and specifically, about arc-continent collisions, switches in subduction polarity, and switches from consuming to transform plate boundaries. Tomotectonics uses land geological observations for validation. We explain the tomotectonic method, with a conceptual separation of its (geophysical) hypothesis-generating stage from its (geological) hypothesis-testing stage.

We generate a full suite of tomotectonic inferences for the North American Cordillera from the slab assemblage now occupying the mantle to depths of 1800-2000 km. We reason why this assemblage originated as a completely intra-oceanic archipelago, at a time of worldwide tectonic reorganization around 200-170 Ma, when the Atlantic began to spread, and the Pacific plate was born. The Archipelago was bounded by two sets of trenches that pulled in seafloor from the east/northeast and from the southwest. On the archipelago's western boundary, purely oceanic plate was consumed beneath intra-oceanic Farallon arcs; beneath the eastern boundary, ocean lithosphere attached to western North America was consumed, until none remained. The resulting collision between the continental margin and the eastern bounding arc (which was built on Insular Superterrane) was diachronous, commencing ~155 Ma (Nevadan orogeny), and continuing through the Sevier orogeny times. Upon collision, subduction polarity was forced to flip at the affected latitudes, so the pre-existing Farallon trench grew southward to accommodate the new kinematic requirement for eastward subduction. The new southern Farallon subduction produced arcs on the continental-margin, including the Sierra Nevada Batholith ~120-80 Ma.

Slab-free areas hindcast that this Andean-type margin at U.S. latitudes did not persist beyond ~80 Ma, and that it must have been followed by a dextral transform regime, i.e., by boundary conditions conducive to large-scale terrane translations. This transform regime ended when the northern Farallon arc, still sitting offshore until ~75-50 Ma gradually collided with the margin to become the continental Cascades arc. In the northeastern boundary arcs of future Central Alaska collided with the continental margin 90-50 Ma, and then gradually collided with the northern Farallon arc. Oblique override of these two oceanic arcs produced a range of collision styles, including the Baja-BC northward sprint and the assembling of Alaska. From its combined accounting of arc override events over the past 170 Ma, tomotectonics indicates large-scale northward displacement of Insular Superterrane since its accretion, in direct and independent support for the "Baja-BC" hypothesis of paleomagnetism.

1. Introduction

The term "tomotectonics" refers to a set of quantitative reasoning tools for reconstructing the paleo-geographies of regions shaped by subduction. Tomotectonics aims to account for all observations that record the processes of (paleo-)subduction, above and below the surface, and to reconcile them in a hypothesis-driven framework. Two types of observations play a fundamental role in that they generate the predictions of the tomotectonic method, and they feature in its name: "tomo" (for seismic tomography of subducted lithosphere in the mantle) and "tectonic" (for plate tectonics). These are largely geophysical observations, which are linked by a null hypothesis about vertical slab sinking that generates a shared, absolute spatial reference frame for slabs and plate motions.

Geological field observations play a different role: to test the tomotectonic predictions, and thus to reject or support the hypothesis. Pertinent geological observations are made in accretionary orogens, which are the surface products of the long-lived subduction processes recorded by the slabs. They contain the volcanic arc terranes that are directly and causally tied to the lithosphere that subducted. This paper applies the tomotectonic method to the North American Cordillera, inferring and evaluating its paleo-geographies since Jurassic times, which is the natural limit of scope in terms of confident geophysical observations, both for the mantle beneath North America and for the Farallon plate record surviving at the surface, on the oldest Pacific plate.

The strength of the tomotectonic approach is its particularly simple, strong working hypothesis, which describes the behavior of subducted oceanic plates once they have entered the mantle. With very few degrees of freedom, the vertical sinking hypothesis is highly predictive – and realistically falsifiable, the hallmark of a useful hypothesis. It does not follow that its falsification is easy in practice because the observational database of land geology is so complicated and incomplete. The essence of subduction is to remove its own traces from the surface into the subsurface. By contrast, the inventory of paleo-seafloor deposited in the mantle should be complete. That leaves the practical challenge of imaging it completely with seismic tomography, a domain where major progress has occurred over the past ~20 years (Earth Model Collaboration 2024, Hosseini et al. 2018, Pavlis et al. 2012).

Part 1 of this study, the prediction-generating part, consists of Sections 2-4 (Figures 1-6). Section 2 presents the relevant observations from mantle tomography and quantitative, global-scale plate reconstructions. Section 3 explains the tomotectonic working hypothesis of vertical slab sinking, which links the two data sets and renders them predictive. Section 4 carries out this predictive program by hindcasting paleo-trenches and their override sequences for North America.

Part 2 consists of Sections 5 and 6, which examine the predicted arc-building and accretion events in light of geological observations. Section 5 presents the validation principle: that every slab in the mantle predicts a (paleo-)arc at the surface, which should correspond with a geologically observed arc of suitable age, spatial extent and composition (e.g., continental versus oceanic). Equally important, every geologically known arc should be paired with a plausible slab in terms of location and depth. Section 5.3 re-runs the tomotectonic override sequence of Section 4.4 in order to spell out its predictions for the paired, real-world arc terranes.

We have been able to identify only one set of slab/arc matches that leaves no orphaned arcs or slabs and invokes no more complicated behavior than admitted by the tomotectonic null hypothesis (Sigloch & Mihalynuk 2013, 2017). It has generated significant debate because it predicts more intra-oceanic subduction and later accretion events (Late Jurassic to Cenozoic) for Cordilleran superterranes than more established interpretations (Monger & Gibson, 2019). On the other hand, the established interpretations have all been challenged from within geology as well (Moores 1970, Moores 1998, Johnston 2008, Hildebrand 2009, Schweickert 2015, Tikoff et al. 2023). Here we focus more on inferring large-scale transform motions from major structural breaks in the younger slab assemblage, and non-deposition – pertinent to "Baja-BC" displacements mostly between 80-50 Ma (Irving 1985, Enkin 2006, Kent & Irving 2010, and extending to 100 Ma according to Tikoff et al. 2023). Such displacements obscure preceding terrane accretions and are seemingly at odds with concurrent continental arc construction (Cowan et al., 1997). However, the mantle is very informative and provides a geometric solution to the Baja-BC conundrum.

The reasoning of Section 5 provides the skeptical reader with a template for proposing and evaluating alternative sets of slabs-arc pairings that satisfy the same observations and simple null hypothesis. Alternatively, the reader could envisage the level of mantle convection complexity required to link slabs to surface geology, and whether such complexity yields a predictive working hypothesis.

Section 6 discusses how all collision types in the Cordillera were shaped by double-sided subduction in one form or another: from the early head-on collision in the U.S./Sierra Nevada segment, to oblique collisions during the Sevier orogeny (Columbian orogeny in Canada) and predominantly transform Baja-BC translation.

In this Penrose Volume contribution, we continue to add tomographic tools for deriving past plate kinematics from tomographic images of subducted oceanic lithosphere. We specifically refine techniques for deciphering periods of transcurrent motion from the tomographic slabscape, applying these tools to the BajaBC debate. Section 7 provides a synopsis and considerations for guiding meaningful discussion and work in the future.

2. Observations for a tomotectonic reconstruction of Cordilleran North America

Tomotectonics makes spatial and temporal superpositions of two types of structures that are observable essentially by geophysical means:

1) The 3-D geometries of subducted oceanic lithosphere in the mantle ("slabs"), obtained from seismic tomography.
2) Quantitative reconstructions of plate motions across the earth's surface over time, mainly based on remnant magnetism of extant seafloor.

For North America (NAM) a superposition of slabs and plate motions for the past ~170 million years (Ma) is shown in Figure 1, which serves as a visual roadmap for this study. The translucent patches outline mantle regions (volumes) where subducted seafloor is observed at certain depths between the surface (0 km) and 1800 km. A first-order observation is that slab distribution is uneven, and that large regions of the mantle do not contain slab at any depth. Outlines of the NAM west coast trace the continent's westward drift over the past 170 Ma, as reconstructed by the "Global R" absolute reference frame (Torsvik et al. 2019). If in a thought experiment, a resident of Washington state on the U.S. west coast could be transported 130 million years (m.y.) back in time with the continent, the reconstruction of Figure 1 hindcasts that they would end up in a present-day latitude and longitude signaled by the "130 Ma" coastline, an absolute position that is presently occupied by Maine on the U.S. *east* coast.

2.1 Tomographically imaged slabs

Figures 2 and 3 render all slabs (or rather, seismically fast P-wave anomalies) in the teleseismic P-wave tomography model of Sigloch (2011), down to ~1800 km depth in the mantle (where this regional model loses resolution). Mantle imaging under North America made a quantum leap in the wake of the USArray Transportable Array deployment across the (western) U.S., when ~400 broadband seismometers rolled across the contiguous U.S. between 2004-2013 (Meltzer et al. 1999). In more recent tomographies, including global models that image deeper (Hosseini et al. 2018), the resolution under North America remains driven by the USArray data set. Other regional tomographies of North America can be inspected at the portal of Earth Model Collaboration 2024. The massive slab complexes to be discussed are well delineated in practically all post-USArray tomographies. Imaging differences or uncertainties persist mainly in the shape of less massive, upper-mantle slabs. Examples concern the spatial continuity of recently subducted Cascadia (Farallon) slab (see review of Pavlis et al. 2012), or the vertical delineation of old, stable continental lithosphere against slab in the transition zone below it (both are seismically fast).

Figure 2 renders two 3-D oblique views of the slab complex into which the Farallon (Juan de Fuca) slab subducts today. Slow seismic anomalies, which are proxies mainly for hotter-than-average mantle (e.g., Yellowstone), are not rendered but can be inspected in Sigloch (2011). We prefer these 3D iso-surface renderings to the more commonly seen 2-D depth slices ("red-blue" maps) because vertical continuity of structure is particularly important in tomotectonics. The disadvantage of oblique views is that their 3-D content cannot always be presented satisfactorily on 2-D paper. As a compromise, we show the same 3-D renderings in "map view", with the virtual camera pointing vertically down – as in Figure 3a, or up as in Figure 3B. With color as a proxy for depth, such "3-D map views" convey the vertical connectivity of structures, and easily tie to surface map overlays. The "inside-out" map view of Figure 3b renders the deepest (magenta) slabs in the foreground, unobscured by the blanket of shallower slabs. The deepest slabs (1100-1800+ km, yellow to magenta (maximum grey) levels) are very steep and spatially concentrated in linear belts. We call them "slab walls". By contrast, slabs above 1000 km show more lateral spread and are less clearly structured. To get oriented in the 3-D renderings, the reader may find it useful to match the slabs cartooned in Figure 1 with the 3-D slab observations in Figures 2 and 3. In section 4, we consider these slab geometries in detail, after discussing in section 3 how we propose to interpret their evolution over time and space.

That seismically fast anomalies (below lithospheric depths) represent subducted lithosphere has become a quasi-certainty as imaging resolution has improved over the decades. Lots of lithosphere is expected under North America from its subduction history, and at least recently subducted slab should remain tomographically visible. Indeed, fast anomalies are now unfailingly imaged in the upper mantle below subduction zones (e.g., the purple slab level beneath Cascadia in Fig. 2). These fast anomalies coincide with the band of seismicity produced within the slab in the upper mantle (<700 km depth), which ground-truths the tomographic detection of slab. The imaged anomalies usually continue below the deepest earthquake depths, and this satisfies *a priori* expectations from geologic or plate tectonic records of longer subduction histories (at least 180 m.y. in the case of the northern Farallon slab of Fig. 2). Finally, there is no plausible alternative for what the fast anomalies might represent other than cold, subducted lithosphere.

2.2 Quantitative plate reconstructions

The primary constraints on quantitative plate reconstructions come from paleo-seafloor spreading ridges. Their spreading histories are recorded as isochrons ("stripes") of alternating seafloor magnetization, which in principle permit very detailed and accurate reconstructions of relative plate motion circuits so long as plates can be linked through symmetrical paleo-spreading at ridges. The activity of trenches destroys these records by subducting the magnetized seafloor. Hence isochron-based reconstructions do not reach back beyond 100-200 Ma, but for North American reconstruction, the situation is very favorable. We require mainly the Atlantic spreading record, which is completely preserved back to Pangean times (>170 Ma, Müller et al. 2008). For eastward subduction, constraints are provided by an exceptionally long (>180 Ma) record of Farallon-Pacific spreading in the Pacific basin (Engebretson et al. 1985), although with the Farallon plate now subducted, we must rely on an assumption of symmetric spreading, which is well supported observationally (Müller et al. 1998).

Seafloor isochrons only permit reconstructing the paleo-plates' motions *relative to each other*. It is crucial to appreciate that the reconstruction of Figure 1 is delivered in *absolute* coordinates relative to the lower mantle. The lower mantle is chosen as reference because it is the most slowly changing among the earth's layers, moving 1-2 orders or magnitude more slowly than tectonics plates, i.e., millimeters per year, versus several centimeters or more. The absolute tie of relative plate circuits to the lower mantle is achieved via intraplate hotspot tracks: the entire lithospheric shell of the earth must be translated relative to the deeper mantle over time, such that in the reconstruction for time T, all seamounts dated to time T in the available hotspot tracks come to overlie the *present-day* positions of their generating hotspot volcano. The mantle plumes presumed to create the volcanic hotspot tracks are expected *a priori* to originate as upwellings from the lowermost mantle. Therefore, the reasoning becomes that hotspot tracks empirically yield the best available proxy for the quasi-stationary lower mantle. Indeed, the set of (Indo-Atlantic) hotspots is observed to have moved only very slowly relative to each other (<10 mm/yr) (Morgan 1983, O'Neill et al. 2005). The simplest explanation is that the hotspots do not move relative to the medium in which they are anchored, i.e., the lowermost mantle. The specification of "Indo-Atlantic" hotspots is important because North American paleo-positioning in Figure 1 is achieved relative to this well-behaved, near-stationary set of hotspots of the Pangean hemisphere. Pacific hotspots, whose stationarity is more questionable (Wessel & Kroenke 2008), are not needed and do not enter any of our reconstruction arguments. Pacific hotspots are not used to infer the sequence of North America drifting and override of the intra-oceanic archipelago that we infer from slab geometries.

3. The tomotectonic null hypothesis of slabs settling vertically

3.1 Predictive power of the vertical sinking hypothesis

Tectonic plates at the surface move horizontally, at typical velocities of centimeters per year relative to the lower mantle (or rather, relative to hotspots, our best proxy of lower-mantle motion). A way of defining vertical slab sinking is that a sliver of tectonic plate loses all of its horizontal motion soon after entering its trench, and subsequently moves only vertically down under the pull of gravity (Fig. 4A). An analogue would be a tablecloth draped too far over the edge of a table, and which starts sliding off the table under the pull of gravity. The part of the cloth still covering the table is moving horizontally, but at the table edge (the "trench"), its motion is abruptly converted into almost exclusively vertical motion, until all of the cloth has "subducted" off of the table, forming a folded pile on the floor below. For this change of the motion vector to occur, the tablecloth needs to be pliable; if instead it was stiff like a sheet of metal, motion vectors for portions above and astride the table would be identical. A defining characteristic of a tectonic plate is that it does behave like a stiff sheet at the surface, in principle not admitting internal deformation. Hence the vertical sinking hypothesis postulates that a plate entering the mantle in a subduction zone loses rigidity and deforms to follow only the pull of gravity, because stress transmission from its still-connected, surficial part has become ineffectual.

We first consider the utility of vertical slab-sinking behavior in paleo-geographic reconstruction that follows from the example of slabs beneath North America in Figures 1 and 3. The vertical-sinking hypothesis predicts that every latitude and longitude where slab is observed (at any depth) must once have hosted a paleo-trench, and its arc, at the surface. The slabs map out their own paleo-trench locations (vertically above them), although we need more information to determine when each trench was actively depositing slab. It is equally straightforward to hindcast the absolute locations where no trench was ever present, namely above the slab-free areas in Figures 1 and 3. No other method of inference provides such straightforward predictions of paleo-trench and -arc geometries. (In this paper, we variably refer to paleo-trenches or paleo-arcs in terms of predictions, sometimes interchangeably. Every subduction zone where plate is consumed must feature both a trench and an arc on the overriding plate – running in parallel, typically spaced by 100-300 km, which is a small distance compared to observational uncertainties in paleo-reconstruction. In the hypothesis-generating, geophysical sections 3 and 4, we typically refer to the paleo-trenches predicted (i.e., plate boundaries), whereas in the hypothesis-testing, geological sections 5 and 6, we refer more to paleo-arcs, as the most survivable and localizable record of the paleo-plate boundary.

The joint consideration of slab geometries with the continent reconstruction of Figure 1 extends the predictions to the type of plate boundary. Recall that the west coast in Figure 1 is reconstructed relative to the lower mantle. Under the vertical-sinking hypothesis, the (lower-mantle) slabs of Figure 1 have not moved laterally since entering their trenches. Hence the slabs and the continent are shown in the same, lower-mantle reference frame, and their absolute coordinates are directly comparable.

Under this hypothesis, the passage of reconstructed North America across the slab-scape in Figure 1 directly translates into a paleo-movie of the continental margin riding into a network of subduction zones. The trenches (slab-filled areas) can only have existed while the continent was not occupying their positions. By the end of the movie (0 Ma), all slabs must have been deposited in their observed positions, vertically below a network of paleo-trenches, the positioning of which must respect plate geometries and other plate tectonic rules. For example, if the orange, northern MEZ slab now located under the U.S. eastern seaboard sank vertically, it could not have been deposited after ~90 Ma because by that time, the continent was overlying all areas occupied by the slab. Hence no trench or arc younger than ~90 Ma can be assigned to those easterly absolute longitudes in a tomotectonic reconstruction. By the same argument, a paleo-trench must have been overlying, or migrating across, the absolute area now occupied by FS slab, and it must have been active before ~70 Ma, because by 70 Ma, the continent was overlying the entire area occupied by FS slab. Between ~170-155 Ma, the west coast traversed a slab-free zone, hence a trench along the west coast is not admissible for those times. For times more recent than ~155 Ma, increasingly large segments of the west coast overlap slab provinces (MEZ, ANG, FS), which means that a trench is required at those times and latitudes along the margin, Andean-style. If FS slab, for example, was laid down after ~130 Ma, then it must have been generated by eastward subduction; the sourcing of slab from west of FS would be inconsistent with NAM occupying this region by ~130 Ma. The vertical slab sinking hypothesis is testable in principle: if somehow, we could be sure that slab FS was deposited more recently than 70 Ma, we would have to conclude that the slab must have sunk significantly non-vertically, translated eastward in the mantle (unless the continental reconstruction was in error, placing NAM too far west).

3.2 The range of slab geometries generated by vertical sinking

There are two conditions for vertical slab sinking: (1) a plate must lose its rigidity upon entering the mantle, and (2) while sinking in the mantle, the slab does not get advected laterally by ambient mantle flow. These conditions may well be met, not perfectly but within the observational uncertainties. A crucial (tomographic) observation in this context is that slabs are much thicker than a single sheet of mature ocean lithosphere (i.e., much thicker than ~100 km) if they are located in or below the mantle transition zone, i.e., below ~400 km depth. Hence the question becomes whether the thickened slabs sink vertically within the observational uncertainties. We can limit the null hypothesis of vertical sinking to thickened slabs, since in tomography models, slabs appear ubiquitously thickened from the mantle transition zone down (Figs. 2 and 3).

This section considers the first condition of slab softening near the trench, leaving the second question of lateral entrainment to section 3.3. Historically, vertical slab sinking has served as the physically plausible starting position from first principles; deviations from it were considered as and when required by observations. The first-ever cartoon of subduction, published by Harry Hess (1965) and reproduced in Figure 4A, spells out vertical sinking beneath a moving trench. Hess conveys the concept of softening with clarity by envisaging a slab as a chain of viscous droplets, each of which should sink vertically if they are relatively dense and not entrained by pre-existing, lateral motion of the low-viscosity mantle through which they sink. The trench in Figure 4A has moved from points A to B, *relative to the mantle*, and Hess spells out how the ratio between trench velocity and slab sinking rate determines the slab dip angle: "If the overriding continent or island arc moved forward at the same rate that the current [i.e., droplet] descends then a plane dipping at 45° will represent the zone along which the motion is taking place." An unrealistic aspect of Hess' cartoon, published a few years before the plate tectonics breakthrough of his postdoc (Morgan 1968), is that the subducting plate does not actively converge onto the trench (zero motion relative to the mantle). Hence it has no horizontal velocity to lose upon entering the mantle, whereas actual subducting plates are typically observed to move trenchward several times faster than their overriding plates (Forsyth & Uyeda 1975, Cerpa et al. 2022). Figure 4, panels B-I explores the slab geometries predicted to result from vertical sinking as a function of the velocities v_{sub} and v_o of the subducting plate and overriding plates, respectively (keeping the slab sinking rate v_z constant in all scenarios). This regime diagram includes the most frequently observed regimes where v_{sub} is significantly faster than v_o or v_z (panels B, D, F and H).

The geometrically simplest case (Fig. 4E) is vertical sinking under a stationary upper plate and arc (v_o=0), with a relatively slow subducting plate. This results in a vertically dipping slab, which remains undeformed because the rate at which it enters the mantle is fully accommodated by the vertical removal of older slab through sinking: $v_{sub} = v_z$, with v_o=0. By contrast, the mantle entry rate in Figure 4D much exceeds the sinking rate ($v_{sub} = 2.5v_z$, a typical value for present-day subduction zones, Cerpa et al. 2022), and this excess of subducted lithosphere is accommodated by slab thickening ("shortening") – most likely through a folding process, as cartooned (Ribe et al. 2007, Stegman et al. 2010) or demonstrated by a tablecloth sliding off a table top. The result is a thickened slab that dips vertically, since the trench is stationary.

Vertical sinking under migrating trenches ($v_o \neq 0$) results in dipping slabs (Figs. 4B/C, F/G, H/I), the dip angle determined by the ratio between trench motion v_o and sinking rate v_z, as already noted by Hess (1965). Whether or not a dipping slab is thickened again depends on whether the slab entry rate exceeds the rate at which accommodation space is generated in the mantle. Not only slab sinking out of the way (v_z), but also lateral trench migration $v_o \neq 0$ contribute to accommodating the slab in this generalized scenario. The "traffic jam" conditions that result in slab thickening prevail in most present-day subduction zones (Cerpa et al. 2022): plate convergence is typically 50-100 mm/yr, of which only one half to one quarter can be accommodated by vertical slab sinking and lateral trench motion. Thus, thickened slabs are expected *a priori*, and are indeed observed: the slabs contoured in Figures 2 and 3 are several times thicker than a sheet of lithosphere, except immediately below the Cascadia trench (purple in Fig. 2).

We interpret the massive slab walls MEZ, ANG and CR/CR2 in Figure 3B to have formed similar to Figure 4D, and slabs FS and FN to have formed as in Figure 4F. Very rapid convergence in Figure 4H produces a flatly subducting slab, a regime which may apply to part of FS slab (Laramide flat subduction episode). While most slabs are predicted and/or observed to thicken, tomography cannot (yet) resolve their internal structure, e.g., the individual folds. For the slabs' continued sinking behavior, it makes no difference how exactly they thickened, but this likely happens by folding (as cartooned), a process shown to be viable and probable by numerical and physical experiments (e.g., Ribe et al. 2007, Stegman et al. 2010, Cerpa et al. 2022). The physics are those of a viscous thin sheet (lithosphere) encountering a semi-rigid backstop (the lower mantle) – commonly observed when pouring honey or cake batter.

Slab thickening is a viscous deformation process; at the depth where it is observed the lithosphere has lost its "plateness". For the currently subducting Farallon (FN) plate, thickening is observed ~400 km under the well-illuminated Cascadia trench (Fig. 2, or more clearly in Sigloch et al. 2008, their Fig. 1). While softening at 400 km depth is not the same as immediately after trench entry, the difference is small for paleo-reconstruction (even less when reconstructing arcs, which form above lithosphere that has already subducted 80-200 km). A massive slab wall should consist of many lithospheric folds, and the sheet from the trench down to the slab merely corresponds to the next limb to be laid down on the slab wall (Fig. 4D). The laying down of the limb implies non-vertical motion, on the scale of the lateral width of the slab wall (400-700 km). Hence the width of a slab wall represents a quantification of the deviation from strictly vertical sinking (in the upper mantle), and the resulting spatial fuzziness needs to be evaluated together with other spatial uncertainties concerning, e.g., the hotspot frame, plate reconstruction, or the shape of the continental paleo-margin before it encountered the arc, and changes thereof during collision or extension (quantified by Sigloch & Mihalynuk 2013, Supplementary Information). Reconstructing the paleo-arc centered above the slab wall probably entails 100-200 km of uncertainty (the arc might have been shifted towards the downgoing or the overriding plate). But this uncertainty is small compared to other interpretable geometries of interest, such as slab length along strike, or the slab-free gaps between two slabs. Despite the widened slab geometries, the overall slab-scape in Figure 3 remains highly structured, with individual slabs well separated.

3.3 The vertical sinking hypothesis for thickened slabs

The width of a slab wall signals and quantifies a moderate amount of non-vertical sinking in the uppermost mantle, associated with the thickening/folding process. Once a slab is thickened, it is not expected to undergo much additional lateral displacement during its continued sinking towards the core. The wider a slab (wall), the more massive it is and the more nearly vertically it is expected to sink because gravity, vertically down, is the only primary force driving mantle convection. Lateral mantle flow ("mantle wind") is a secondary effect that translates material between regions of (active) downwelling or upwelling. Even if lateral flows were pronounced, they are not likely to effectively entrain thickened slabs because those are the most massive sinkers in the mantle, and because the ambient mantle is less viscous and will therefore tend to flow around a slab in toroidal motion rather than carrying it along.

Lateral entrainment can be quantified by numerical modelling, although a fully realistic setup – 3-D spherical geometry; self-consistent, spontaneous plate formation and subduction rather than forced plate motions; sufficient rheology contrasts in the upper mantle to produce slab folding – remain beyond today's computational possibilities. Van der Wiel et al. (2024) found 2 mm/year average lateral displacement for 10-15 mm/year vertical sinking in the lower mantle, which translates to 266-400 km of lateral displacement while sinking through the lower mantle. As a caveat, their slabs did not fold nor thicken significantly until the lowermost mantle, biasing upward the lower-mantle value (of 2 mm/year) for lateral displacement. If folding had happened in the upper mantle as observed by tomography (and achieved in a 2-D model by Cerpa et al. 2022, through the implementation of an asthenosphere), then the resulting, more massive slabs would probably have incurred even less lateral motion in the lower mantle. In a physically much more approximate setup, Steinberger et al. 2012 also obtained several hundred kilometers of lateral slab displacement during sinking from surface to core. In summary, models are not fully realistic but point towards several hundred kilometers of lateral slab displacement while sinking through the lower mantle, which may still be an overestimate.

A strong observational indicator for vertical sinking, in both upper and lower mantle, is that the slab walls of Figure 3B have remained so vertical and structurally intact, despite their great "height" of >1000 km in places (MEZ, ANG) and their great age (proportional to the amount of lithosphere they contain). By far the simplest explanation for the formation of these slab walls is vertical sinking beneath a stationary arc-trench system (Fig. 4D). The alternative of non-vertical sinking (plus a non-stationary trench exactly compensating for this non-vertical sinking) seems contrived, especially considering the massive slab volumes that would need to have moved around laterally. To remain vertical into the lower mantle, entrainment into lateral flow could not have been significant without destroying the observed vertical wall geometries of Figure 3A/B.

We conclude that first-order considerations, observations and simulations all point to vertical sinking of slabs through the upper and lower mantle, with lateral deviations not exceeding a few hundred kilometers, a small amount relative to slab dimensions of 10^3-10^4 km. Most non-vertical sinking is probably due to the thickening (folding) process in the upper mantle, with the subsequent descent of thickened slab even more nearly vertical. While remaining a hypothesis, this proposition is likely to accrue more support from simulations and from tomotectonic analyses in other regions. Vertical sinking of lower-mantle slabs makes very strong predictions about paleo-geography at the surface. Even where predictions contradict widely held *interpretations* of Cordilleran geology, they are worth pursuing because the vertical sinking hypothesis is so plausible and because the resulting inferences arising from it are straightforward, detailed and geologically testable.

3.4 Vertical slab sinking not tenable for North America?

We have repeatedly encountered a perception that for the slab assemblage under North America, vertical slab sinking has been rejected conclusively. This would be correct only if framed by the current consensus interpretation of paleo-geography: "Vertical slab sinking beneath *an always margin-hugging Farallon trench* is untenable" – whereas for intra-oceanic subduction of the early Farallon and other plates, the question has not been asked. Tomographic interpretations that guided geodynamic models prior to Sigloch and Mihalynuk (2013) had not considered anything but margin-hugging Farallon subduction, and have indeed shown that vertical sinking under a margin-hugging, migrating trench would have generated slab assemblages significantly different from the observed (Lithgow-Bertelloni & Richards 1998) – more evenly spread beneath the continent, rather than concentrated in slab walls with strikes not resembling the contour of the ancestral western continental margin. Bunge and Grand (1997) attributed this mismatch to one specific episode of non-vertical sinking, namely flat subduction during Laramide times (they used ~70-40 Ma), although their numerical forward modelling did not actually produce the postulated, non-vertical sinking. Liu et al. (2008) did achieve highly non-vertical sinking for the same Laramide scenario, but only by replacing forward modelling of Farallon subduction with adjoint (inverse) modelling, and by additionally adopting an unusual mantle rheology *a priori*. Whereas forward modelling predicts present-day slab geometries by numerically subducting plates over a past time period, adjoint modelling solves for paleo-mantle structure at the simulation's starting time (tens of m.y. ago), by minimizing the misfit between observed and simulated mantle structure at present day. Specifically, Liu et al. (2008) investigated whether a paleo-mantle state could be found that was capable of driving sufficiently effective lateral flow to translate the Laramide Farallon slab eastward in the upper mantle (into the MEZ slab), given that the (margin-hugging) trench was too westerly to deposit MEZ slabs in forward models (Bunge & Grand 1997). Hence the adjoint model was basically asking for lateral slab displacement. It could in principle conclude that non-vertical sinking was physically possible *if all input boundary conditions (including paleo-trench locations) were correct*. It could not diagnose *whether* the simulated paleo-trench locations were correct, even less whether non-vertical sinking was actually required. For the same reasons, the adjoint modelling recently deployed by Fuston (2022) cannot diagnose that non-vertical sinking is required in the real mantle – unless it was certain that their *a priori* placement of paleo-trenches (for explaining Insular superterrane evolution) was correct. Note that we consider passage of a "flat slab" beneath western North America very likely for Laramide times (in geometric agreement with Liu et al. 2008, Humphreys, 2009; Humphreys et al., 2024). Formation of flat slab need not be restricted to low angle injection of ocean lithosphere, but can alternatively, and perhaps more commonly, be produced by *vertical* sinking combined with rapid lateral trench motion, Figure 4H/I.

Bunge & Grand (1997) or Liu et al. (2008) could not have envisaged anything but a margin-hugging Farallon trench, which justified their escalation from forward to adjoint modelling in order to obtain sufficiently non-vertical sinking. The Cascadia slab of Figure 2 had not yet been imaged, and thus the slab walls under the U.S. eastern seaboard and across Canada ("MEZ" and "ANG") appeared to be the only possible resting places for 180 m.y. of demonstrated Farallon subduction. For lack of additional slabs, MEZ-ANG slabs needed to be matched with the Farallon plate, and the trench must have been margin-hugging from plate kinematics as then understood. This situation fundamentally changed with the imaging of the Cascadia (FN/CR) slab into the lower mantle (Sigloch et al. 2008) – a slab that currently receives Farallon lithosphere and arguably always has (c.f. section 4). This discovery made it possible and necessary to question the margin-hugging nature of the (northern) Farallon trench, and to envisage additional intra-oceanic trenches (Sigloch & Mihalynuk, 2013). Hence it is natural to revisit the physically appealing and predictive hypothesis of vertical slab sinking under North America.

3.5 Uniformity of slab sinking

There is no need to hypothesize further specifics about slab sinking, and in particular, no need to stipulate sinking rates *a priori*. If deeper slabs are found spatially adjacent to shallower slabs, there is an intuitive expectation that the deeper slabs subducted earlier, because all slabs sank through essentially the same medium. We will occasionally use this expectation to arbitrate between two explanatory alternatives (e.g., for slab W), but there is no need to elevate this expectation to a part of the hypothesis. The slabs will turn out to embody this principle automatically, e.g., deeper slabs where trenches are known to have been in the deeper past.

There are many opportunities to *estimate* sinking rate from the slab geometries –we present some, and proper quantifications can be found in Sigloch & Mihalynuk (2013) and Mohammadzaheri et al. (2021). These estimates indicate that the slabs sank at ~10 mm/yr (±2 mm/yr), more or less everywhere across the Americas, which is a remarkably uniform result. It has led to misconceptions that tomotectonics *assumes* or imposes a sinking rate arbitrarily. To counter this impression, the present study limits mention of sinking rate, leaving it largely implicit in the tomotectonic observables. An explicit sinking rate is only needed when making an actual tomotectonic movie, where slabs grow at a rate commensurate with plate advances (e.g., Sigloch & Mihalynuk 2017; and as translated to map view in Figure 5) – in which case ~10 mm/year is the only value that "works" with vertical sinking.

We finish with a single striking observation that suggests a basically uniform sinking rate: the deep ends of the slab walls of Figure 3B all reach to 1800-2000 km depth, across the entire study domain. (The regional tomography of Figures 2 and 3 loses resolution around these depths, but global scale tomographies confirm 1800-2000 km as the deep ends of these slab walls (Hosseini et al, 2018). Below 1800-2000 km, copious volumes of slab are present into the lowermost mantle, but in geometrically different arrangements. This suggests a comprehensive and relatively sudden reconfiguration of paleo-trenches across the area, *plus a constant sinking rate across the domain*, otherwise the slabs that were deposited after the reconfiguration event (and which are the subject of our study) would not all have reached the same depth of ~1800-2000 km. What was this event? Section 4 will yield the answer without reference to a sinking rate, but at 10 mm/year, a slab depth of 1800 km translates to a mantle entry time of 180 Ma. This is the time when Central Atlantic opening started appreciably, setting North America on its westward drift, and also when the Pacific plate (and possibly the Farallon plate) were born – indeed a major reconfiguration that may have fundamentally reset paleo-Pacific subduction zones. These observations are all mutually consistent – supporting uniform slab sinking, as well as clear correspondences between deep mantle structure and known, major surface events. The slab breaks at 1800-2000 km depth thus provide a natural limit for the scope for our reconstruction. An older archipelago, below ~2000 km, is not as sharply resolved by tomography, and the uncertainties on absolute paleo-positioning at the surface (in absence of hotspot tracks) become unworkable beyond Jurassic times.

4. Tomotectonic reconstruction of North America

4.1 A western and an eastern slab complex under North America

We are ready to execute the predictive stage of tomotectonics. One by-product is Figure 5, which makes paleo-trench predictions by "transcribing" the slab-scape of Figure 3 using the tomotectonic null hypothesis. The tomography model is sliced into horizontal maps in depth increments of 100 km. At each depth, a paleo-trench line is drawn above every slab present and colored according to the depth-to-color scheme of Figure 3. For slab walls, it is easy to draw the inferred trench lines (centered inside the narrow slab). For the almost vertical slabs, the lines change little with depth, resulting in tightly clustered lines in Figure 5. For dipping slabs, the transcription is subject to larger uncertainties, and paleo-coastlines or interpolations may also be used, as will be explained.

The assemblage of slabs under North America clearly separates into two groups (Figs. 1 and 3): a Western Slab Group comprising slabs CR, W and FN; and an Eastern Slab Group, comprising slabs MEZ, ANG, and FS. Slabs within each group are spatially connected and separated from the other group by slab-free mantle. Figures 1 and 3A show a small overlap between the two slab groups (easternmost CR and westernmost FS), but only laterally, not in depth. This does not violate the vertical sinking hypothesis: the area hosted two different trenches, at different times. The older trench deposited the deeper CR, and the more recent trench deposited FS. The deepest slabs in both groups are slab walls (MEZ, ANG, deep CR), and they all reach to the same depth of 1800-2000 km (magenta to grey color level in Fig. 3B).

4.2 Tomotectonic reconstruction of the Western Slab Group (northern Farallon slabs)

The three slabs of the Western Group (FN, CR, and W) are jointly rendered in Figure 2. The view angle of Figure 2A emphasizes spatial continuity, making clear that the three slabs form a single system that slopes down to the east. By contrast, the view angle of Figure 2B highlights intra-slab breaks and structural divisions. Slab W is seen to be a separate fragment in Figure 2B, but clearly in a spatial correspondence with CR in Figure 2A. The subdivision of the main slab into FN and CR in Figure 1 may seem arbitrary from Figure 3A (FN is the upper-mantle part, corresponding to the purple, light and dark blue levels), but Figure 3B shows that this upper-mantle slab is almost "floating" freely, due to gaps towards the slab components surrounding it.

For visual clarity, Figure 2 masks out certain slab parts by comparison with Figure 3, which renders *all* seismically fast structure (below 400 km depth). Figure 2 omits the deep slab fragment CR2, west of today's west coast. It also masks out an upper-mantle slab that strikes east-west under southern Saskatchewan, Alberta and B.C. (dark blue in Fig. 3A), and which does not participate in the sloping continuity of the Western Group but rather seems to rest on top of it. (We later return to this slab as the speculated Orcas slab.)

4.2.1 FN slab – northern Farallon slab in the upper mantle, margin-hugging trench

"FN" stands for Farallon North. Near the trench, the slab must represent Farallon lithosphere because the Farallon (Juan de Fuca) plate is subducting into it today. Below the present-day coastline of the Pacific Northwest (PNW) in Figures 2 and 3, shallow slab is imaged beneath the active Farallon (Juan de Fuca) subduction, but neither north nor south of it. This provides a first reassurance that the tomography "works": a slab is imaged below a confirmed (present-day) subduction zone, no slab is imaged below adjacent non-subduction zones.

For depositing the upper-mantle slab FN to the east of the trench, a margin-hugging trench is the only plausible scenario i.e., a continuation of the present-day situation into the past. The continental margin gradually traversed FN slab over the past ~70 m.y. (Fig. 1), and FN slab shallows to the west (Fig. 2A). Westward shallowing is consistent with deposition of FN under a westward migrating (marginal) trench, so that easterly FN is deeper because it had more time to sink, as in Figure 4F.

Magnetic isochrons on the Pacific plate trace the growth of the (northern) Farallon plate from ~180 Ma to 0 Ma (Atwater, 1989; Engebretson et al., 1985), spreading towards the Western Slab Group. Since these slabs represent the paleo-trenches closest to the reconstructed Pacific-Farallon spreading ridge over time (e.g., Engebretson et al., 1985; Seton et al., 2012), and since Farallon plate is still subducting into this slab today, the Farallon plate must have subducted into FN in the past as well.

In summary, FN holds Farallon lithosphere, and today's Farallon trench is built on the continental margin. The margin's eastward progression back into the past in Figure 1 matches the FN slab's eastward down dip: everything points to a margin-hugging trench in the past as well.

4.2.2 CR slab – northern Farallon slab in the lower mantle, intra-oceanic subduction

At first glance, lower-mantle CR slab (turquoise levels and below in Figures 2 and 3) seems to smoothly continue the downward dip of FN slab (with a margin-hugging Farallon trench as the explanation), but there are serious problems with this proposal. With increasing depth, CR slab appears increasingly spread out laterally in Figure 2A because at those depths CR is no longer dipping east. Rather it has steepened into a slab wall and rotated counterclockwise relative to FN and the coastline, with its long axis striking NW-SE (especially clear in Fig. 3B). If the deep CR dips at all, it is to the west, in the "wrong" direction for subduction beneath a west-migrating continental margin. Deposition of the voluminous slab wall portion of the CR required a stationary trench striking highly oblique to the coastline (Fig. 1). At yellow/green depth levels in Figures 2 and 3, the CR slab looks segmented and complex, including the detached fragment W – again, not a good match to the paleo-coastline.

CR is much more voluminous than FN, requiring a trench that dwelled in the area, but the coastline did not dwell: by >80 Ma, it shows no overlap with CR slab in Figure 1. The northern Farallon plate was spreading since >180 Ma, requiring the continental margin outlined in Figure 1 to leave the CR slab 100 m.y. too early to be consistent with the widely held idea of (northern) Farallon plate subducting since its inception (~180 Ma) under North America. Prior to 80 Ma, the NAM margin in Figure 1 traverses the slab-free zone to the northeast of CR, which for tomotectonics implies no trench along the margin. Finally, CR2, an isolated slab as deep as CR, is present just offshore the present-day west coast in Figures 3A and 3B – further west than the margin ever was – so that CR2 cannot be due to vertical sinking under a margin-hugging trench.

The inevitable conclusion is that CR and CR2 cannot have been deposited into a margin-hugging trench by vertical sinking, unlike FN. Therefore, prior to about 80 Ma, the northern Farallon trench must have sat *offshore* the NAM west coast, or in absolute coordinates, NAM sat well east of the stationary Farallon (CR) trench. Jointly, FN and CR are voluminous enough to account for the observed 180 m.y. of northern Farallon spreading and subduction.

Hence, by coincidence, FN is not only the upper-mantle part of the northern Farallon slab, but also the part that was deposited by an Andean-style (Cascades) trench. CR, the lower-mantle Farallon slab, was deposited by an intra-oceanic trench. The geometric complexities at intermediate depths of CR presumably reflect the prolonged, oblique override of CR by NAM which gradually "accreted" the CR Farallon trench. A corollary of this tomotectonic prediction is that before 80 Ma, the Farallon trench sat offshore at Pacific Northwest latitudes. This has many implications, including that Baja-BC terranes could have shuffled northward *inboard* of this trench (section 5).

In terms of trench lines for Figure 5, the deep slab wall of CR is easy to transcribe (compare to Fig. 3B). For the dipping FN slab, paleo-coastlines were equated to trench lines since a margin-hugging trench has been inferred. The intermediate-depth (turquoise) trenches above the fragmented, rotating slab were drawn as best guesses/interpolations, and they are almost certainly too simplistic. The strikes of trenches drawn above W are guesswork since the slab lacks a clear strike, and we do not fully understand W's functioning relative to CR. The very deepest (magenta, grey) trench levels of CR are also guesswork – were the two separate slab walls originally connected into one long, E-W striking slab (Sigloch & Mihalynuk 2013)? The strike and shape of the offshore CR fragment is not well imaged. The overall complexity of the Western Group is real and not an imaging shortfall – much of its paleo-geographical meaning remains to be deciphered.

4.2.3 AL slab – intra-oceanic and most southerly Farallon subduction

The Alisitos (AL) slab is a stunted slab wall of ~300 km "height", occupying depths of ~1400-1100 km in the mantle, which strikes perpendicular to MEZ slab wall, extending 2400 km westward from Yucatan to offshore southern Baja. The AL slab lies outside the mantle volume illuminated by the regional tomography of Sigloch (2011) and is therefore not visible in Figure 3, but it is robustly resolved by global tomographies (e.g., Hosseini et al. 2020). AL slab reaches less deep than CR, which initiated at >180 Ma, but deeper than southern Farallon (FS) slab, which initiated ~130 Ma. The AL slab completed the line of Farallon offshore trenches (together with CR, C2) that closed off the archipelago towards the west (Fig. 5B), prior to the inception of FS trench.

4.3 Tomotectonic reconstruction of the Eastern Slab Group

4.3.1 FS slab – southern Farallon slab in the transition zone and lower mantle

The Eastern Slab Group consists of FS, MEZ and ANG slabs. FS should have subducted more recently than MEZ and ANG, due to its more westerly and shallower position. The paleo-coastline of Figure 1 traverses FS from ~130 Ma (±15 Ma) to ~75 Ma (± 10 Ma), so deposition must have concluded by the later date. The slab occupies the same depths as lower FN and intermediate CR, for which we have inferred similar ages.

FS slab features a linear, sharp truncation towards its southwest, where the mantle becomes slab free. This truncation (yellow line in Fig. 1, the "Big Break") approximately coincides with the strike of the paleo-coastline at ~75-80 Ma. The simplest explanation for this coincidence is that the FS trench was built on the margin, and that (vertical) deposition into this marginal trench suddenly stopped at 75-80 Ma. The slab's elongation in WSW-ENE direction, which is the direction of margin advance, likewise suggests that FS was deposited beneath the migrating NAM margin.

In Figure 3B, FS slab tends to deepen toward the east (and the south), albeit irregularly. This also points to deposition below the migrating margin: easterly FS slab regions have had more time to sink. The gentle overall dip of FS suggests that its trench migrated relatively rapidly: FS slab geometry best corresponds to Figure 4H, where the slab flattens in and below the transition zone.

An eastward-subducting, margin-hugging trench during Cretaceous times, just south of the northern Farallon system, must be another Farallon trench. The reason is cartooned in Figure 6. When Farallon-Pacific (FAR-PAC) spreading was still nascent (time 170 Ma), the associated spreading ridge segment was short (as recorded by Pacific isochrons), so the CR slab is wide enough latitudinally to account for the young Farallon plate (Fig. 6A). But over Cretaceous times and by 80 Ma (Fig. 6B), the FAR-PAC ridge had extended southward (Atwater, 1989; Engebretson et al., 1985), too far to be accounted for by CR slab only – since CR slab visibly did not grow southward. Hence an additional Farallon trench segment must have developed to the south of CR. In fact, FS slab exactly mirrors the lengthening of the Farallon spreading ridge by a commensurate lengthening of the trench: FS starts out at a very narrow coastal trench between 150 and130 Ma but widens southward to underlie much of the U.S. and Mexican paleo-margins before the 80-Ma coastline reaches the Big Break.

In summary, all aspects of FS point to subduction of the southern Farallon plate over the Cretaceous period (roughly 150-75 Ma), beneath the NAM margin. Figure 6B sums up Farallon subduction shortly before the Big Break: beneath the continental margin of Mexico and California, but still offshore in the Pacific Northwest.

4.3.2 Slab-free window between the present-day margin and FS slab

Next we consider the significance of the slab free area southwest of the Big Break in Figure 1, extending from FS slab to the current margins of southern California and Mexico. South of the northern Farallon/Cascadia trench, a dextral transform plate boundary runs along the *present-day* margin (the San Andreas system). From Pacific isochrons, Atwater (1970) inferred this transform system back to ~30 Ma, to the reconstructed "landfall" of the PAC-FAR spreading ridge on the margin.

Tomotectonics can diagnose the existence of this same transform regime from the absence of slab beneath the present-day margin (indicating that it is not a trench; and a continent-ocean boundary cannot be a spreading ridge either). However, Figure 1 shows that the slab-free window extends eastward from the coast not only to the 30-Ma paleo-coastline, but all the way to the Big Break, which corresponds to the ~75-80 Ma coastline. Hence tomotectonics hindcasts that a transform plate boundary has held sway along the Californian and Mexican margin since ~75 Ma, when the margin-hugging southern Farallon (FS) trench suddenly shut down at the Big Break event.

Slab W (traversed by the coast ~20-50 Ma) might signal a localized, temporary interruption of this transform regime, but it is unlikely. We noted that slab W is deep and blends into the overall geometries of CR, hence it likely represents older subduction. If slab W does not interrupt the subduction-free period after the Big Break, then the current San Andreas regime along the margin is in full spatial and temporal continuity with the transform regime of ~50-80 Ma that was inferred from rock paleomagnetism to have transported the Baja-BC microcontinent northward (Irving, 1985; Kent & Irving 2010). This is a straightforward consequence of the wide slab-free window, combined with the vertical sinking hypothesis.

4.3.3 MEZ and ANG slab walls

MEZ slab is among the longest and most voluminous slabs in the whole mantle. It is an enormous slab wall that runs from northeast Canada to Florida under the NAM eastern seaboard, and from there on to Peru (Fig. 1). MEZ wall is >1,000 km "high" under Florida (occupying depth levels ~1800 km to ~800 km in the mantle column, Fig. 3), but only ~300 km "high" under Nova Scotia (occupying ~1800-1500 km depth).

MEZ lies in spatial eastward continuation of the southern Farallon (FS) slab and continues the eastward-deepening trend, although at a dramatically steeper angle than FS. The intuition might thus be that MEZ represents Farallon plate older than FS. Tomotectonics indicates that this cannot be the case.

The deposition of a voluminous, linear slab wall requires a trench that remains stationary above MEZ for a long time (Fig. 4D). By contrast, the paleo-coastline in Figure 1 marches right across MEZ (and ANG) without dwelling on the slab and without showing any correspondence with the slab's shape. In reverse time, NAM leaves behind FS slab by ~130 Ma. By 155 Ma, the margin leaves behind the eastern promontory of MEZ slab wall and traverses only slab-free mantle until 170 Ma – the temporal limit of our study, when the NAM east coast has reunited by with Pangaea and the Central Atlantic closed (see Fig. 6A).

The swift and oblique march of the west coast across MEZ means that a *margin-hugging* Farallon trench could not have deposited the slab wall by vertical sinking. What about a stationary, offshore Farallon trench, as observed in the case of CR? The problem with eastward (Farallon) subduction into MEZ is that it would prevent NAM from moving westward, away from Pangea, between 170 Ma and the moment it reaches MEZ (which is ~155 Ma at the MEZ promontory, and later further south). The slab-free zone between MEZ and NAM at 170 Ma is occupied by seafloor at the paleo-surface, and this seafloor must subduct in order to let NAM move westward (Fig. 6A). The only slab available to subduct into is MEZ, which means *westward* subduction of the seafloor between Pangaea and MEZ, into MEZ trench.

MEZ slab could, therefore, not have hosted an eastward subducting trench at the same time, meaning no Farallon trench, not even an intra-oceanic one. This is the decisive argument against MEZ as a Farallon slab. Westward subduction into MEZ solves other problems: the huge latitudinal extent of MEZ does not match the short isochron segment of the FAR-PAC spreading ridge recorded for Jurassic times (Fig. 6A). The FS slab, narrowing then disappearing to the east, already explains the history of southern Farallon growth.

By contrast, the north-south extent of MEZ is of the correct length and strike to let all of North America break free from Pangaea at once, and to start significant westward drift by ~170 Ma. The northern MEZ segment from Nova Scotia to Florida closely matches the Central Mid-Atlantic spreading ridge in length and strike, and from 170 Ma to today. The situation is cartooned in Figure 6A, which highlights (in blue) the seafloor west of NAM that needs to subduct into MEZ (and ANG). ANG slab served the same role as MEZ, enabling NAM to move west. MEZ trench pulled on the NAM margin at U.S. and Mexican latitudes, whereas ANG pulled on the B.C. margin. As required for this functioning, ANG slab wall is the spatial northwestward extension of MEZ, and very similar in character. ANG strikes oblique to the paleo-margin, and it reaches far to the west. This means that the margin took a very long time to override ANG slab – in Figure 6B, its trench is still pulling on the northern margin at 80 Ma, when MEZ has long been overridden.

4.4 Chronological sequence of archipelago override

Pulling all tomotectonic inferences together, we play forward the "movie" of continent-trench collisions, using Figures 1, 3, 5 and 6. All trenches start up around the same time (same depth of ~1800-2000 km), while NAM is still with Pangea, i.e., between 200 and 170 Ma (Fig. 6A). All trenches are originally intra-oceanic in the proto-Pacific basin west of Pangaea, where they are free to remain stationary and to build the observed slab walls MEZ, ANG and CR.

MEZ and ANG trenches are exerting a westward pull on the NAM plate, whose western plate boundary is not the continental margin but an ocean basin (the "Mezcalera-Angayucham Ocean" in Fig. 6A). From ~200-170 Ma, the Central Atlantic rifts along a line parallel to northern MEZ slab. Central Atlantic rifting transitions to proper spreading ~170 Ma (recorded by Atlantic isochrons, e.g., Seton et al. 2012). The Atlantic opens at the expense of the Mezcalera-Angayucham Ocean, which narrows by westward subduction into MEZ and ANG slabs.

Around 155 Ma, the NAM west coast at U.S. latitudes starts to collide with the northern MEZ trench, under-riding the MEZ arc and deforming the margin (orange barbs in Fig. 1). The collision gradually spreads in latitude as broader swaths of MEZ arc (and later ANG arc) are overridden (Fig. 1, coastlines at 130, 110 Ma). The gradual override of northeastern MEZ slab ~155-110 Ma is recorded by the westward shallowing slab "ramp" it forms in Figure 3A: under the 150-Ma paleo-coastline, the slab had 150 Ma to sink since the end of subduction, and its upper truncation now lies ~1500 km deep (red level of the 3-D isosurface in Fig. 3A); under the 110 Ma-line, its shallowest part lies 1100 km deep (yellow level) and has been sinking for 110 m.y. (This ramp is among the best opportunities to estimate slab sinking rate, Sigloch and Mihalynuk, 2013). In Figure 5, the slab ramp translates to trench lines on northern MEZ "retreating" westward, from pink to red to yellow levels: no more trench where the Mezcalera Ocean has disappeared.

At conterminous U.S latitudes, subduction cannot cease with the consumption of all Mezcalera Ocean lithosphere because NAM continues to be pulled westward, by still-active trenches of northern ANG and southern MEZ. NAM is pulled into the area presently underlain by eastern FS slab, which forced the ocean lithosphere occupying this absolute position beneath the advancing U.S. west coast, depositing FS slab. Hence subduction polarity flips along the California/Mexico margin: NAM margin turns into the overriding plate (green barbs in Fig. 1), with Farallon plate subducting underneath it. MEZ and ANG trench segments shrink while FS trench grows along the margin. CR trench (northern Farallon) sat in the same stationary, intra-oceanic position the entire time.

At 80 Ma (Fig 6B), these override events have run their course, and things are about to change. The southern Farallon (FS) trench on the margin abruptly shuts down ~80-75 Ma and will never be re-established (Big Break of FS slab). A transform system takes over that persists to present-day (San Andreas), as signalled by the slab-free corridor southwest of FS slab. The reason for this shutdown of the continental arc is not obvious, perhaps related to the beginning, oblique collision of NAM with northern Farallon (CR) arc -- or to plateau subduction (Livaccari et al., 1981; Humphreys et al., 2024) which cannot be inferred purely tomotectonically. At the end of a protracted override (recorded by the fragmentation of upper CR slab), the seafloor that remained between CR trench and NAM in Figure 6B has been squeezed out, and the northern Farallon trench has "accreted" (by ~50 Ma). It continues as the margin-hugging Cascades trench that is still active today (FN slab).

In the far north, ANG arc is under-ridden by NAM very gradually and obliquely into Cenozoic times, always by westward subduction. Once ANG subduction is completed, the northern margin turns into the transform system in B.C. that continues to the present day (slab-free area between northwestern ANG slab and present-day margin).

5. The match between tomotectonic arcs and geologic arcs

So far, we have used only the tomotectonic observables of slab geometries and quantitative plate reconstructions for making the paleogeographic inferences of Section 4; these are linked by the null hypothesis of slabs sinking in the absolute positions where they entered the mantle. Geological observables remain an untapped, independent data set for testing the tomotectonic hypothesis and its predictions.

The principal link for hypothesis testing is the volcanic arc, which is an inevitable surface manifestation of any subduction zone. Tomotectonics hindcasts absolute paleo-arc locations: above the observed slabs. If the tomotectonic method works properly, every paleo-arc predicted from slab should have an observed counterpart in the accretionary orogen. The converse is equally important: every geologically observed arc should be matchable to a suitable "tomotectonic arc", i.e., a slab.

Figure 6 shows the large-scale assemblage of arc terranes since ~170 Ma that need to be explained along the present-day west coast of North America (left part of the map). Terranes are grouped into belts of superterranes, based on shared characteristics of their basement terranes. Furthest north and west are the Jura-Cretaceous arcs of Central Alaska (colored red). South of them, several superterrane belts run parallel to the continental margin. From outboard to inboard they are the Farallon terranes (green); the Insular (INS) and Guerrero (GUE) superterranes (orange); the Intermontane Superterrane (IMS) and the basement of the "Native" arc (purple), both of which hosted a Triassic-Jurassic arc that shut down almost simultaneously on IMS and Native arc ~170 Ma (e.g. Mihalynuk et al., 2004; Dickinson, 2008. Given that our reconstruction starts at 170 Ma (incipient westward drift of NAM), the IMS-Native arc is too old to be associated with a slab, but it is inseparable from arguments about Insular arc because they are now juxtaposed across a suture and their activity periods overlapped at times before 170 Ma (INS Mesozoic arc started ~205 Ma; Canil and Morris, 2024). IMS was an intra-oceanic arc but for our argument it is tectonically equivalent to NAM because it had accreted to the NAM margin by ~170 Ma, before the start of the reconstruction. The cyan belt running between INS and IMS, or INS and stable NAM, is a belt of collapsed basins of oceanic character, interpreted to mark the suture of the Mezcalera Ocean.

The color scheme for the superterranes reflects their basements, as opposed to reflecting the most recent arcs intruding into those basements (which would leave most terranes green, since intruded by recent Farallon arcs). This color scheme was chosen for a visual match of each geological arc terrane to the temporally *first* slab to have caused arc magmatism on them since 170 Ma.

The right part of Figure 6 schematically reconstructs the four superterrane groups (Farallon, INS-GUE, Central Alaska, IMS-Native) above their matched slabs, hence the absolute paleo-positions where these arc terranes grew, according to tomotectonics. At the outset, before 170 Ma, the MEZ slab wall (orange) as associated with Jurassic-aged arc on the INS-GUE microcontinent; the ANG slab wall (red) is host to the Central Alaskan Jura-Cretaceous arc terranes; the CR slab wall is associated with oldest Farallon terranes. A first plausibility check is that the relative positions of basement terranes above slabs reflect their relative spatial relationships at present: Central Alaska furthest north; Farallon outboard of INS, and INS outboard of IMS/Native arc; and GUE south of INS.

As time progresses, these slab walls correlate with arc magmatism that continues into Cretaceous times, until the regime changes because an arc is overridden by NAM, or because a terrane is "handed over" to a different, younger slab, or evolves into a transform regime. As they accrete to western NAM, older arcs (INS-GUE, IMS-Native) arcs are predicted to be overprinted by younger (FS, FN) arcs as archipelago override progresses (Section 4.4). It is crucial to expect and recognize such arc juxtapositions and successions in the geologic record of a given terrane when assessing the accuracy of tomotectonic predictions.

The set of slab-to-arc matches presented in Figure 6 will arguably yield the “correct” solution, in the sense that the archipelago override sequence, hindcast by tomotectonics in Section 4.4, will terminate with the spatial configuration of today’s Cordilleran accreted terranes, and will satisfy the geologically known timing constraints on arc magmatism and margin deformation, which are presented in Figure 7. Moreover, the association of the Jurassic arc on INS with northernmost MEZ slab wall, which we argue is inevitable to honor geological constraints (and vertical sinking), will be shown to also honor (and in fact independently predict) the paleomagnetic observations of large northward displacements of INS relative to NAM.

To justify the matches of geological arcs to tomotectonic arcs (i.e., slabs) of Figure 6, we proceed from younger to older as in section 4, from more certain Farallon arcs and slabs (section 5.1) to older arcs that can be paired with the deep, eastern slab walls MEZ and ANG.

5.1 Northern and southern Farallon arcs (eastward subduction)

5.1.1 FN slab paired with the Cenozoic, margin-hugging Cascades arc

The northern Farallon slab (FN), still subducting into the upper mantle, clearly must be matched with the Cenozoic, still active Cascades arc. From FN slab's connection to the active trench and eastward dip, the tomotectonic inference (in section 4.2.1) of an arc built on the NAM margin might seem trivial, but recall that the margin-hugging character of this arc was hindcast to be limited to Cenozoic times, i.e. relatively recent -- despite the observation that both the slab and the Farallon isochrons on the Pacific plate reach to much more older times. The prediction of a recent Andean-style arc instead followed from the vertical sinking hypothesis, because in Cretaceous times NAM was located too far east for vertical deposition of the deeper (older) Cascadia slab CR under a hypothetical margin-hugging trench. It is therefore an important observation that the observable Cascades arc is no older than 47 Ma (du Bray et al, 2014;

Dragovich et al., 2016; Tepper and Clark, 2024; with a continuous arc axis is only apparent since ~40 Ma, see Fig. 1 of Glazner, 2022; or ~45 Ma, Humphreys and Grunder, 2022) -- consistent with the tomotectonic prediction of absence of earlier continental arc, but presence of intra-oceanic CR arc in this absolute location back to ~180 Ma. While proponents of a much longer-lived northern Farallon arc might invoke it covered under Columbia River basalts or translated north on BajaBC terranes, the fact remains that observations at present do not seem to require an arc built on the continental margin of the Pacific Northwest margin beyond ~50 Ma, consistent with tomotectonic inference.

5.1.2 CR slab paired with intra-oceanic northern Farallon arcs aged ~180-50 Ma

This lower-mantle slab wall predicts the presence of intra-oceanic, mature arc terranes oceanic arc, both due to its considerable volume (Fig. 2), a proxy for subduction duration, and because the associated, northern Farallon isochrons reach ~180 Ma. The geologic record preserves only a limited number of suitably old and oceanic arc terranes to associate with CR slab. The CR arc may be best preserved in the subsurface beneath Vancouver Island (Clowes et al., 1987) as the downdip extent of the Pacific Rim terrane ("PR" in Fig. 7; Sigloch & Mihalynuk 2013, 2017).

Other parts of CR arc may have been entrained and transported north with BajaBC, of which Vancouver Island is the trailing southern end. During the margin-wide dextral transform regime predicted by Figure 1 for ~80-50 Ma (section 4.4), intra-oceanic CR arc would have sat outboard of the translating fault(s) and hence expected to be carried north. The successor of this transform regime continues to today, albeit at a slower rate (e.g., Baranov-Leech River hypothesis of Cowan, 2003; Garver and Davidson, 2015). That such a big and old slab has only fragmentary arc relics illustrates some practical challenges in making slab/arc matches. However, this is equally true for any accounting of pre-Cascades subduction in the Pacific Northwest (PNW) from geology or plate tectonics alone. FAR-PAC isochrons record Farallon spreading towards the PNW since 180 Ma, irrespective of mantle evidence. If the pre-Cascades arc were postulated to have grown on the margin, the problem of the "missing" arc would be aggravated because a margin-hugging arc should not be displaced as easily as the intra-oceanic CR arc inferred from tomotectonics.

5.1.3 Aleutian slab paired with Aleutian arc

For completeness, the Pacific plate subducts northward beneath southern Alaska today. This subduction zone has been building the upper-mantle Aleutians slab (Gorbatov, et al., 2000; van der Meer et al., 2018, Fuston & Wu, 2021), associated with the Aleutians arc since at least 46 Ma (Jicha and Kay, 2018). This straightforward, present-day match is mentioned here because according to the Baja-BC hypothesis of paleomagnetism, transform shuffling transported southern (INS) to essentially their present resting places by ~50 Ma (e.g., Kent and Irving, 2010) -- just before the Aleutian arc started to grow on and outboard of those newly arrived terranes. Kula northward subduction (speculatively since ~85 Ma, Wood and Davies, 1982, Seton et al., 2012) immediately preceded Aleutian subduction in that region and is presumably associated with KI slab in Figures 5 and 3, (Sigloch and Mihalynuk, 2017). According to Pacific isochrons, the Kula plate was located outboard of the northern Farallon plate (CR slab), which itself was already intra-oceanic according to tomotectonics. Hence Kula plate was not in direct contact with the NAM margin according to tomotectonics and probably tangential to BajaBC events, whereas previous authors considered the Kula plate adjacent to the PNW margin (Engebretson et al., 1985) and hence as a potentially major northward driver of BajaBC terranes along the margin.

5.1.4 Farallon South (FS) slab paired with Cretaceous margin-hugging arcs in the U.S. (Sierra Nevada, Klamaths, Idaho) and Mexico (Peninsular)

FS is inferred to be Farallon arc built on the NAM margin (section 4.3.1); at the end of its inferred lifetime, the arc had its largest extent and covered the ~80 Ma margin from Mexico to the northern U.S. (yellow line in Fig. 1).

At California latitudes, pairing FS slab with the arc that built the Sierra Nevada Batholith (SNB, essentially ~125-80 Ma, Paterson and Ducea, 2015) seems relatively straightforward. FS slab fits the timing, subduction polarity and continental nature of the SNB arc. Figure 6 shows this arc in translucent lime green, originating at the eastern tip of FS slab, in the inner corner between MEZ and ANG slab walls. The dashed, retreating trench lines schematically represent the subsequent, southwestward migration of this arc with the NAM margin while the FS slab is inferred to grow below it from ~140 or 130 Ma to ~80 Ma.

In Mexico, we pair FS slab with the margin-hugging Peninsular arc, more specifically with its 99-86 Ma La Posta suite (Hildebrand and and Whalen, 2014). We cannot pair FS with additional, older parts of Peninsular arc because its earlier phase, the Alisitos arc (>116-106 based on unambiguous zircon U-Pb ages on extant Alisitos Fm.; Schmidt et al., 2014), has oceanic character (so we pair it with the intra-oceanic AL slab in section 5.1.5). FS arc earlier than La Posta would not be expected anyway since MEZ arc override, which must precede FS onset, was ~110 Ma according to Fig. 1.

In Idaho, we pair FS arc with the SNB-equivalent arc that intrudes IMS and NAM craton 125-90 Ma (Gray et al., 2024; Giorgis et al., 2005; and citations therein).

In section 5.2.2, we reason from tomotectonic principles that FS slab must additionally be paired with the Coast Plutonic Complex of northern British Columbia (~127 Ma to 76 Ma; Currie, 1996; Zagorevski et al., 2016), to where it must have been translated after forming vertically above FS.

5.1.5 AL slab paired with Alisitos intra-oceanic arc

AL slab is paired with the Alisitos arc, which forms part of the Peninsular arc of Mexico. Alisitos arc is of oceanic character, was active since >116-106 (see above section) and docked to the Mexican (GUE superterrane) margin ~100 Ma (Johnson et al., 1999; Hildebrand and Whalen, 2014). AL slab sits in a clearly outboard position (west of MEZ, deep) relative to NAM, hence should always have been intra-oceanic arc. Stationed along AL slab, the Alisitos arc will accrete at roughly its observed latitudes on the MX margin (Clennett et al. 2020). Located at a depth ~1050-1400 km, the AL slab would have sunk 10 mm/yr if subduction ended at 106 Ma, consistent with the other slab walls across the Archipelago (Sigloch & Mihalynuk 2013).

5.2 Arcs associated with Mezcalera and Angayucham westward subduction

Section 5.1 has matched all eastward (Farallon) arcs inferred by tomotectonics with actually observed geological arcs. The tomotectonically inferred arcs (i.e., slabs) remaining to be matched are MEZ and ANG slab walls.

5.2.1 ANG slab wall paired with Central Alaskan arcs (Koyukuk)

The Jura-Cretaceous arcs of Central Alaska are a straightforward match with ANG slab wall. Figure 1 shows how NAM underrode ANG slab very slowly over Cretaceous times and into the Cenozoic – a prolonged, oblique collision that would have slowly plucked the originally linear, >3,000 km long arc off its slab and crumpled its slivers into the tightly folded oroclines seen in Figure 6 (in red). The northerly latitude of ANG slab ensures that Central Alaska accretes north of all Farallon and MEZ arcs, as observed. This huge slab provides a satisfying placement for Central Alaskan arc terranes that have been difficult to place or to relate to more southerly events in reconstructions based purely on geology (e.g. Patton and Box, 1989) or purely on plate reconstructions (e.g., Seton et al. 2012).

5.2.2 MEZ slab wall paired with Insular and Guerrero microcontinents

The proposition is to place INS and GUE microcontinents above the northernmost part of MEZ slab (which will be overridden by the U.S. margin), and GUE just south of INS, above the part of MEZ that will be overridden by the Mexican margin – see Figures 1 and 6. The correct positioning of INS is central to the archipelago model and differs from Always-Andean models (Hamilton, 1969; van der Heyden, 1992; Monger and Gibson, 2019, and many others), Ribbon-continent models (Johnston, 2001, 2008; Hildebrand, 2009, 2013) or the Hit-and-Run model (Maxon and Tikoff, 1996; Tikoff et al., 2023), so we justify it in some detail with tomotectonic reasoning.

The approach is to reason backwards in time from the margin-hugging Farallon FS arc. INS basement can be tied to MEZ slab based on the geometric relationship and genetic succession between MEZ and FS slabs, when combined with the observation that FS arc intruded INS (and Guerrero).

Recall how the tomotectonic inference of sections 4.3.3 and 4.4 predicted a smooth hand-off from westward subduction into the intra-oceanic MEZ slab and under the (yet-unnamed) MEZ-arc, to eastward Farallon subduction into FS slab and beneath the continental NAM margin. This subduction flip was inferred from the spatial relationship between MEZ and FS slabs: at any latitude, FS is observed immediately west of the MEZ slab wall and spread out laterally as if deposited by a migrating (margin-hugging) trench – in the override sequence, FS is the functional "replacement" of MEZ slab, which keeps NAM's westward drift going by moving seafloor out of the way.
The geological link is that the plutons from the earlier (westward) MEZ-arc and the later (eastward) FS arc *must have intruded into the same basement terrane*, the MEZ-arc basement that was initially stationed above MEZ slab and was subsequently accreted and carried away by the NAM margin.

Section 5.1.4 paired the margin-hugging FS slab at Mexican latitudes with Peninsular arc, more precisely its younger part, the 99-86 Ma La Posta Suite (whereas the >116-106 Ma Alisitos arc is inferred to have grown offshore). This FS arc intrudes GUE basement; it follows that the MEZ arc must also have intruded GUE. Hence GUE microcontinent is the wanted "MEZ-arc", i.e., must be stationed above MEZ slab prior to its override.

At U.S. latitudes, section 5.1.4 paired FS slab with the Sierra Nevada Batholith (SNB) arc, dated 140-90 Ma, which intrudes into NAM craton and what may lie outboard of it but is covered by Great Valley sediments. We cannot make a link of FS arc to INS (or another outboard terrane) here.

FS slab was also paired with contemporaneous arc in Idaho (125-100 Ma), which intrudes NAM craton and IMS. Again, we cannot show that FS arc intruded INS here, despite the suspicion that INS may originally have lain west of IMS at this latitude.

In northern B.C., FS arc is the Coast Plutonic Complex (125 (maybe 135) to 76 Ma), which intrudes into both INS and IMS, stitching them together. If we accept that IMS was accreted to the NAM margin by ~170 Ma, i.e., long before the margin-hugging FS arc started, then the observation of FS intruding into IMS post-170 Ma is equivalent to saying that FS intruded into NAM. Here, FS arc is also intruding INS basement, just outboard of the NAM-IMS margin. This means that INS must indeed be the "MEZ-arc" that we are seeking to position above MEZ slab: INS was lining the "NAM margin" (i.e., IMS) by the time FS arc started up at 135 or 125 Ma. INS basement was subsequently intruded and stitched to NAM-IMS by the FS arc.

Plutons on this part of INS that are older than FS arc must therefore be plutons generated by westward (MEZ) subduction, according to the tectonic inference. Indeed, the plutonism on INS is observed to reach back much longer (e.g., ~205-160 Ma Bonanza arc), meaning the deep slab wall of MEZ is "needed" to account for this long-lived arc magmatism on INS.

We showed that GUE superterrane must likewise have been stationed above MEZ slab prior to the onset of the FS arc on it. Old plutonic parts of GUE seem to reach back to at least 164 Ma (Shaw et al., 2003) but MEZ slab wall can readily account for their ages. We note that on geological grounds, GUE had been argued to be a close correlative of INS. We have independently confirmed, or at least supported, this correlation by showing that both INS and GUE must have been stationed above MEZ slab, intruded by the same arc.)

Along MEZ slab, INS should arguably have been stationed north of GUE, preserving their relative latitudinal positions at present-day. This means that INS must have occupied the northernmost part of MEZ slab prior to its accretion to NAM-IMS. (No other correlatives of INS are found farther north in the Cordillera, which might need to be placed north of INS along MEZ slab.)

5.2.3 Tomotectonics infers large-scale northward displacement of INS (BajaBC)

The margin-hugging FS is a southerly slab that was never traversed by the B.C. margin (Fig. 1). Also, no slab other than FS was inferred to represent margin-hugging arc in section 4 (except for FN, which is much too young). Hence the margin-hugging (IMS-intruding) arc aged 135-76 Ma on B.C. basement terranes (IMS and INS) can only be paired with FS slab in the tomotectonic logic.

The fact that we have identified a margin-hugging Farallon arc geologically manifested on B.C. terranes therefore implies that *these basement terranes were not always located at B.C. latitudes, but rather further south above the FS slab, while FS arc was active* (all under the tomotectonic hypothesis of vertical sinking). FS slab was active until ~80 Ma (Big Break, Fig. 1), so we can infer that at 80 Ma, INS terranes now located in northern B.C. were located somewhere along the Big Break line in Fig. 1, somewhere between Idaho and northern Mexico, where they were intruded by FS arc. They must have moved from there to northern B.C. since 80 Ma. This is essentially the same inference as the BajaBC hypothesis of paleomagnetism (e.g., Enkin 2006, Kent & Irving 2010), but reached completely independently of paleomagnetism.

We can obtain an additional constraint on INS translation. Section 5.2.2. inferred that INS must have been positioned above the northeasternmost segment of MEZ slab prior to the activity period of the FS arc slab on INS (which started ~140 Ma in the SNB) -- c.f. Fig. 6. The absolute latitude and longitude of MEZ slab are tightly constrained by the tomographic image (Figs. 1 and 3), particularly the location where the slab ends in the northeast. The latitudes along the NAM margin where INS (northeastern MEZ) first collided depend on the plate reconstruction (Sigloch & Mihalynuk 2013, Supplement), but they were U.S. latitudes, perhaps reaching into southern B.C. Today, however, the northern part of INS is located in southern Alaska, far north of the U.S or southern B.C. This means that (northern) INS must have been displaced since its accretion at ~155 Ma, from the U.S. or southern B.C. to northern B.C. and southern Alaska. Again, this is essentially a restatement of the paleomagnetic inference about BajaBC (whose core is formed by INS), without having used any paleomagnetic data points.

5.3 Existence of the Jura-Cretaceous Mezcalera Ocean that separated Insular microcontinent from NAM and Intermontane

Tomotectonics infers an open ocean, the Mezcalera Ocean, between NAM and the MEZ arc (INS-GUE) at >170 Ma (Figs. 1, 5, 6), which persisted to ~155 Ma at its narrowest point (offshore the U.S. margin), and to ~110 Ma offshore the Mexican margin. In Section 5.2 we have tomotectonically reasoned that MEZ slab wall hosted the INS-GUE microcontinent; and that arc plutons on the INS-GUE basement terranes must be attributed to westward MEZ subduction if their ages are older than "FS-slab ages". Hence, we should also show from the geological record that an open ocean plausibly existed *east* of the intra-oceanic INS-GUE during “pre-FS slab times", since without this ocean, there would have been no lithosphere to subduct westward and build the MEZ slab.

Hence, we should demonstrate geological structures exist immediately east (inboard) of the INS-GUE terranes that are consistent with an oceanic suture, and with predicted suturing dates between 155 Ma (MEZ override by U.S. margin, this includes terranes now in B.C.) and 110 Ma (MEZ override by Mexico margin). Structures suggestive of such a suture are indeed present immediately east of INS, in the form of a belt of a dozen “collapsed basins”, which are featured and named on the map Figure 6. in cyan. Half of them (e.g. Tlikakila in the north to Arperos in the south) contain mantle or mélange rock. All contain turbidite deposits consistent with relict ocean basin fill of Late Jurassic and Early Cretaceous age. In B.C., these suture basins run between INS and IMS and had previously been dated (U-Pb zircon on pinning plutons; van der Heyden 1989, 1992) as having closed by 170 Ma, which would be contradiction to the tomotectonic inference of an open Mezcalera Ocean at 170 (Figure. 1). But Gehrels et al. (2009) and Butler et al. (2006) reanalyzed a subset of the plutons and found that all of the old stitching ages were compromised by xenocrystic cores, and actual crystallization ages were younger (120-100 Ma) and consistent with our predicted Late Jurassic to Early Cretaceous closure dates. The evidence for the nature and timing of the collapsed basins is discussed in detail by Sigloch & Mihalynuk (2017, 2020). A key observation is that the basins span the Cordilleran margin as a continuous belt, as predicted from the latitudinal extent of the Mezcalera-Angayucham Ocean (Fig. 6), and that they reach closure dates of 155 Ma and younger, as predicted.

The possibility of a wide Mezcalera Ocean has since been doubted based on the observation that INS arc, which would have up to 1000-2000 km west of NAM before 170 Ma, is flooded with sediments of NAM provenance. We do not consider this a valid counterargument because the seafloor conveyor ultimately transports all sediments that are shed into the Mezcalera Ocean to its MEZ trench and INS arc, where the sediments stack up if they do not subduct. Modern-day analogue systems equally have their oceanic arcs flooded with sediments from the approaching continental margins, as detailed in section 6.2 and Fig. 8B.

Inferences about the arc on INS, and the existence of the suture, are confounded by the occurrence of arc on IMS (Stikinia and Quesnellia) that shut down by 170 Ma but temporally overlapped with observed Mesozoic arc on INS (which started ~205 Ma; Canil and Morris, 2024). The simplest explanation might be that INS and IMS arcs were caused by the same subduction zone and slab, and that therefore no Mezcalera Ocean could have been open between INS and IMS post-205 Ma. However, the observation of suture basin fills that reach to much younger ages than 205 or 170 Ma shed strong doubt on this hypothesis and permit envisaging an open ocean basin until well after 170 Ma, and two separate subduction zones simultaneously subducting the Mezcalera seafloor westward beneath INS and eastward beneath IMS (or beneath the cratonic margin of the southwest U.S., the "Native arc"), for the period when basin fill was being deposited. This conclusion can be reached from geological evidence alone (Dickinson & Lawton 2001), or from slab evidence alone, and the two support each other.

We acknowledge the issue of not being able to confidently pair a slab with the Native arc and IMS arc, because no slab is imaged vertically below the NAM margin at 170 Ma. Global tomographies show a deeper set of slabs (>2000 km deep) below the archipelago discussed, and also east of it, albeit less sharply resolved. This observation points to several additional paleo-trenches in the region for the time period of the IMS/Native arc. A likely explanation is that the NAM margin was actually located above one (of two) of those candidate slabs before 170 Ma (i.e., above "Atlantis" slab (van der Meer et al. 2010) or deepest ANG slab), but that the available, absolute mantle reference frames are significantly off for times before Atlantic opening, preventing a confident match. The uncertainties of absolute paleo-positioning multiply into Jurassic times, with neither surviving seafloor nor hotspot tracks available, and lingering questions about True Polar Wander (Fu & Kent, 2018). The observation that everything reconfigured between 200-170 Ma in this hemisphere -- onset of Atlantic rift-then-drift, initiation of subduction into all Farallon slab walls -- suggests that some major disruption, perhaps in the mantle, may be confounding attempts to continue the absolute mantle reference frame into the past.

5.4 Archipelago override sequence including geologic arc terranes

Summarizing all tomotectonic inferences, we replay the archipelago override sequence of Section 4.4 with the matched geologic arc terranes as shown in Figures 7, 6 and 5. Slab pull as the driving force is emphasized in this accounting of archipelago override, justified by the observation that 90% of present-day plate motions can be explained by trench configurations and a perpendicular pull force towards every trench, (Forsyth & Uyeda, 1975).

5.4.1 Birth of the archipelago and convergence of NAM before 155 Ma

In the proto-Pacific basin between 200-180 Ma, a vast grouping of intra-oceanic arcs starts up relatively simultaneously (Fig. 5B, at 170 Ma). This new Archipelago sits >1,000 km west of NAM and consists of arcs that added to the Insular-Guerrero Superterrane, a Mesozoic-Paleozoic microcontinent (stationary above MEZ slab wall); and of arcs that will form Central Alaska, striking NW-SE along a >3,000 km trench (ANG slab wall). Farther west, the juvenile Farallon arc (CR slab) parallels the strike of the Alaskan (ANG) arcs over ~2,000 km length, sitting ~1,500 km south of them. On and close to the NAM margin, a long chain of older arcs is shutting down by ~170 Ma (the combined Native/IMS arc), is overprinted, or transitions southward into extensional volcanic fields (e.g. Saleeby and Dunne, 2015; Tosdal and Wooden, 2015; Busby and Centeno-García, 2022). The period of ~200-170 Ma thus leaves two separate arcs in the geological record: the Andean-style Native arc on the NAM cratonic margin by eastward subduction, which marches offshore to the north as the IMS arc; and the intra-oceanic INS-

GUE arc, built by westward subduction into MEZ slab. Western NAM sheds sediments into the ocean basin to its west (the Mezcalera Ocean), across a continent-ocean margin that has become quasi passive since the shutdown of the Native and accretion of the IMS arc by ~170 Ma. NAM is exposed to westward pull because the seafloor west of it, which newly forms part of the NAM plate, continues to subduct westward into the MEZ and ANG slab, beneath the INS-GUE and Central Alaskan arcs (Figs. 5 and 6). A rift zone between eastern North America and west Africa, active since ~200 Ma, transitions to full westward drift by ~170 Ma, opening the Central Atlantic along a spreading ridge that closely parallels the INS-GUE trench on the opposite side of NAM.

Thus, North America breaks away from Pangaea and is pulled into the Archipelago, with INS-GUE trench consuming the seafloor immediately west of NAM, the Mezcalera Ocean (Fig. 6). As this Mezcalera Ocean narrows, the INS-GUE arc above MEZ slab gets flooded with detrital NAM sediments, transported to it by the westward ocean plate conveyor. All NAM sediments shed into the Mezcalera basin ultimately reach the INS arc, where they either subduct or become part of its accretionary prism, wedged between INS and NAM. This prism and any remnant ophiolotic rocks of the Mezcalera seafloor, will mark the suture of the Mezcalera Ocean.

5.4.2 NAM gradually collides with INS-GUE, forcing a trench on the margin (155-80 Ma)

Around ~155 Ma, NAM first collides with northern INS at conterminous U.S. latitudes. The absolute latitude (and longitude) of INS collision is well defined by the eastward-protruding prong of northernmost MEZ slab. The collision region on NAM depends on the plate reconstruction, but it was at U.S. latitudes, possibly extending into southern B.C. (Sigloch & Mihalynuk 2013, Supplement). In California and Oregon, this localized first collision sutures INS to the craton, with the suture marked by the Calaveras mélange belt (Sierra Nevada) and the Western Jurassic belt (Klamaths) as defined by Dickinson (2008). This juxtaposes, across the suture belt, the westward INS arc (which goes extinct due to the collision ~150 Ma) against the east Native arc (extinct since ~170 Ma). At Pacific Northwest latitudes, INS does not collide with NAM craton directly, but rather with the pre-accreted IMS lining the margin (Stikinia, in its more southerly, pre-BajaBC position). Mezcalera mélange basins at these latitudes therefore juxtapose INS arc (active to ~150 Ma or somewhat younger) against IMS arc (extinct since ~174 Ma, Mihalynuk et al., 2004). Following BajaBC and later translations since ~90 Ma, those INS-IMS suture basins are now found in B.C. and southern Alaska, including the Tyaughton-Methow, Gravina-Nutzotin and Kahiltna basins (figure 6, cyan colors and basins legend).

This continent-microcontinent collision deforms the NAM margin locally around the first collision point with the MEZ prong (Fig. 7, thick orange line); from there, the stresses radiate northward, southward and inland through the lithosphere, including to latitudes that have not yet collided (scalloped symbols in Fig. 7, radiating out from “Nv”). This is our interpreted cause of the regionally localized Nevadan orogeny since ~155 Ma, which is regionally confined but later spreads into the all-encompassing, thin-skinned orogenies of the Sevier (U.S.) and the northern Sevier/Columbian (Canada) belts, as more southern segments of INS collide (orange thick line in Fig. 7), and stresses radiate out from a wider collision zone (scalloped symbols radiating from labels “Sv” and “Sv^N”). The obducted INS loads the continental margin, which develops topography that sheds sediments inland (Passage Beds of B.C. and Alberta) ~155 Ma. The collided segment (U.S. segment) of northern INS arc is extinguished.

NAM continues to be pulled into the Archipelago by the still-subducting segments of the Mezcalera Ocean and of the Angayucham Ocean, south and north of the collided segment. As NAM overrides MEZ arc (INS) and rides into the interior of the Archipelago, the seafloor sitting west of MEZ slab wall

is newly forced to subduct under the continental margin, i.e., eastward, generating FS slab and an associated new arc in the NAM lithosphere. This is the SNB arc, the batholithic roots of which intrude and overprint the two older arcs: the just-accreted INS arc, and the more inboard Native Triassic-Jurassic / IMS arc. Figure 8A summarizes the genesis of the three juxtaposed and overprinting arcs for Sierra Nevada latitudes.
As NAM continues to be pulled west by the southern MEZ and by ANG trenches, the continent collides with wider and wider latitudinal swaths of INS-GUE arc segments, which go extinct and are replaced by eastward subduction of southern Farallon (FS) slab, generating the Sierra Nevada Batholith (~125-80 Ma, peaking at 100 Ma; Paterson and Ducea, 2015) and allied arcs on the continental margin of Mexico (La Posta suite plutons, 100-90 Ma; Walawender et al., 1990) and Idaho (Wallowa and Idaho batholiths, 125-90 Ma; Gray et al., 2024; Giorgis et al., 2005; and citations therein). The progressive accretion of INS arc segments widens the deformation of the margin into the Sevier (U.S. & Mexico) and Columbian (Canadian) orogenies. Suture basins between INS and cratonic NAM forming south of the latitudes of initial MEZ collision have later closing dates; MEZ westward subduction and override finishes by ~100 Ma with the collapse of northern Guerrero microcontinent against nuclear Mexico (Fitz-Díaz et al., 2018), and subduction flip to Farallon (FS) subduction outboard of Guerrero.

In a geometric twist, this new Farallon (FS) eastward arc on Guerrero is not pristine but has an offshore predecessor, the Alisitos arc, aged ~140-105 Ma (based on slab; >116-~106 based on unambiguous zircon U-Pb ages on extant Alisitos Fm.; Schmidt et al., 2014) which was stationed above the AL, as part of a closed curtain of Farallon offshore arcs (Fig. 5B). The first seafloor subducting into FS slab was therefore not Farallon plate, strictly speaking (since Farallon plate was already subducting into CR and AL slabs), but rather intra-archipelago seafloor that had been passively sitting prior to MEZ collision. This is the first seafloor consumed into FS, but as FS trench rolls westward with the NAM margin, they approach the intra-oceanic AL slab (Fig. 6). Around 110 Ma the AL slab is evidently no longer needed since its function of consuming southern Farallon plate can be taken over by the new FS trench along the NAM margin. The Alisitos arc shuts down, is pulled towards the FS trench (welded passively into Farallon seafloor) and accretes to the Guerrero margin by ~100 Ma (Johnson et al., 1999; Schmidt et al., 2014), shortly after the accretion of Guerrero to nuclear Mexico and the onset of FS subduction on Guerrero's outboard margin. In the geologic record, Alisitos arc thus looks like a "surplus" Farallon arc, of intra-oceanic signature and older ages than expected in its FS (Peninsular/La Posta) arc surroundings, on account of its 30 m.y. of prior history. Outboard of the accreted Alisitos arc, FS subduction resumes until the Big Break (or end of the La Posta suite ~86 Ma).

By ~100 Ma, all MEZ westward subduction has ceased, but ANG westward subduction will continue much longer (to ~50 Ma, Fig. 1). The Farallon plate (FS & CR slabs) has reached its maximum latitudinal extent, with southern Farallon (FS) slab subducting into an Andean-style trench segment along the MX and California margins, whereas northern Farallon arc (CR) remains offshore at PNW latitudes, almost unchanged since its inception at >180 Ma (Fig. 5B, 5C).

5.4.3 Gradual accretion of Central Alaska to B.C. above ANG slab (110-50 Ma)

From ~110 Ma onward, NAM collides with future Central Alaskan arcs along ANG slab (Figs. 1 and 6). According to Fig. 1, the colliding segment is in B.C., where IMS (Quesnellia) and Yukon-Tanana terrane form the outboard NAM margin (Stikinia and Insular will arrive from the south only after 90 Ma). The collisions with ANG arcs (Koyukuk) over 60 m.y., sustains and intensifies the deformation of the margin (Fig. 7, Columbian "Sv^N" orogeny). We propose that the tightening of INS against the Idaho margin 105-90 Ma, with thickening of crust into the Idaho batholith (Georgis et al., 2008; Tikoff et al., 2023), may have been caused or intensified by the onset of ANG arc collisions. The ANG arcs themselves, colliding at high angle according to the strike of the slab, slowly crumple into the intensely deformed oroclines of Central Alaska, in the "Great Alaskan Terrane Wreck" style of Johnston (2001).

As southern segments of the ANG trench are overridden, they are not polarity-flipped into Farallon subduction -- unlike the handover from MEZ to FS) -- given that immediately southwest of ANG, no FS-like, shallow slab is observed. Evidently the Orcas micro-plate (Orcas basin in Fig. 1), which has acted as a spacer between ANG and CR subduction since >180 Ma, is able to slide out of the way towards the northwest (parallel to its two arcs) or push the CR trench westward, rather than subduct beneath the encroaching NAM. The Yukon margin and northern BC continued to be pulled into the Koyukuk arc.

By 80 Ma, Figure 1 shows a complex situation in the PNW. NAM has partly overridden the space of the Orcas microplate and must be pushing the plate westward. The CR slab shows geometric complications (tears, gaps at green levels in Fig. 2), probably in reaction. The northwestern edge of FS slab (i.e., the continental margin) is also encroaching in the space occupied by CR slab – this offshore Farallon segment with its old oceanic arcs (Pacific Rim, etc.) will inevitably accrete, but Orcas microplate must move out of the way first (see Fig. 5C at 80 Ma).

5.4.4 Margin-hugging Farallon arc gives way to transform margin and BajaBC (80 Ma to present)

Surprisingly, the continental FS arc to the south suddenly shuts down ~80 Ma. Its extinction is recorded both by the absence of slab southwest of the Big Break (which approximately coincides with the margin location around 80 Ma, Fig. 1), and by the geological dates on SNB arc activity ~125-80 Ma. A possible reason may be the geometric disturbances of FS trench in the PNW – which would be consistent with the observation that the SNB-equivalent arc in Idaho (northwestern edge of FS) shut down slightly earlier, ~85 Ma. Still, a continued growth of FS arc by taking over CR arc, now immediately adjacent, would have seemed more intuitive.

This leaves the long-standing alternative that the SNB (FS arc) was terminally disrupted by the accretion of an enormous oceanic plateau. These were the inferred conjugates ("other halves") of the Hess and Shatsky Rises found on today's Pacific plate (Livaccari et al., 1981; Humphreys, 2009; Humphreys et al., 2015, this volume), which would have been transported to the FS trench by ~90 Ma on the Farallon plate. We consider this hypothesis likely as at least a contributor to FS shutdown. Figure 7 includes the timing and spatial extent of plateau ("SRC") arrival at the margin, and the basement-cored Laramide deformation radiating out from it.

The demise of the margin-hugging FS trench transforms the continental margin (still a plate boundary) into a transform boundary (Fig. 1, blue margin segments west of the Big Break). This mechanically decouples outboard terranes along the Mexican and U.S. margins from stable NAM, and couples them more to the Farallon plate, which is now in transform motion (transpression) relative to NAM. Such transform boundaries run within the soft continental lithosphere, a process that now determines the longitudinal extent of BajaBC (which is incompletely known). According to paleomagnetic constraints, INS and at least western parts of IMS were slivered off. Figure 9A/B shows our speculative *main* BajaBC fault as yellow line (as implemented by Clennett et al. 2020), which is drawn to run just inboard of the most robust paleomagnetic sites with significant displacement.

Crucially, the *entire* NAM margin is inferred to have been a transform regime for a short time window following the Big Break ~80 Ma, because the CR trench to the north is still (barely) sitting offshore, and

NAM is pushing away the Orcas microplate obliquely (Fig. 1). Baja-BC can therefore move north relatively unimpeded and *inboard* of the northern Farallon arc, assisted by the small, moveable Orcas plate, as spelled out in Figure 9B.

This transform corridor stays open for some tens of m.y. (recorded by disruption and retreat of upper CR slab in Fig. 2), until by ~50 Ma the Orcas plate has disappeared, the northern Farallon trench (CR) has obliquely accreted to the PNW and is directly succeeded by FN, the northern Farallon arc now building on the continental margin (Cascades arc). This new margin-hugging arc acts like a roadblock that ends the free passage of Baja-BC terranes.

In the far north, the Koyukuk arcs, which have been crumpling against the B.C. margin, are further impacted by the arrival of Baja-BC from the south, and Baja-BC gets wedged against the backstop of the Koyukuk arcs (Fig. 9B). As the Orcas microplate gets squeezed away and ultimately subducts, the INS and Central Alaskan arcs are compressed into the big terrane agglomerate that is now Alaska (Fig. 9B).

During the period of this transform corridor, (~80-50 Ma) the continental margin is newly exposed to "slab windows", where hot asthenosphere comes in direct contact with continental lithosphere previously hydrated by arc (FS). This is the case in the slab-free zone southwest of the Big Break (Fig. 1), to which we attribute the spatially diffuse and migrating ignimbrite flare-up in the U.S. and Mexico after the FS shut down, i.e., post-Laramide (Glazner, 2022). BajaBC on its way north traverses an additional, analogous slab window, just inboard of CR trench, where slab deposition is disrupted or paused at the time (slab break and tears in Fig. 2 at transitional depths between CR and FN) while Orcas plate is pushed out, and asthenosphere comes in direct contact with pre-hydrated INS and IMS lithosphere that is additionally weakened by large-scale transform faults. This CR slab window can account for the 65-54 Ma voluminous sweep of magmatism in the Coast Plutonic Complex of B.C. In Alaska, it can account for widespread 75-65 Ma magmatism into the transpressional zone between BajaBC (INS-Peninsular) and ANG (Farewell terrane), followed by a broad sweep of 65-51 Ma (Jones et al., 2021) (whereas 104-80 Ma plutons in INS (Peninsular) would still have been proper FS arc.)

Once the Koyukuk arc is completely extinct -- ANG slab is largely overridden by 50 Ma -- the northern B.C. margin remains a transform boundary without slab interaction to the present-day, still carrying parts of INS northward, albeit more slowly, at ~41 mm/yr (Leonard, et al., 2007). The transform regime also continues to present along the Sierra Nevada sector (San Andreas), still slivering off continental fragments and transporting them north (Baja California, Salinian block, Transverse Ranges) but only until they reach the impasse of the Juan de Fuca (northern Farallon) plate and its Cascades arc.

6. Discussion

Discussion items focus on the Insular Superterrane, its arcs, and its translations. INS has been the focal point of Cordilleran controversies. For its early history, this concerns the timing and style of its accretion to NAM and IMS – before 170 Ma (Gehrels et al. 2009, Monger & Gibson 2019), since 155 Ma (Sigloch & Mihalynuk 2013, 2017), or ~100 Ma (Tikoff et al. 2023)? For INS has been at the center of the unresolved BajaBC debate between the geological and paleomagnetic communities, waged mostly against large-scale terrane translations ~90-50 Ma as irreconcilable with a presumably margin-hugging Farallon arc.

6.1 Objections to the archipelago model based on detrital zircons and plutons

Objections to the archipelago model (and the ~15 m.y. period of westward-only subduction at conterminous U.S. latitudes) have centered on supposedly discrepant geological characteristics of the Jura-Cretaceous suture between under-riding NAM and overriding Insular Superterrane. The substantial width of the Mezcalera Ocean inferred by tomotectonics, initially 1000-2000 km at its narrowest (Fig. 6A), has been considered incompatible with observed flooding of its intra-oceanic INS arc with old zircons, a lack of old detrital zircon sources in the archipelago, and a margin of NAM that was too distant to be the source. Another criticism has concerned the lack of a persistent sedimentary basin on the leading (western) edge of the subducting NAM plate.

Detrital zircons have been pointed to as a 'crucial test' of the archipelago model (LaMaskin et al., 2022), in that zircons derived from cratonic NAM, and from the Native Triassic-Jurassic arc built upon its margin, should be absent in INS if it was intra-oceanic and on the overriding plate. We argue that quite to the contrary, sediments derived from the continent and its margin are expected to be an increasingly predominant component during arc-continent convergence, given that the seafloor conveyor transports all continental sediments to the oceanic trench, where they stack up if they do not subduct. Modern examples for continent-beneath-arc collisions confirm this to be the case (Fig. 8B). In Australia-beneath-Banda subduction (forming Timor), as well as in China-beneath-Luzon subduction (forming Taiwan), sediments that contain zircons derived from the continent are observed on both the fore and back sides of the converging arc. Both Timor (e.g. Harris, 2011) and Taiwan (e.g. Beyssac et al., 2007) are comprised primarily of continentally derived sediment, some of which transits the arc and is carried onto the overriding plate. Even isotopically primitive igneous rocks of the Luzon arc are overwhelmed by old, inherited zircons likely originating from the Chinese cratonic margin (Shao et al., 2015). In both cases, a sizeable ocean basin has been consumed, as required for the Mezcalera Ocean.

Hence the observed abundance of old continental zircons on INS does not constitute a 'crucial test' against an open Mezcalera Ocean ending in NAM-beneath-INS arc collision; modern-day analogues demonstrate quite the opposite. In the case of the Insular Superterrane, objections based on lack of old zircons may even be moot because basement of the superterrane itself includes possible sources of Early Paleozoic strata with abundant Precambrian zircons (e.g. Beranek et al, 2012; and noted, but discounted by LaMaskin et al., 2022).

Likewise, criticisms based on the lack of sediment load and minor, if any, exhumation on the leading edge of the subducting continental plate are at odds with fundamental features of modern analogues. In both the Timor and Taiwan examples, amphibolite-grade metamorphic rocks are exhumed continent-ward of the colliding arc because the arc acts as a backstop for strata scraped off the subducting continental plate (Fig. 8B). In the case of Timor, imbricated Australian passive margin sequence may be backthrust over the Banda forearc (Harris, 2011; Tate et al., 2017). In the case of Taiwan, the subducting continental margin (China) is interpreted as a relict Andean-type arc (Cui et al., 2021), analogous to the extinct, Native-Jurassic arc that formed the leading edge of NAM prior to its collision with INS. Thus, the Luzon-China collision may be the best modern analogue for initial impingement of western NAM (California) with the Mezcalera arcs at ~155 Ma.

We acknowledge that the creation of a plate model showing terrane motion paths and accurate relationships with other terranes while preserving recognizable terrane outlines is a challenge. With these constraints, our models (Henderson et al., 2014; Clennett et al., 2020) have not yet generated satisfactory motions for Klamath terranes (as pointed out by LaMaskin, et al., 2022), and this clearly requires future work. However, whether the Mezcalera suture lies between *bona fide* intra-oceanic arc of the Rogue-Chetco arc (Yule et al., 2006) bounded by the Orleans Fault, or includes arc, ophiolite, and mélange belts (e.g. Rattlesnake Creek terrane as used by Wyld and Wright, 1988) as far east as the North Fork terrane (as defined by Snoke and Barnes, 2006), does not alter the fundamental mantle underpinnings of the continental-scale suture between INS and NAM/IMS.

6.2 Insular microcontinent collision in the Sierra Nevada and Klamaths ~155 Ma

The tomotectonic prediction is that first collision and accretion of MEZ arc (INS) was at U.S. latitudes ~155 Ma, suturing the first segment of the Mezcalera-Angayucham Ocean and deforming the margin in the Nevadan orogeny (Fig. 7). We examine the spatiotemporal relationship between the fill of the interpreted suture basins, and magmatism on either side of the basin and across it, on the example of the Sierra Nevada and Klamaths (Fig. 8). If arc plutons intrude on both sides of the suture basin *before* the time of suturing then they could not have originated from the same subduction zone (slab), due to the width of the separating ocean -- whereas *after* suturing, a single subduction zone can lead to intrusion of plutons on both sides of the suture.

Figure 8C shows map of the mélange basins in the Sierra Nevada and Klamaths, with a compilation of plutonism colored by age. The Calaveras mélange belt (as used by Dickinson, 2008) extends between the orange line (limit towards INS) and the purple line (limit towards NAM and superadjacent "Native" Triassic-Jurassic arc (NTJ). The cyan line divides the mélange belt into an eastern part, representing NTJ subduction complex; and a western part, the Don Pedro terrane (Blake et al., 1982; here following refinements of Schweickert, 2015) representing the highly strained arc, suture basin and mélange of eastern INS. In the Sierra Nevada, Schweickert (2015) identifies as the interface (cyan line) the Sonora fault (known as Rich Bar fault in northern Sierra Nevada). Key constraints on the timing of the Sonora fault are the Sonora dike swarm (159 – 157 Ma; Sharp, 1988; see inset Fig. 8C) which the Sonora fault cuts, and the Guadalupe intrusive complex (153-151 Ma; Saleeby et al., 1989; Ernst et al., 2009; 'G' on Fig. 8C), which plugs the fault. We show possible extensions of this interface within the Klamaths in Figure 8C.

This suture interpretation implies that a sliver of INS survives, immediately west of the orange line (Foothills terrane in the Sierra Nevada foothills), which disappears beneath the basin fill of the Great Valley. The basin fill of the mélange belt indicates that the basin (Mezcalera Ocean) closed between 157 and 153 Ma at this latitude.

Plutons younger than 155 Ma (green) extend across and overprint the mélange belt. These plutons are attributed to margin-hugging eastward subduction into FS slab, according to both our model and the Always-Andean model; they cannot discriminate between the two models.

Say we accept that the NTJ arc was active to ~170 Ma (Dickinson 2008) -- we fix this likely date to develop a tangible argument but revisit the question shortly. In that scenario, both models predict plutons older than 170 Ma (purple in Fig. 8C) on both sides of the mélange belt – the Always-Andean model because it considers plutons of the NTJ arc to intrude both the craton and what lies to the west, because the Calaveras mélange is not considered to present a wide, open ocean; and the tomotectonic model because it considers eastward NTJ arc and westward MEZ-INS arc to have been active simultaneously before 170 Ma, on either side of the Mezcalera Ocean. (INS-Bonanza arc reaches back to ~205 Ma in B.C., Canil & Morris 2024). Hence plutons older than 170 Ma do not discriminate between models either.

What might discriminate between, or at least affect the relative plausibility of a model, is the location of plutonism (orange in Fig. 8C) for the time period between the demise of the NTJ arc (~170 Ma, Dickinson, 2008) and closure of the suture basin (~157-153 Ma), based on ages of sediments. The tomotectonic model predicts arc plutons during this period only on west of the suture (i.e., on INS), caused by the westward subduction that closed the Mezcalera Ocean basin by ~155 Ma (predicted for this latitude). The Always-Andean model, rejecting an open basin at this time, presumably predicts arc plutons on both sides of the mélange belt, and cutting across the mélange. (Although what would be the significance of the young mélange?)

The relevant (orange) plutons in Fig. 8C are largely confined to west of the suture in both the Sierra Nevada and the Klamaths, which is consistent with westward subduction. There are some exceptions, although not very numerous, especially if we were willing to discount plutons east of the mélange dated 170-165 Ma (orange with red fill), as this may be the too close to the postulated end date of NTJ (170 Ma) to be separable from expected, purple plutons.

This leaves, as potentially problematic to the tomotectonic model, the area of the 166 Ma Standard Pluton (zoom area in Fig. 8C, east of the mélange on cratonic NAM), which calls for closer examination if the characteristics of primary arc, generated by subducting slab, are present. For example, if the 166 Ma Standard pluton represents the NTJ arc axis at the time of intrusion, it is unusual in that it apparently cuts its own accretionary complex (between the cyan and purple lines). Together with other plutons of this age range that intrude mélange and primitive arc terranes between the purple and orange lines, their true arc character remains open to doubt.

This type of pluton argument can support one model or another, but probably not reject a model. Even if orange plutons were found only west of the orange line, supporters of the Andean model might reply that at these times, the arc happened to reach less far inboard. The westward subduction model could be rejected if no orange plutons were found west of the orange line, which is clearly not the case.

Westward subduction could probably not even be rejected if *some* orange plutons east of the purple line turned out to be of true arc character, because the described potential for discriminating between competing models depends on our readiness to accept that Native arc plutonism stopped at 170 Ma, i.e. well before the mélange belt was completely formed. If one was to admit the possibility of the Native arc extending to as recent as basin fill times (155 Ma), then all possibility for model discrimination based on plutons would be lost. In that case, both models would predict primary arc plutons on both sides of the mélange belt to 155 Ma – the Andean model from a single eastward subduction zone reaching across the mélange belt, and the tomotectonic model from one eastward and one westward subduction zone, acting simultaneously to close the Mezcalera Ocean. In summary, westward subduction under INS *cannot be ruled out* as long as arc plutons were intruded into INS up until mélange belt end (~155 Ma), which is observed (orange in Fig. 8C).

A major obstacle to this type of argument is the extensive overprinting by later FS arc, but this, too, is predicted – by the Andean-style model because all purple, orange and green plutons would have been generated by a single, long-lived subduction zone; and by the tomotectonic model because subduction handoff and flip, from MEZ to FS, occurred on a single terrane (INS, the surviving sliver west of the orange line in Fig. 8C). The only surprise (for the tomotectonic model) is the presence of the additional NTJ arc -- although less surprising given that additional (older) slabs are blurrily imaged below 1800-2000 km in the general area, and considering how the slabs studied here indicate several active arcs at any time.

The two-arc model in California may seem contrived, but only until one engages with the significance of the young mélange belt. Prior geologic studies have reached the same conclusion as our tomotectonic prediction, namely that westward subduction was at least partly responsible for closing the basin that became the Calaveras mélange (Schweickert 2015, Dickinson 2008) or its equivalent in Mexico (Arperos Basin of Dickinson & Lawton 2001), which they envisage closing Banda-arc style, with subduction of the Mezcalera Ocean both to the east and the west.

The possibility of westward subduction could be rejected only if the possibility of the mélange recording an ocean basin was discarded completely. Conversely, the presence of the relatively young mélange (suture) basin east of INS-GUE, all along the Cordillera, provides the strongest positive support for the westward subduction model. The suture question may be clearing up in Mexico, where Mezcalera Ocean closure is predicted (Fig. 1) and observed much later, ~110 Ma (Arperos basin fill). This would leave a ~60 m.y. time period (~170 Ma to ~110 Ma) without NTJ arc equivalent. Some workers even doubt the presence of NTJ-equivalent arc in Mexico, as the "Nazas arc" may not represent arc plutonism (Busby and Centeno-Garcia, 2022). In that case, pre-FS aged arc may be present only on GUE basement, outboard of the Arperos (suture) basin. On GUE, arc plutons reach to at least 164 Ma (Schmidt et al. 2014), as predicted tomotectonically for westward subduction under INS-GUE.

6.3 Alternatives to westward subduction?

The difficulty of rejecting westward subduction from geologic evidence should be viewed in combination with the high likelihood of westward subduction that is implied by the wall-like geometries of the MEZ-ANG slabs, and by their enormous volumes. Explaining this 3-D slab-scape -- not just a few selected slabs or 2-D sections -- by anything but vertical sinking under stationary, long-lived trenches is unlikely to be supported by any realistic numerical modelling of subduction (i.e., self-consistently, freely subducting, not forced). Considering U.S. latitudes in isolation, it might be defensible to place the NAM margin above MEZ slab for all times before 155 Ma, because the Mezcalera Ocean was narrowest there, and uncertainties in absolute reference frame may be sufficient at 170 Ma to assert that the ocean did not exist (Sigloch & Mihalynuk, 2013, Supplement). This could "salvage" the Always-Andean Farallon subduction model for the U.S., but not for Mexico, where the distances between NAM margin and MEZ slab were too large, and implied ocean closure too recent to invoke said uncertainties.

Explaining the ANG slab wall by anything but westward subduction seems contrived, but this slab has seen little engagement. If westward subduction is required for ANG, then how to envisage otherwise for MEZ, when the two look so similar? The question is what a fully-fledged alternative to the tomotectonic model could look like, one that attempted to explain all slabs jointly, in addition to all geological observations (including the mélange belts). How many additional degrees of freedom, at the surface or in the mantle, would this model incur if it were kept free of westward subduction? Would it make any predictions? Could numerical modelling reproduce it? Geological testing of the suture in individual field areas is essential, but these larger questions of tectonic self-consistency should be kept in mind, precisely *because* it is so difficult to reject westward subduction under INS from geological evidence alone.

6.4 The Andean-style Farallon arc: smaller and shorter-lived than expected

Our archipelago model converges with the "mainstream" model following the override of INS-GUE above MEZ (since ~155 Ma, diachronous from north to south). By contrast, the most widely accepted model envisages margin-hugging eastward subduction since the Early Jurassic times of NTJ arc (Gehrels et al. 2009, Monger & Gibson 2019). The tomotectonically inferred FS slab has the characteristics of the margin-hugging Farallon arc inferred mainly from U.S. geology, but it is more limited in space and in time. In the land record, FS arc looks much bigger than in the mantle because this "classical" Farallon arc was smeared all across the B.C. and southern Alaska margin after its demise, whereas those margins never actually hosted a margin-hugging arc, according to the slabs (section 5.2).

The margin-hugging Farallon (FS) system was also shorter lived (~130-80 Ma) than usually envisaged. It started after MEZ (INS-GUE) override, i.e. after 155 Ma, but this is difficult to detect because older MEZ arc can easily be confounded for this FS arc, since it was constructed on the same INS-GUE basement and immediately preceded the FS arc (section 5.2).

The mantle records additional Farallon arcs (slabs CR, CR2, AL) that have left scant land records compared to FS. The northern Farallon arc (CR slab) existed before, during and after the lifetime of the margin-hugging FS arc, but it was intra-oceanic from >180 Ma to ~50 Ma. The intra-oceanic nature of northern Farallon subduction is a robust tomotectonic inference, given how deep the CR slab reaches and how far east NAM lay at those times (Fig. 1). A segment of this deepest Farallon system (CR2 slab) is located west (outboard) of even today's NAM margin, which itself is located further west than ever before. It is this *very* outboard, intra-oceanic CR/CR2 slab that is associated with the oldest and most complete isochron record since >180 Ma – a data set that strongly contributed to the notion of an Always-Andean margin since Early Jurassic times. In fact, this old oceanic Farallon arc has left hardly any land record, to the extent that we can identify only one associated arc terrane (Pacific Rim terrane, section 5.1.2).

In contrast, the margin-hugging FS arc has left hardly any seafloor isochron record because its inferred lifetime of ~130-80 Ma almost completely overlaps with the Cretaceous Superchron, a long period of non-reversal of the earth's magnetic field, during which seafloor was not magnetized with isochrons. This means that we have a good land record for the Farallon plate when we have little oceanic record, and vice versa. Awareness of these disconnects between oceanic and on-land records needs to enter our thinking about Farallon subduction. The archipelago model may feel disorienting because non-Farallon subduction zones (MEZ, ANG) are suddenly proposed to have played major roles, yet remained largely hidden from the land geologic record. But from the CR and Alisitos slabs, we can recognize that the supposedly familiar Farallon subduction record remains equally obscure for any segment that was intra-oceanic.

The early terminal shutdown of the margin-hugging FS arc (around 80 Ma) is another important tomotectonic inference. It is consistent with the observed shutdown of the main phase of SNB and allied arcs, but not with arguments that the SNB arc recovered sometime after the Laramide orogeny, albeit in diffuse form. Given the lack of slab west of the Big Break (Fig. 1 & 3), we interpret that the southwestern U.S. remained free of a continental arc after 80 Ma. The observed, spatially diffuse sweeps of "arc-like" magmatism across the western U.S. noted by various workers (see summary in Glazner, 2022) likely represent slab-window magmatism. NAM lithosphere, continuing westward and pre-hydrated by the flat FS slab that it had recently traversed, was melt-prone when it encountered the asthenosphere of the slab-free window. In absolute coordinates, the upper mantle region traversed by western NAM during the diffuse magmatic sweeps would have last been occupied by Baja-BC, which had however shuffled north most recently. Intruding magma would have found ready pathways due to the pervasive shearing and slivering of terranes during BajaBC translations. The blue-shaded (transform) areas in Fig. 7 essentially coincide with the times and margin regions predicted to have been affected by this type of magmatism. While we cannot currently account for spatial details of the magmatic sweep, we argue that the events look unsurprising considering the slab-free mantle underneath, and that there is no compelling reason to interpret the sweep as "true" arc magmatism caused by subducting lithosphere.

6.5 Reconstructed northward journey of BajaBC

The most important result of this study is that tomotectonic inference comes to essentially the same conclusions as paleomagnetism in the long-standing "BajaBC" debate about large-scale, margin-parallel translation of the Insular microcontinent and additional terranes (section 5.2.2, 5.2.3): INS accreted essentially across U.S. latitudes (since 155 Ma) but has moved north to spread across the British Columbia margin today. The bulk of this translation should have occurred after 80 Ma (Big Break, end of margin-hugging arc in U.S.)

The "BajaBC" hypothesis (Irving 1985) was developed to explain paleomagnetic measurements on Cordilleran terrestrial rocks, reproduced many times (Enkin 2006, Kent & Irving 2010), which indicate that Insular microcontinent and western parts of Intermontane microcontinent (Stikinia) originally accreted far south of their current locations, relative to NAM. Southern INS, now located in southern British Columbia, originally occupied Baja Californian (Mexican) latitudes (Irving 1985, Kent & Irving 2010). Alaskan parts of INS should accordingly have accreted at conterminous U.S. latitudes. The northward shuffle of 1500-2000 km happened between 80 Ma and ~50 Ma because rocks magnetized around 90 Ma show the full latitudinal offset, and rocks across most of British Columbia that were magnetized after 50 Ma show no significant offset relative to the North American craton. The 50 Ma to present history of northwest-most British Columbia and southern Alaska is much different. There, the evolving transform margin and its transition into the Aleutian arc accommodated significant northward offset from 50 Ma to present (see Hillhouse and Coe, 1994; Murphy, 2018).

Figure 9A shows the trajectories over time of the half dozen most robust paleomagnetic data sets that gave rise to the Baja-BC hypothesis. Data from many more sites support the timing of the northward sprint but are less robust. The blue/green trajectories follow the paleomagnetic sample sites back in time and space to where and when they were magnetized: Carmacks at 70 Ma, Churn Creek/Mount Tatlow at 95 Ma, 103 Ma for Spences Bridge, etc. (Enkin, 2006). All positions are given in absolute coordinates relative to the lower mantle. The Baja-BC sites are implemented to move northward rapidly between 70 Ma and 50 Ma. This timing is biased by paleomagnetic data (Carmacks volcanics formed 70 km, 1900 km south of their current location); tomotectonics would predicts translation after 80 Ma (end of FS arc, i.e.., SNB and allied arcs) and until ~50 Ma (establishment of a margin hugging arc in the PNW, Cascades magmatism evident by 45 Ma; Humphreys and Grunder, 2022).

The yellow line in Figure 9A is our speculated location of the main Baja-BC transform fault ran. It is necessary to commit to a location when building a quantitative model like Clennett et al. (2020). We run the main Baja-BC shear inboard of all displaced sites of Figure 9A, but no more inboard than necessary (a conservative solution), and through locations that could plausibly hide a major fault. Mainly we run the fault through Cache Creek accretionary complex (IMS) in B.C. and through presumed, left-behind IMS correlatives in the U.S. (in or west of the Blue Mountains; Mihalynuk & Diakow, 2020; Tikoff et al., 2023).

In B.C., we speculate that the fault runs through the Cache Creek accretionary complex, sliding Stikinia past Quesnellia (as in Fig. 9B at 70 Ma). Displacement of Quesnellia is inferred to have been much less than Stikinia; however, paleomagnetic data on layered Mesozoic volcanic rocks of Quesnellia that are not compromised by resetting and pass all confidence tests, have yet to be obtained. Hence, we position the main Baja-BC shear zone conservatively between Quesnellia and Stikinia; in the intensely imbricated and poorly exposed Cache Creek terrane which separates them and could well hide this shear zone. In the Pacific Northwest U.S., its offset must be distributed somewhere between the dashed and the non-dashed line. This restores IMS and NTJ to a single, long arc chain for times before 90 Ma: NTJ stays in California, Stikinia moves to the PNW, and QN stays in B.C.

There is no paleomagnetic evidence that the Guerrero superterrane in Mexico underwent significant displacement, hence we run the fault outboard of it. The same is true for the Sierra Nevada in California, where we run the fault slightly outboard of the NAM-INS suture (identified with the Calaveras mélange belt and Mariposa collapsed basin in the Sierra Nevada (Don Pedro terrane); Fig. 6 and section 6.2). Hence run the fault under the Great Valley (inspired by Wright and Wyld, 2007), with the implication that the Franciscan subduction complex outboard of the valley did not form at these latitudes but further south, and still above the same slab (FS). We continue the speculated fault *inboard* of the Klamaths, in order to implement ~1000 km northward translation of the Klamaths (Housen and Dorsey, 2005), past the stationary Sierra Nevada, which is recorded by Ochoco basin strata correlative with the Hornbrook Formation (Surpless and Beverly, 2013) that straddle the Klamath block (Housen, 2018). This restores the Klamaths' Mesozoic arc belts south to a margin segment now devoid of such arcs (whereas the MEZ slab predicts that INS-GUE should have accreted all along the margin to Mexico). We reiterate the speculative nature of this "main" fault and the fact that many terranes must have moved relative to each other (multiple faults), as also implemented in Clennett et al. (2020). At the regional scales considered in this study, the uncertainties about the exact location of the fault(s) do not change the primary conclusion that INS must have moved from U.S. to B.C. latitudes.

6.6 The Orcas (Resurrection) microplate assembles Alaska between 80-50 Ma

The small, oceanic Orcas plate plays a big role in the assembly of Alaska (Fig. 9B). Orcas plate is inferred tomotectonically as occupying the space between the intra-oceanic slab walls CR and ANG (Fig. 5B). As such, the Orcas plate must be as old as the slab walls (>180 Ma), henec as old as the archipelago itself. The maturing arcs of CR (Pacific Rim) and ANG (Koyukuk) were welded into Orcas plate, which acted as the overriding plate to both arcs. At least Koyukuk was a constituent part of future Alaska, and we predict that some "missing" CR arcs of section 5.1.2 might yet be identified there, e.g., in the inner Chugach subduction complex (Sigloch & Mihalynuk 2020).

The oroclinal crumpling of the ANG arcs, terrane-wreck style (Johnston, 2008) can be explained by North America moving parallel over the slab during its slow override (Fig. 1, yellow absolute motion arrow), causing collisions at almost 90° angle with the Koyukuk arc segments. Since the arcs were welded into Orcas, this small plate must have moved along to some extent, pushed northwestward by NAM (Quesnellia/Yukon Tanana) margin. This escape motion of Orcas made space for BajaBC to follow (Fig. 9B).

By 85 Ma, the NAM margin with BajaBC abutted the southeastern plate boundary of Orcas (Fig. 9B), which must always have been a transform boundary, connecting the ANG and CR trenches (Fig. 1 at 90/80 Ma, blue coastlines). One way to understand BajaBC is that this continental terrane package became functionally part of the microplate because the Orcas' transform boundary stepped into the softer, more shearable lithosphere of the continent. Thus, the Orcas plate acquired the final constituent of future Alaska. All that was left was for the Orcas seafloor to disappear, to fuse BajaBC, Central Alaska, and potentially some CR arcs.

The northwestward escape motion of Orcas is probably recorded in the perturbed slab geometries of the northern Farallon slab, between its CR and FN levels (Fig. 3). It is not obvious where exactly the Orcas plate subducted in the end, as it would have formed only a small slab. One guess is a small, seismically fast anomaly in the upper mantle that strikes east-west under southern Saskatchewan, Alberta and B.C. (dark blue in Fig. 3A). This anomaly is not rendered in Fig. 2, which visually masks out "lithosphere", which may accidentally include shallow slab). This anomaly is not part of the sloping continuity of the northern Farallon group (FN/CR) but rather seems to rest on top of it. Its location in Figure 9B is marked by the gray oval and two "??". The alternative is the Orcas plate was carried along northwestward until southern Alaska had reached essentially its present-day location, and that it was the first seafloor to subduct into the incipient Aleutians trench, ahead of the Pacific plate that subducts today.

The angle between the NAM margin and ANG slab (Fig. 9B) survives as today's curve of the southern coast of Alaska and B.C., which envelops the Gulf of Alaska. From magmatic sweeps along its coastlines, Haeussler et al. (2003) inferred a short-lived Cenozoic microplate in the elbow between Alaska and B.C., called Resurrection plate. The Resurrection hypothesis was revisited by Miller et al. 2023 and supported by Fuston & Wu (2021) from upper-mantle geometries of the Farallon (FN) and Aleutian slabs.

At 85 Ma in the tomotectonic reconstruction, southern Alaska and B.C. wrap around Orcas seafloor (Fig. 9B), which will occupy this space (the future Gulf of Alaska) until it subducts and is replaced by Pacific seafloor. Hence the final demise stage (60-50 Ma) of the Orcas plate is kinematically equivalent to the Cenozoic Resurrection plate (in an odd mismatch of naming), except that the deep ANG and CR slabs indicate a much longer history for this plate. Evidently the Orcas/Resurrection plate left a magmatic sweep record on the margin when it was finally squeezed into the mantle. The 80-50 Ma northward sprint of Baja-BC must be a manifestation of the mobility of the Orcas plate during this squeeze phase. The intra-oceanic northern Farallon arc (CR) could only make landfall on the continent (as Cascades continental arc) as and when the Orcas plate, into which the CR arc had always been welded, disappeared into the mantle.

7. Conclusions and outlook

We have applied the tomotectonic method to the formation of the North Americal Cordillera since 170 Ma. The method is based on a simple, predictive, falsifiable null hypothesis, and a separation of geophysical (slab and plate tectonic) observations for making predictions, from geological observations for testing the predictions. The link between tomotectonics and geology is made by volcanic arcs above subducted paleo-lithosphere (slabs).

Since breaking away from Pangaea in early Jurassic times, North America has overridden a vast archipelago of intra-oceanic subduction zones and their arc terranes. This is supported by robust evidence in the mantle and at the surface. Here we use "archipelago" as an oceanic area bounded by trenches that are oriented to pull in seafloor from opposite sides: a large-scale zone of plate convergence. All arc and microcontinent collisions of Cordilleran North America since ~155 Ma have been shaped by this double-sided nature of subduction.

The accretion of Insular Superterrane, including the Sierra Nevada orogeny and arc succession was a case of subduction flip within the spacious interior of the archipelago. Collapse of the Central Alaskan arcs into oroclines against the continental margin, by westward subduction, was possible in the lee of the nearby, opposite-facing Farallon trench. The northward sprint of Baja-BC and the assembly of Alaska 80-50 Ma occurred in the same setting of double-sided subduction. Tomotectonics infers large-scale northward displacement of Insular Superterrane (relative to stable North America) since it was accreted.

This inference is completely independent of the paleomagnetic argument for Baja-BC, and supportive of it.

With very few degrees of freedom, the tomotectonic method capably predicts the known regional tectonic regimes (subduction, compression, transform) and their changes along various sectors of the NAM west coast from ~170 Ma to today. It contributes absolute paleo-locations where these events occurred. A useful contribution to tomotectonic hypothesis testing would be tools for better discriminating igneous rocks formed in an arc above subducting lithosphere from similar magmatic rocks formed in other environments.

Acknowledgements

We thank Gene Humphreys, Terry Pavlis and Basil Tikoff for their reviews, and Associate Editor Margi Rusmore for additional comments and editorial handling, all of which helped to improve this manuscript. We thank editor Nancy Riggs and her team for the editorial handling. We are grateful to the organizers of the excellent Penrose conference that gave rise to this paper and volume: Stacia Gordon, Basil Tikoff, Elena Centeno-Garcia, William Matthews, and their organizing team. K.S. acknowledges funding by the European Research Council under the European Union's Horizon 2020 research and innovation program, grant 639003 DEEP TIME and by the French government through the UCAJEDI Investments in the Future project, reference number ANR-15-IDEX-01. We dedicate this work to Eldridge Moores.

References

Atwater, T., 1970, Implications of plate tectonics for the Cenozoic tectonic evolution of western North America: Geological Society of America Bulletin, v. 81, p. 3513–3536.

Atwater, T., 1989, Plate tectonic history of the Northeast Pacific and western North America, in Winterer, E.L., Hussong, D.M., and Decker, R.W. eds., The eastern Pacific Ocean and Hawaii, Geological Society of America, Decade of North American Geology, v. N, p. 21–72.

Barth, A.P., Wooden, J.L., Jacobson, C.E. and Economos, R.C., 2013, Detrital zircon as a proxy for tracking the magmatic arc system: The California arc example. Geology, v. 41, p. 223-226.

Beyssac, O., Simoes, M., Avouac, J.P., Farley, K.A., Chen, Y.G., Chan, Y.C. and Goffé, B., 2007, Late Cenozoic metamorphic evolution and exhumation of Taiwan: Tectonics, v. 26, TC6001 [online]

Blake, M.C., Jones, D.L., and Howell, D.G., 1982, Preliminary Tectonostratigraphic Terrane Map of California: U.S. Geological Survey Open-File Report 82–593, 2 maps, 9 p.

Bunge, H.P., and Grand, S.P., 2000, Mesozoic plate-motion history below the northeast Pacific Ocean from seismic images of the subducted Farallon slab: Nature, v. 405, p. 337-340.

Busby, C.J., and Centeno-García, E., 2022, The "Nazas Arc" is a continental rift province: implications for Mesozoic tectonic reconstructions of the southwest Cordillera, US and Mexico: Geosphere, 18, p. 647-669.

Busby, R.W., and Aderhold, K., 2020, The Alaska transportable array: As built. Seismological Research Letters, v. 91, p.3017-3027.

Canil, D., and Morris, R.A., 2024, Continentalization of an intraoceanic arc as exemplified by the Jurassic Bonanza arc of Vancouver Island, Canada: Geological Society of America Bulletin, v. 136, p. 880-892.

Castellanos-Melendez, M.P., Dilles, J., Guillong, M., Bachmann, O., and Chelle-Michou, C., 2024, From birth to death: The role of upper-crustal thermal maturation and volcanism in porphyry ore formation revealed in the Yerington district: Earth and Planetary Science Letters, v. 647, p.119053.

Cerpa, N.G., Sigloch, K., Garel, F., Heuret, A., Davies, D.R., and Mihalynuk, M.G., 2022, The effect of a weak asthenospheric layer on surface kinematics, subduction dynamics and slab morphology in the lower mantle: Journal of Geophysical Research: Solid Earth, v. 127, p. e2022JB024494.

Chapman, A.D., Saleeby, J.B., Wood, D.J., Piasecki, A., Kidder, S., Ducea, M.N., and Farley, K.A., 2012, Late Cretaceous gravitational collapse of the southern Sierra Nevada batholith, California: Geosphere, v. 8, p. 314-341.

Clennett, E.J., Sigloch, K., Mihalynuk, M.G., Seton, M., Henderson, M.A., Hosseini, K., Mohammadzaheri, A., Johnston, S.T., and Müller, R.D., 2020, A quantitative tomotectonic plate reconstruction of western North America and the eastern Pacific basin: Geochemistry, Geophysics, Geosystems, v. 21, p.e2020GC009117.

Clowes, R.M., Brandon, M.T., Green, A.G., Yorath, C.J., Brown, A.S., Kanasewich, E.R., and Spencer, C., 1987, LITHOPROBE-southern Vancouver Island: Cenozoic subduction complex imaged by deep seismic reflections: Canadian Journal of Earth Sciences, v. 24, p. 31–51.

Cowan, D.S., 2003, Revisiting the Baranof-Leech River hypothesis for early Tertiary coastwise transport of the Chugach-Prince William Terrane: Earth and Planetary Science Letters, v. 213, p. 463–475, doi: 10.1016/s0012-821x(03)00300-5.

Cowan, D.S., Brandon, M.T., and Garver, J.I., 1997, Geological tests of hypotheses for large coastwise displacements; a critique illustrated by the Baja British Columbia controversy: American Journal of Science, v. 297, p. 117-173.

Crafford, A.E.J., 2007, Geologic map of Nevada: US Department of the Interior, US Geological Survey, Pamphlet, 46 p., and Data Series 249.

Cui, Y., Shao, L., Li, Z.X., Zhu, W., Qiao, P., and Zhang, X., 2021, A Mesozoic Andean-type active continental margin along coastal South China: New geological records from the basement of the northern South China Sea. Gondwana Research, v. 99, p. 36-52.

Currie, L.D., 1996. The geology and mid-Jurassic amalgamation of Tracy Arm terrane and Stikinia of northwestern British Columbia: unpublished Ph.D. thesis, Carleton, Ottawa, 385 p.

DeCelles, P.G., 2004, Late Jurassic to Eocene evolution of the Cordilleran thrust belt and foreland basin system, western USA. American Journal of Science, v. 304, p.105-168.

Dickinson, W.R., 2008, Accretionary Mesozoic-Cenozoic expansion of the Cordilleran continental margin in California and adjacent Oregon: Geosphere, v. 4, p. 329–353, doi: 10.1130/GES00105.1.

Dickinson, W.R., 2018, Tectonosedimentary Relations of Pennsylvanian to Jurassic Strata on the Colorado Plateau: Geological Society of America Special Paper 533, 184 p., https://dx.doi.org/10.1130/2018.2533.

Dickinson, W.R., and Lawton, T.F., 2001, Carboniferous to Cretaceous assembly and fragmentation of Mexico: Geological Society of America Bulletin, v. 113, p. 1142–1160.

Dragovich, J. D., Littke, H. A., Mahan, S. A., Anderson, M. L., MacDonald, J. H., Jr., Cakir, Recep, Stoker, B. A., Koger, C. J., DuFrane, S. A., Bethel, J. P., Smith, D. T., and Villeneuve, N. M., 2013, Geologic map of the Sultan 7.5-minute quadrangle, Snohomish and King Counties, Washington: Washington Division of Geology and Earth Resources Map Series 2013-01, 1 sheet, scale 1:24,000, plus 52 p. text.

du Bray, E.A., John, D.A., and Cousens, B.L., 2014, Petrologic, tectonic, and metallogenic evolution of the southern segment of the ancestral Cascades magmatic arc, California and Nevada: Geosphere, v. 10, p. 1-39.

Dumitru, T.A., Wakabayashi, J., Wright, J.E., and Wooden, J.L., 2010, Early Cretaceous transition from nonaccretionary behavior to strongly accretionary behavior within the Franciscan subduction complex: Tectonics, v. 29, http://onlinelibrary.wiley.com/doi/10.1029/2009TC002542/full.

Ernst, W.G., Saleeby, J.B., and Snow, C.A., 2009, Guadalupe pluton–Mariposa Formation age relationships in the southern Sierran Foothills: Onset of Mesozoic subduction in northern California?: Journal of Geophysical Research, v. 114, p. B11204, doi:10.1029/2009JB006607.

Earth Model Collaboration, 2024, A repository of Earth models providing the NSF SAGE and GAGE research community model preview visualization tools, facilities to extract model data/metadata, and access to the contributed processing software, URL: Earth Model Collaboration / EarthScope Consortium | Observable (observablehq.com) [accessed July, 2024].

Engebretson, D.C., Cox, A., and Gordon, R.G., 1985, Relative motions between oceanic and continental plates in the Pacific basin: Geological Society of America Special Paper 206, p. 1–60.

Enkin, R.J., 2006, Paleomagnetism and the case for Baja British Columbia: Paleogeography of the North American Cordillera, in Haggart, J. Enkin, R.J. and Monger, J.W.H., eds., Paleogeography of the North American Cordillera, Evidence For and Against Large-Scale Displacements: Geological Association of Canada Special Paper 46, p. 233–253.

Fitz-Díaz, E., Lawton, T.F., Juárez-Arriaga, E., and Chávez-Cabello, G., 2018, The Cretaceous-Paleogene Mexican orogen: Structure, basin development, magmatism and tectonics: Earth-Science Reviews, v.183, p.56-84.

Forsyth, D., and Uyeda, S., 1975, On the relative importance of the driving forces of plate motion: Geophysical Journal International, 43, p. 163-200.

Fu, R.R., and Kent, D.V., 2018, Anomalous Late Jurassic motion of the Pacific Plate with implications for true polar wander: Earth and Planetary Science Letters, v. 490, p. 20-30.

Fuston, S. L., 2022, Reconciling North American Tectonics with the Deep Mantle through Structurally Unfolding Subducted Slabs and Mantle Convection Modeling: Ph.D. thesis, University of Houston, 115 p.

Fuston, S., and Wu, J., 2021, Raising the Resurrection plate from an unfolded-slab plate tectonic reconstruction of northwestern North America since early Cenozoic time: GSA Bulletin, v. 133, p. 1128-1140.

Garver, J.I., and Davidson, C.M., 2015, Southwestern Laurentian zircons in upper Cretaceous flysch of the Chugach-Prince William terrane in Alaska: American Journal of Science, v. 315, p. 537-556.

Gehrels, G., Rusmore, M., Woodsworth, G., Crawford, M., Andronicos, C., Hollister, L., Patchett, J., Ducea, M., Butler, R., Klepeis, K., Davidson, C., Friedman, R., Haggart, J., Mahoney, B., et al., 2009, U-Th-Pb geochronology of the Coast Mountains batholith in north-coastal British Columbia: Constraints on age and tectonic evolution: Geological Society of America Bulletin, v. 121, p. 1341–1361, doi:10.1130/B26404.1.

Giorgis, S., Tikoff, B., and McClelland, W., 2005. Missing Idaho arc: Transpressional modification of the 87Sr/86Sr transition on the western edge of the Idaho batholith: Geology, 33, p.469-472.

Giorgis, S., McClelland, W., Fayon, A., Singer, B., and Tikoff, B., 2008, Timing of deformation and exhumation in the western Idaho shear zone, McCall, Idaho: Geological Society of America Bulletin, v. 120, p. 1119–1133, https://doi.org/10.1130/B26291.1.

Glazner, A.F., 2022, Cenozoic magmatism and plate tectonics in western North America: Have we got it wrong?, in Foulger, G.R., Hamilton, L.C., Jurdy, D.M., Stein, C.A., Howard, K.A., and Stein, S., eds., In the Footsteps of Warren B. Hamilton: New Ideas in Earth Science: Geological Society of America Special Paper 553, p. 1–14, https://doi.org/10.1130/2021.2553(09).

Gorbatov, A., Widiyantoro, S., Fukao, Y., and Gordeev, E., 2000, Signature of remnant slabs in the North Pacific from P-wave tomography: Geophysical Journal International, v. 142, p. 27-36.

Gray, K.D., Johnson, K., Foster, D.A., and Isakson, V., 2024. Jura-Cretaceous synorogenic magmatism and relations to supercontinental rifting in the northwestern US Cordillera: Geological Society of America Bulletin, v. 136 , p. 3735-3768.

Hamilton, W., 1969, Mesozoic California and the underflow of Pacific mantle: Geological Society of America Bulletin, v.80, p. 2409-2430.

Haeussler, P. J., Bradley, D. C., Wells, R. E., and Miller, M. L., 2003, Life and death of the Resurrection plate: Evidence for its existence and subduction in the northeastern Pacific in Paleocene–Eocene time: Geological Society of America Bulletin, v. 115, p. 867-880.

Harris, R., 2011, The nature of the Banda Arc–continent collision in the Timor region, in Brown, D., and Ryan, P.D., eds., Arc-continent collision: Springer, pp. 163-211.

Hess, H. H., 1965, Mid-Oceanic Ridges and Tectonics of the Sea-Floor, in Whittard, W.F., and Bradshaw, R., eds., Submarine Geology and Geophysics: Proc. 17th Symposium of the Colston Research Society, 5-9 April 1965, Bristol, p. 317-332.Hildebrand, R.S., 2009, Did Westward Subduction Cause Cretaceous–Tertiary Orogeny in the North American Cordillera?: Geological Society of America Special Paper 457, 71 p., https://doi.org/10.1130/SPE457. Hildebrand, R.S., 2013, Mesozoic assembly of the North American Cordillera: Geological Society of America Special Paper 495, 169 p.

Hildebrand, R.S., 2013, Mesozoic Assembly of the North American Cordillera: Geological Society of America Special Paper 495, 169 p., doi:10.1130/2013.2495. For permission to copy, contact editing@geosociety.org.

Hildebrand, R.S., and Whalen, J.B., 2014, Arc and slab-failure magmatism in Cordilleran batholiths II–The Cretaceous Peninsular Ranges batholith of southern and Baja California: Geoscience Canada, v. 41, p.399-458.

Hillhouse, J. W., and Coe, R. S., 1994, Paleomagnetic data from Alaska, in Plafker, G., and Berg, H. C., eds., The Geology of Alaska: Boulder, Colorado, Geological Society of America, The Geology of North America, v. G-l, p. 797-812

Hosseini, K., and Sigloch, K., 2015, Multifrequency measurements of core-diffracted P waves (Pdiff) for global waveform tomography: Geophysical Journal International, v. 203, p. 506–521.

Hosseini, K., Matthews, K.J., Sigloch, K., Shephard, G.E., Domeier, M., and Tsekhmistrenko, M., 2018, SubMachine: Web-based tools for exploring seismic tomography and other models of Earth's deep interior: Geochemistry, Geophysics, Geosystems, v. 19, p. 1464-1483.

Hosseini, K., Sigloch, K., Tsekhmistrenko, M., Zaheri, A., Nissen-Meyer, T., and Igel, H., 2020, Global mantle structure from multifrequency tomography using P, PP and P-diffracted waves: Geophysical Journal International, v. 220, p.96-141.

Housen, B.A., and Dorsey, R.J., 2005, Paleomagnetism and tectonic significance of Albian and Cenomanian turbidites, Ochoco basin, Mitchell Inlier, central Oregon: Journal of Geophysical Research: Solid Earth, v. 110, p. 1-22, doi:10.1029/2004JB003458.

Humphreys, E., 2009, Relation of flat subduction to magmatism and deformation in the western United States, in Kay, S.M., Ramos, V.A., and Dickinson, W.R., eds., Backbone of the Americas: Shallow Subduction, Plateau Uplift, and Ridge and Terrane Collision: Geological Society of America Memoir 204, p. 85-98, doi: 10.1130/2009.1204(04)

Humphreys, E.D., and Grunder, A.L., 2022, Tectonic controls on the origin and segmentation of the Cascade Arc, USA: Bulletin of Volcanology, v. 84, p.102.

Humphreys, E.D., Schmandt, B., Bezada, M.J., and Perry-Houts, J., 2015, Recent craton growth by slab stacking beneath Wyoming: Earth and Planetary Science Letters, v. 429, p. 170–180, doi: 10 .1016 /j .epsl .2015 .07 .066 .Müller, R.D., Sdrolias, M., Gaina, C., and Roest, W.R., 2008, Age, spreading rates, and spreading asymmetry of the world's ocean crust: Geochemistry, Geophysics, Geosystems – G3, v. 9, doi: 10.1029/2007GC001743.

Humphreys, E.D., Clennett, E.J., Wu, J., and van Buer, N.J., 2024, Reconciling Baja-BC and flat Shatsky conjugate subduction beneath the western U.S. THIS VOLUME.

Irving, E., 1985, Whence British Columbia: Nature, v. 314, p. 673-674.

Jicha, B.R., and Kay, S.M., 2018, Quantifying arc migration and the role of forearc subduction erosion in the central Aleutians: Journal of Volcanology and Geothermal Research, v. 360, p. 84-99.

Johnson, S.E., Tate, M.C., and Mark Fanning, C., 1999, New geologic mapping and SHRIMP U-Pb zircon data in the Peninsular Ranges batholith, Baja California, Mexico: Evidence for a suture?: *Geology*, v. *27*, p.743-746.

Johnston, S.T., 2008, The Cordilleran ribbon continent of North America: Annual Review of Earth and Planetary Sciences, v. 36, p. 495–530, doi: 10.1146/annurev.earth.36.031207.124331.

Johnston, S.T., 2001, The Great Alaskan Terrane Wreck: reconciliation of paleomagnetic and geological data in the northern Cordillera: Earth and Planetary Science Letters, v. 193, p. 259–272.

Kent, D.V., and Irving, E., 2010, Influence of inclination error in sedimentary rocks on the Triassic and Jurassic apparent pole wander path for North America and implications for Cordilleran tectonics: Journal of Geophysical Research B, Solid Earth, v. 115, p. 1-25, doi: 10.1029/2009JB007205.

Kent, D.V., Olsen, P.E., and Muttoni, G., 2017, Astrochronostratigraphic polarity time scale (APTS) for the Late Triassic and Early Jurassic from continental sediments and correlation with standard marine stages. Earth-Science Reviews, v.166, p.153-180.

Leonard, L.J., Hyndman, R.D., Mazzotti, S., Nykolaishen, L., Schmidt, M., and Hippchen, S., 2007, Current deformation in the northern Canadian Cordillera inferred from GPS measurements: Journal of Geophysical Research: Solid Earth, v. 112, p. 1-15, B11401, doi:10.1029/2007JB005061

Livaccari, R. F., Burke, K., and Sengor, A. M. C., 1981, Was the Laramide orogeny related to subduction of an oceanic plateau?: Nature, v. 289, p. 276–278.

Lithgow-Bertelloni, C., and Richards, M. A., 1998, The dynamics of Cenozoic and Mesozoic plate motions: Reviews of Geophysics, v. 36, p. 27-78.

Liu, L., Spasojevic, S., & Gurnis, M. (2008). Reconstructing Farallon plate subduction beneath North America back to the Late Cretaceous. Science, 322(5903), 934-938.

Ludington, S., Moring, B.C., Miller, R.J., Stone, P.A., Bookstrom, A.A., Bedford, D.R., Evans, J.G., Haxel, G.A., Nutt, C.J., Flyn, K.S., and Hopkins, M.J., 2007, Preliminary integrated geologic map databases for the United States, Western States—California, Nevada, Arizona, Washington, Oregon, Idaho, and Utah (ver. 1.3, December 2007): U.S. Geological Survey Open-File Report 2005–1305, accessed September 14, 2009, at https://pubs.usgs.gov/of/2005/1305/.Meltzer, Anne, et al., 1999, The USArray initiative: Geological Society of America Today v. 9, p. 8-10.

Mihalynuk, M.G., and Diakow, L.J., 2020, Southern Nicola arc geology. British Columbia Ministry of Energy, Mines and Low Carbon Innovation, British Columbia Geological Survey Geoscience Map 2020-01, 1:50,000 scale, two sheets.

Mihalynuk, M.G., Erdmer, P., Ghent, E.D., Cordey, F., Archibald, D.A., Friedman, R.M., and Johannson, G.G., 2004, Coherent French Range blueschist: Subduction to exhumation in < 2.5 m.y.?: Geological Society of America Bulletin, v. 116, p. 910–922, doi: 10.1130/b25393.

Miller, R. B., Umhoefer, P. J., Eddy, M. P., and Tepper, J. H., 2023, Upper-plate response to ridge subduction and oceanic plateau accretion, Washington Cascades and surrounding region: Implications for plate tectonic evolution of the Pacific Northwest (USA and southwestern Canada) in the Paleogene: Geosphere, v. 19, p. 1157-1179.

Monger, J.W., and Gibson, H.D., 2019, Mesozoic-Cenozoic deformation in the Canadian Cordillera: The record of a "Continental bulldozer"?: Tectonophysics, v. 757, p.153-169.

Moores, E.M., 1970, Ultramafics and orogeny, with models of the US Cordillera and the Tethys: Nature, v. 228, p. 837–842.

Moores, E.M., 1998, Ophiolites, the Sierra Nevada, "Cordilleria," and orogeny along the Pacific and Caribbean margins of North and South America: International Geology Review, v. 40, p. 40–54.

Morgan, W. J., 1968, Rises, trenches, great faults, and crustal blocks: Journal of Geophysical Research, v. 73, p. 1959-1982.

Morgan, W.J., 1983, Hotspot tracks and the early rifting of the Atlantic: Developments in Geotectonics, v. 19, p. 123-139).

Müller, R. D., Roest, W. R., and Royer, J. Y., 1998, Asymmetric sea-floor spreading caused by ridge–plume interactions: Nature, v. 396, p. 455-459.

Müller, R.D., Sdrolias, M., Gaina, C., and Roest, W.R., 2008, Age, spreading rates, and spreading asymmetry of the world's ocean crust: Geochemistry, Geophysics, Geosystems – G3, v. 9, doi: 10.1029/2007GC001743.

Murphy, D.C., 2018, Latest Cretaceous–early Eocene Pacifi c-Arctic?-Atlantic connection: Co-evolution of strike-slip fault systems, oroclines, and transverse fold and-thrust belts in the northwestern North American Cordillera, in Piepjohn, K., Strauss, J.V., Reinhardt, L., and McClelland, W.C., eds., Circum-Arctic Structural Events: Tectonic Evolution of the Arctic Margins and Trans-Arctic Links with Adjacent Orogens: Geological Society of America Special Paper 541, p. 1–22, https://doi.org/10.1130/2018.2541(28).

O'Neill, C., Mueller, D., and Steinberger, B., 2005, On the uncertainties in hot spot reconstructions and the significance of moving hot spot reference frames: Geochemistry, Geophysics, Geosystems – G3, v. 6, doi: 10.1029/2004GC000784.

Pană, D., 2021. ^{40}Ar/^{39}Ar dating of phyllonite in the southern Rocky Mountain Trench and adjacent Rocky Mountains unravels kinematic links between the Omineca and Foreland belts of the southern Canadian Cordillera. The Journal of Geology, v. 129, p. 255-281.

Paterson, S.R., and Ducea, M.N., 2015, Arc magmatic tempos: Gathering the evidence: Elements, v. 11, p. 91-98.

Patton Jr, W.W., and Box, S.E., 1989, Tectonic setting of the Yukon-Koyukuk basin and its borderlands, western Alaska: Journal of Geophysical Research: Solid Earth, v. 94, p. 15807-15820.8, DOI: 10.2113/gselements.11.2.91

Pavlis, G.L., Sigloch, K., Burdick, S., Fouch, M.J., and Vernon, F.L., 2012, Unraveling the geometry of the Farallon plate: Synthesis of three-dimensional imaging results from USArray: Tectonophysics, v. 532–535, p. 82–102, doi: 10 .1016 /j .tecto .2012 .02 .008 .

Pavlis, T.L., Amato, J.M., Trop, J.M., Ridgway, K.D., Roeske, S.M., and Gehrels, G.E., 2019, Subduction polarity in ancient arcs: A call to integrate geology and geophysics to decipher the Mesozoic tectonic history of the Northern Cordillera of North America: GSA Today, v. 29, p. 4-10.

Ribe, N.M., Stutzmann, E., Ren, Y., and van der Hilst, R., 2007, Buckling instabilities of subducted lithosphere beneath the transition zone: Earth and Planetary Science Letters, v. 254, p. 173–179, doi: 10.1016/j.epsl.2006.11.028.

Saleeby, J. B., E. E. Geary, S. R. Paterson, and O. T. Tobisch, 1989, Isotopic systematics of Pb/U (zircon) and 40Ar/39Ar (biotite-hornblende) from rocks of the central Foothills terrane, Sierra Nevada, California: Geological Society of America Bulletin, v. 101, p. 1481–1492, doi:10.1130/0016-7606(1989) 1012.3.CO;2.

Saleeby, J., and Dunne, G., 2015, Temporal and tectonic relations of early Mesozoic arc magmatism, southern Sierra Nevada, California, in Anderson, T.H., Didenko, A.N., Johnson, C.L., Khanchuk, A.I., and MacDonald, J.H., Jr., eds., Late Jurassic Margin of Laurasia—A Record of Faulting Accommodating Plate Rotation: Geological Society of America Special Paper 513, p. 223–268, doi:10.1130/2015.2513(05).

Schmidt, K.L., Wetmore, P.H., Alsleben, H., and Paterson, S.R., 2014, Mesozoic tectonic evolution of the southern Peninsular Ranges batholith, Baja Cali fornia, Mexico: Long-lived history of a collisional segment in the Mesozoic Cordilleran arc, in Morton, D.M., and Miller, F.K., eds., Peninsular Ranges Batholith, Baja California and South ern California: Geological Society of America Memoirs, v. 211, p. 645–668, http://dx.doi.org/10.1130/2014.1211 (20).

Schweickert, R.A., 2015, Jurassic evolution of the Western Sierra Nevada metamorphic province, in Anderson, T.H., Didenko, A.N., Johnson, C.L., Khanchuk, A.I., and MacDonald, J.H., Jr., eds., Late Jurassic Margin of Laurasia—A Record of Faulting Accommodating Plate Rotation: Geological Society of America Special Paper 513, p. 299–358, doi:10.1130/2015.2513(08).

Seton, M., Müller, R.D., Zahirovic, S., Gaina, C., Torsvik, T., Shephard, G., Talsma, A., Gurnis, M., Turner, M., Maus, S., and Chandler, M., 2012, Global continental and ocean basin reconstructions since 200 Ma: Earth-Science Reviews, v. 113, p. 212–270, doi: 10.1016/j.earscirev.2012.03.002.

Sharp, W.D., 1988, Pre-Cretaceous crustal evolution in the Sierra Nevada region, California, in Ernst, W.G., ed., Metamorphism and Crustal Evolution of the Western United States, Rubey Volume VII: Englewood Cliffs, New Jersey, Prentice-Hall, Inc., p. 821–864.

Shaw, S.E., Todd, V.R., and Grove, M., 2003, Jurassic peraluminous gneissic granites in the axial zone of the Peninsular Ranges, southern Califor nia, in Johnson, S.E., Paterson, S.R., Fletcher, J.M., Girty, G.H., Kim brough, D.L., and Martín-Barajas, A., eds., Tectonic Evolution of North western Mexico and the Southwestern USA: Geological Society of America Special Papers, v. 374, p. 157–183, http://dx.doi.org/10.1130/0-8137 2374-4.157.

Sigloch, K., 2008, Multiple-Frequency Body-Wave Tomography [Ph.D. thesis]: Princeton, New Jersey, Princeton University, 249 p.

Sigloch, K., 2011, Mantle provinces under North America from multifrequency P-wave tomography: Geochemistry Geophysics Geosystems, v. 12, Q02W08, doi: 10.1029 /2010GC003421 .

Sigloch, K., and Mihalynuk, M.G., 2013, Intra-oceanic subduction shaped the assembly of Cordilleran North America: Nature, v. 496, p. 50–56, doi: 10 .1038/nature12019 .

Sigloch, K., and Mihalynuk, M.G., 2020, Comment on GSA Today article by Pavlis et al., 2019: "Subduction polarity in ancient arcs: A call to integrate geology and geophysics to decipher the Mesozoic tectonic history of the northern Cordillera of North America": GSA Today, v. 30, p. e47-e50, https://doi.org/10.1130/GSATG431C.1.

Sigloch, K., McQuarrie, N., and Nolet, G., 2008, Two-stage subduction history under North America inferred from multiple-frequency tomography: Nature Geoscience, v. 1, p. 458–462, doi: 10 .1038 /ngeo231.

Stegman, D. R., Farrington, R., Capitanio, F. A., and Schellart, W. P., 2010, A regime diagram for subduction styles from 3-D numerical models of free subduction: Tectonophysics, v. 483, p. 29-45.

Steinberger, B., Torsvik, T. H., and Becker, T. W., 2012, Subduction to the lower mantle–a comparison between geodynamic and tomographic models: Solid Earth, v. 3, p. 415-432.

Surpless, K.D., and Beverly, E.J., 2013, Understanding a critical basinal link in Cretaceous Cordilleran paleogeography: Detailed provenance of the Hornbrook Formation, Oregon and California: GSA Bulletin, v. 125, p. 709-727.

Tardy, M., Lopierre, H., Bourdier, J.L., Coulon, C., Hernández, L.E.O., and Yta, M., 1992, Intraoceanic setting of the western Mexico Guerrero terrane--implications for the Pacific-Tethys geodynamic relationships during the Cretaceous: Revista mexicana de ciencias geológicas, v. 10, p. 118-128.

Tate, G.W., McQuarrie, N., Tiranda, H., van Hinsbergen, D.J., Harris, R., Zachariasse, W.J., Fellin, M.G., Reiners, P.W. and Willett, S.D., 2017, Reconciling regional continuity with local variability in structure, uplift and exhumation of the Timor orogen: Gondwana Research, v. 49, p. 364-386.

Tepper, J.H., and Clark, K.P., 2024, Initiation of the Cascade arc: Geology, v. 52, p. 297–301, https://doi.org/10.1130/G51888.1

Tikoff, B., Housen, B.A., Maxson, J.A., Nelson, E.M., Trevino, S., and Shipley, T.F., 2023, Hit-and-run model for Cretaceous–Paleogene tectonism along the western margin of Laurentia, in Whitmeyer, S.J., Williams, M.L., Kellett, D.A., and Tikoff, B., eds., Laurentia: Turning Points in the Evolution of a Continent: Geological Society of America Memoir 220, p. 659–705, https://doi.org/10.1130/2022.1220(32).

Tomek, F., Žák, J., Verner, K., Ježek, J., and Paterson, S.R., 2024, A complex interplay between pluton emplacement, tectonic deformation, and plate kinematics in the Cretaceous Sierra Nevada magmatic arc, California: Tectonics, v. 43, p. e2023TC007822.

Torsvik, T.H., Steinberger, B., Shephard, G.E., Doubrovine, P.V., Gaina, C., Domeier, M., Conrad, C.P., and Sager, W.W., 2019, Pacific-Panthalassic reconstructions: Overview, errata and the way forward: Geochemistry, Geophysics, Geosystems, v. 20, p. 3659-3689.

Tosdal, R.M., and Wooden, J.L., 2015, Construction of the Jurassic magmatic arc, southeast California and southwest Arizona, in Anderson, T.H., Didenko, A.N., Johnson, C.L., Khanchuk, A.I., and MacDonald, J.H., Jr., eds., Late Jurassic Margin of Laurasia—A Record of Faulting Accommodating Plate Rotation: Geological Society of America Special Paper 513, p. 189–221, doi:10.1130/2015.2513(04).

Van der Meer, D.G., Van Hinsbergen, D.J., and Spakman, W., 2018, Atlas of the underworld: Slab remnants in the mantle, their sinking history, and a new outlook on lower mantle viscosity: Tectonophysics, v. 723, p. 309-448.

van der Wiel, E., van Hinsbergen, D. J., Thieulot, C., and Spakman, W., 2024, Linking rates of slab sinking to long-term lower mantle flow and mixing: Earth and Planetary Science Letters, v. 625, 118471.

Walawender, M.J., Gastil, R.G., Wardlaw, M., Gunn, S.H., Eastman, B.G., McCormick, W.V., and Smith, B.M., 1990, Geochemical, geochronologic, and isotopic constraints on the origin and evolution of the eastern zone of the Peninsular Ranges batholith, in Anderson, J.L., ed., The Nature and Origin of Cordilleran Magmatism: Geological Society of America Memoir 174, p. 1–18.

Wessel, P., and Kroenke, L.W., 2008, Pacific absolute plate motion since 145 Ma: An assessment of the fixed hot spot hypothesis: Journal of Geophysical Research: Solid Earth, v. 113, B06101, 21 p.

Woods, M.T. and Davies, G.F., 1982, Late Cretaceous genesis of the Kula plate: Earth and Planetary Science Letters, v. 58, p.161-166.

Wright, J.E., and Wyld, S.J., 2007, Alternative tectonic model for Late Jurassic through Early Cretaceous evolution of the Great Valley Group, California, in Cloos, M., Carlson, W.D., Gilbert, M.C., Liou, J.G., and Sorensen, S.S., eds., Convergent Margin Terranes and Associated Regions: A Tribute to W.G. Ernst: Geological Society of America Special Paper 419, p. 81-96.

Yonkee, W.A., and Weil, A.B., 2015, Tectonic evolution of the Sevier and Laramide belts within the North American Cordillera orogenic system. Earth-Science Reviews, v. *150*, p.531-593.

Zagorevski, A., Mihalynuk, M.G., Joyce, N., and Anderson, R.G., 2017, Late Cretaceous magmatism in the Atlin Tagish area, northern British Columbia (104M, 104N), in Geological Fieldwork 2016: British Columbia Ministry of Energy and Mines, British Columbia Geological Survey Paper 2017-1, p. 133-152.

Figure captions

Figure 1. Roadmap figure for this study: the superposition of subducted lithosphere (slabs) in the mantle with continental drift, reconstructed with respect to the mantle. Coloured polygons show outlines of major slabs under North America from teleseismic P-wave tomography (Sigloch 2011). Slabs inferred to have been deposited by westward subduction are coloured in orange, those generated by eastward (Farallon) subduction in green. Darker colour shades are applied to lower-mantle slabs (MEZ, ANG and CR/CR2/W; light shades to shallower slabs: FS (400-1000 km deep), FN (0-700 km), and to the shallow western end of ANG. Superimposed are time snapshots tracking the westward migrating margin of North America, reconstructed in a mantle reference frame, which is constrained between 0-120 Ma by moving hotspots (Dubrovine et al., 2012) and 120-170 Ma by true polar wander-corrected paleomagnetic data (Torsvik et al., 2019). Colored arrows connecting the northern end points of the paleo-coastlines highlight three distinct episodes of absolute plate motion.
If the slabs sank vertically in place then a continental margin overlying a slab indicates a continent-arc interaction – because a slab constrains a paleo-subduction zone, which must have hosted a paleo-arc. Symbols on the paleo-margins indicate the nature of the tectonic regime along the margin, as inferable from the tomotectonic principles developed in the text. Orange barbs: NAM-beneath-arc collision (westward subducting slab located underneath). Green barbs: subduction beneath NAM (eastward subduction), with arc built on NAM. Light blue lines and arrows: transform boundary along the margin

(no slab underneath). Black line: (quasi-)passive continental margin (no slab underneath, and no pre-existing plate boundary along the margin). Yellow line traces the sharp western edge of FS slab, associated with a sudden transition from eastward subduction to transform margin ~80 Ma. The starting point of our inference is ~170 Ma, the time when North America separated from Pangaea, and when absolute paleo-positioning in plate reconstructions becomes reasonably reliable.
Slab abbreviations: MEZ – Mezcalera, ANG – Angayucham, CR & CR2 – Cascadia Root, FN – Farallon North, FS – Farallon South, AL – Alisitos. W is a non-interpretive name.

Figure 2. Mantle tomography: 3-D isosurface rendering of seismically fast anomalies imaged under the western U.S.A., from the surface to ~1800 km depth, in the teleseismic P-wave tomography model of Sigloch (2011). The isosurface rendering threshold is dVp/Vp>0.25%. Color signals depth and changes in increments of 200 km. This structure represents subducted oceanic lithosphere (slab) of the former Farallon plate, dipping eastward down from beneath the Cascades (Juan de Fuca) trench. Surface topography of the North American Cordillera and the Pacific basin are overlain in translucent gray, with strong vertical exaggeration. Yellowstone (red triangle) and its vertical downward continuation are shown for visual reference. Seismically slow anomalies are not rendered (e.g., Yellowstone plume). Shallow fast anomalies representing the thick continental lithosphere of NAM are masked out as they would block the 3-D view on the slabscape. Panels A and B present alternative view angles on the same scene, comprising the FN and CR slabs of Figure 1 (subdivided at ~600 km depth, where structural breaks are visible especially in panel B). Slab W is also visible in the foreground. Deep CR2 slab under the Pacific is not rendered.

Figure 3. Three-dimensional isosurface rendering of all seismically fast P-wave anomalies (subducted slabs) in the upper and lower mantle beneath North America. Tomography model, rendering threshold and color scheme as in Figure 2. (A) Top-down view of fast structure below 400 km (in order to exclude the overlying lithosphere, which is fast but does not represent slab). Strictly speaking, the view is from ~390 km down due to slight interpolation smoothing of the contouring algorithm, explaining why the shallowest anomalies appear in dark blue, as part of the 200-400 km layer. (B) Inside-out view of all fast structure from the surface down, with the deepest structure (slab walls MEZ, ANG, CR/CR2) emerging to the foreground. Imaging limitations include artifacts, especially near the margins of the regional dataset: resolution lost into the ocean basins and north of 55°. Two downward smearing artifacts are labeled with white x's and are not interpreted.

Figure 4. (A) The tomotectonic null hypothesis of vertical slab sinking, as envisioned by the very first cartoon of subduction to be published, by Harry Hess in 1965. Motions are drawn in a mantle reference frame, with the overriding plate moving laterally but not the subducting plate. (B)-(I) Range of possible slab geometries predicted for when oceanic lithosphere sinks vertically after entering the trench, as a function of the parameters v_o, the velocity of the overriding plate (or arc) on the x-axis, and of K, a measure for the vigor of subduction, on the y-axis. Dashed lines represent the viscosity discontinuity between upper mantle (UM) and lower mantle (LM), where the mantle becomes 1-2 orders of magnitude more viscous, resisting further slab sinking. Motions are drawn relative to the mantle, and velocity arrows are drawn to scale relative to each other. v_z, the slab sinking velocity in the lower mantle, is kept fixed in all panels (a typical value being 10 mm/year). Kinematic ratio $K = v_{sub}/v_{acc}$ is the ratio of slab length subducted per unit time versus the length of accommodation space created for it, by means of the vertical sinking away of older slab and the migration v_o of the trench away from the site of older subduction (see Cerpa et al. 2022, eq. 1, for exact definition). K>1 indicates "traffic jam conditions", where plate

convergence is too rapid to be accommodated undeformed, so that slab is forced to thicken (probably by folding). The average value observed for present-day trenches is K~2.5 (Cerpa et al. 2022), with the associated slab types highlighted by grey shaded panels D, F, H. $v_o < 0$ (trench advance, panels B & C) is practically not observed.

Figure 5. Paleo-trenches in absolute (mantle) coordinates, as predicted by the observed slab geometries of Figure 3 if the slabs sank vertically. **(A)** Slab-to-trench transcriptions are drawn in depth increments of 100 km, using the same depth-to-colour mapping as Figure 3. Tracks of paleo-trench (or arc) locations are shown as thick lines if inferred to be produced by westward subduction, and thin lines if produced by eastward subduction or subduction of ambiguous polarity (mostly Farallon). For laterally extended slabs (FS, FN, CR, presumably produced as in figs 4F/H), the arc lines are shown as dashed when a locus of slab deposition is poorly constrained laterally, for a given depth. The colour bar also shows an indicative mapping of slab depth to time of subduction, using 10 mm/year as a typical, heuristic value for slab sinking rate. The coastlines of NAM reconstructed at times 170 Ma (black), ~80 Ma (green), and present day (grey). Grey polygons indicate slab footprints at 800 km depth (in light grey) and at 1400 km (dark grey). Label SN marks the approximate position of the Sierra Nevada batholith; the arrow denotes possible extents of the Hess-Shatsky Rise conjugate plateau. Arc abbreviations: A = Aleutian, KI = Kula-Izanagi. Purple-grey stars on western NAM mark the previous generation of arcs IMS & NJ, extinct and accreted by 170 Ma.

(B) Tomotectonically inferred trenches and plates at 170 Ma, before NAM started its westward drift. All arcs are intra-oceanic at this time. AL trench will start up ~130 Ma, when the Farallon plate has grown southeastward. Trenches/arcs active at the respective reconstruction times are highlighted with barbs and the colors corresponding to their depths, and are plotted on the basemap of panel A.

(C) Trenches and plates at 80 Ma when override is far advanced, with the westward subduction system almost overridden. Farallon plate subducts into a margin-hugging trench in the south (FS) but remains offshore farther north (CR).

Figure 6. Arc terranes matched to slabs. Every substantive slab should be associated with a geologically known arc, and every known arc should be associated with a slab. Arc (super-)terranes are shown in their present positions in the Cordillera on the left part of the map. The same arc terranes are schematically reconstructed above their matched slabs and paleo-trenches, in absolute positions relative to the lower mantle. Colour legend gives the interpreted matches of slabs to geologically known arcs. Superterranes, slabs, arcs and trenches are coloured green if associated with Farallon Ocean subduction; orange if associated with Mezcalera Ocean subduction, and red if associated with Angayucham Ocean subduction. The reconstruction time for the arcs and slab walls corresponds to ~170 Ma (before Archipelago override began), except in the case of the SW-ward migrating southern Farallon (Sierra Nevada Batholith) arc, which is shown in several time snapshots migrating across the area occupied by its associated FS slab. North America is reconstructed at 170 Ma, 140 Ma and 0 Ma. Intermontane Superterrane (IMS) and its continental prolongation, the Native Jurassic arc (NJ) are coloured purple; by 170 Ma, their arc activity had ceased and IMS is shown docked against NAM. The interpreted suture of MEZ arcs (Insular & Guerrero Superterranes INS, orange) against IMS/NJ terranes, is represented by a dozen of collapsed oceanic basins colored cyan and numbered/labeled in the legend.

Abbreviations: Guerrero-Insular arc terranes include WR (Wrangellia), AX (Alexander), PE (Peninsular), GU (Guerrero), WF (Western Jurassic, Western Hayfork, Foothills, and related terranes), SA (Santa Ana). Terranes are associated with Farallon subduction include CG—Chugach; FR—Franciscan; PR—Pacific Rim; SC—Siletz-Crescent; VC—Vizcaino.

IMS Superterrane (purple) includes terranes BM (Blue Mountains, CC (Cache Creek), QN (Quesnel), ST (Stikine) and YTT (Yukon Tanana). NJ (Native Jurassic arc) is the onshore continuation of IMS arcs, as is presumably its along-strike continuation of extensional magmatism in Mexico ("Nazas arc", cf. Busby and Centeno-García, 2022), shown by purple asterisks.

Figure 7. Predicted and observed tectonic events along the NAM continental margin over geological time. The x-axis represents past time (in Ma), the y-coordinate is a distance measure roughly proportional to latitude, which runs the length of the western NAM margin, from northern MX to AK. The reference frame is stable NAM: a point in (x,y)-space represents, at time x, a coast-perpendicular swath at length y, from the immediate offshore to several hundred kilometers into the interior. A coast-proximal point on stable NAM over time runs on a horizontal trajectory (although outboard, translating elements in its swath may change); a vertical line represents synchronous events on and near the margin at fixed time x. Three separate layers of information are distinguished by the use of color. Layer 1 (margin): Colored areas represent the tectonic regime of the marginal plate boundary, as inferred by tomotectonics: white — quasi-passive margin, blue — transform boundary, green — Farallon or Pacific subduction zone, bold green, orange or red: override of an active arc on the CR, MEZ or ANG slab, respectively. Blue arrows are proportional margin-parallel motion during BajaBC times (fast) and its aftermath (moderate). Yellow line: Big Break.
Layer 2 (interior): Black elements denote geologically observed deformation in the hinterland of swath y at time x. Orogeny abbreviations: Nv – Nevadan, Sv— Sevier, SvN — Sevier North (Columbian), Lm — Laramide orogeny. HSC: Hess Shatsky Conjugate plateau. Scalloped symbols show extents of observed continental deformation (orogeny, DeCelles, 2004; Yonkee and Weil, 2015; Pană, 2021), which is interpreted to radiate to the hinterland and margin-parallel from the (colored) locations of arc- or plateau collision (Humphreys et al., 2025, this volume). Layer 3 (Insular microntinent): grey vertical bars represent the latitudinal extent of INS every 10 m.y. INS is located offshore while in the white (x,y) space and accreted while in a colored (x,y) space.

Figure 8. Collisional deformation since ~155 Ma, when NAM first rode into the intra-oceanic MEZ arc and welded it onto the continent's westward-subducting margin. **(A)** Progression of deformation in three time slices before, during and after suturing. **At 160 Ma**, arc magmatism above the westward-subducting Mezcalera Ocean, at the leading edge of North America (NAM), adds crust to the Insular Superterrane (INS) arc and lithosphere to the MEZ slab wall. Circa 155 Ma, the last of Mezcalera lithosphere is consumed between NAM and easternmost INS: NAM collides with INS microcontinent, resulting in the Nevadan orogeny **At 140 Ma,** deformation at the California margin and upward truncation of the slab wall. As NAM is still being pulled westward (by intact trench segments in and out of the figure plane), subduction polarity at the collided segment is forced to flip. **At 100 Ma,** subduction has flipped to eastward beneath the margin. Its slab, deposited by subduction of the Southern Farallon plate), creates an east-dipping blanket (100 Ma panel) as the trench is forced westward in front of advancing NAM. This subduction is building new, margin-hugging arcs that overprint the NAM-INS suture (including the Sierra Nevada batholith). Both north and south of the initial collision site, NAM continues to collide with microcontinental INS, resulting in widening Sevier deformation (Columbian orogeny in Canada).
(B) Generalized cross-section through a modern continent-beneath-arc suture, such as between Australia and Asia, Asia beneath the Philippine arc, or NAM beneath INS or ANG. This spatial zoom into the green box in the 140-Ma panel of A is based on a stylized cross section through central Taiwan (after Angelier et al., 1990; Beyssac et al., 2007; section oriented normal to the suture). All of these sutures show widespread distribution of units containing old detrital zircons, tectonically exhumed forearc (tectonically removed), and high grade, rapidly exhumed metamorphic rocks immediately inboard of the suture. Kmg is Cretaceous orthogneiss (Chipan gneiss) that has cooled through 240 °C in the past million years (Beyssac et al., 2007). PS and TN are volcanic (green) and plutonic (pink) representations of magmatic

rocks of the Penghu Island group and of Tatun volcano (magma chamber imaged by Huang et al., 2021 has no perceivable connection to the mantle wedge), projected from south and north into the line of the section.
(C) Map of accretionary mélanges and plutons pertaining to the inferred Mezcalera Ocean suture between INS and cratonic NAM in California. Colored lines delineate two accretionary mélanges in the Sierra Nevada against their surrounding basement: Calaveras, associated with NJT/IMS arc on NAM; and Mariposa, associated with MEZ arc on INS. Cyan line traces the interpreted boundary between the two complexes. Schweickert (2015) maps the Calaveras complex in Sierra Nevada foothills as bordered by Mariposa Formation or similar strata of the Don Pedro terrane. An equivalent contact has not been identified in the Klamath Mountains, but possible traces are shown, based on the compilation of Dickinson (2008). Plutons are colored by age, see legend. The choice of age bins is hypothesis driven around events at 170 Ma (end of NJT arc) and 155 Ma (closure of the mélange basins), see text. Inset: zoom into the area of the ?extension-related, east-west-elongated Standard pluton (166 Ma) and Calaveras Complex, which are cut by the Sonora dike swarm (159-157 Ma) (after Schweickert, 2015). Pluton distribution and ages after (Ludington et al. 2007), except where superseded in California by Cecil et al. (2012) and Schweickert (2015). Pluton ages in Nevada are from John et al. (1994), Castellanos-Melendez et al. (2024). Paleozoic plutons are omitted.

Figure 9. Margin-parallel terrane translations based principally on paleomagnetic data from Late Cretaceous and Eocene strata. These data constrain the tomotectonic terrane reconstruction model of Clennett et al. (2020), which is modified in the figures. (A) Present-day terrane map shows the current locations of a half-dozen units that are very robustly constrained. The green/blue lines, with nodes every 10 Ma and date labels (in Ma) at key times, represent the spatio-temporal trajectories into the past of these units, back to when they were deposited. A 1000-km scale bar is shown for reference. Trajectories are in absolute coordinates relative to the lower mantle, according to our Clennett et al. 2020 reconstruction. This reconstruction honors the displacement constraints of the most solid paleomag sites, Carmacks & Mount Tatlow/Churn Creek, but Spences Bridge is not honored since it does not fully pass the fold test. The model is based on globally derived apparent polar wander paths (APWP), which reach the same conclusion as for APWP derived solely from North American rock units (Housen, 2021; Tikoff et al., 2022). The *main* BajaBC translations are implemented 70-50 Ma along the yellow line, which runs mainly through Intermontane terranes (and their left-behind correlatives in the Blue Mountains/U.S.). This Baja-BC fault line is necessarily speculative, but it must run inboard of all paleomag sites that show significant offsets (details in section 6.2). The trajectory of the Sierra Nevada, illustrative of a non-translated site on stable NAM, is shown in dark green. Accreted superterrane packages follow the colour scheme of Figure 7; additional pericratonic blocks are colored dark and light purple.

(B) Tomotectonic reconstruction of the assembly of Alaska from Baja-BC and Angayucham terrane translations. This 85-Ma snapshot f the Clennett et al. 2020 model reconstructs the configuration of Baja-BC (comprising at a minimum the terranes west of the yellow line) at the onset of its northward sprint. The locations of the Angayucham (red barbs) and northern Farallon trenches (green solid barbs) are constrained by the ANG and CR slabs, respectively. The terranes of the then-active ANG arc (Koyukuk, future Central Alaska, in red) were welded into the Orcas microplate, but gradually being dislodged and rotated by the obliquely colliding NAM – the "Great Alaskan Terrane Wreck" of Johnston (2001). The northern Farallon arc terranes (Pacific Rim, PR, and others now underplating INS) were also intruded into the Orcas plate and slowly accreted against INS. During its northward sprint, Baja-BC effectively became part of the Orcas plate, separated from NAM by the "Baja-BC fault" (yellow line) or collection of faults.

Baja-BC passes *inboard* of, and unimpeded by, the CR Farallon trench, which still sits offshore. As NAM advances westward, Orcas is squeezed out toward the west or north. It may have subducted into one of two small slabs observed under the grey areas (see text). Due to the small size and mobility of the plate, its disappearance can be rapid, and the Baja-BC and Central Alaskan terranes on it are transported along (the "sprint" phase). As the Orcas seafloor subducts, the northern Farallon trench persists and makes landfall on NAM, becoming the continental Cascades arc by ~50 Ma, which shut off this northwestern passage for shuffling terranes. Baja-BC and Central Alaska collapse against each other and against NAM, completing the assembly of Alaska. The angle between the yellow line (paralleling the NAM margin) and the ANG slab (red line) sets the angle of the Alaskan orocline.